

**ON-LINE PRECONCENTRATION OF VAPOR FORMING ELEMENTS
ON RESISTIVELY HEATED W-COIL PRIOR TO THEIR
DETERMINATION BY ATOMIC ABSORPTION SPECTROMETRY**

**A THESIS SUBMITTED TO
THE GRADUATE SCHOOL OF NATURAL AND APPLIED SCIENCES
OF
MIDDLE EAST TECHNICAL UNIVERSITY**

BY

OKTAY CANKUR

**IN PARTIAL FULFILLMENT OF THE REQUIREMENTS FOR THE DEGREE
OF
DOCTOR OF PHILOSOPHY**

**IN
CHEMISTRY**

MAY 2004

Approval of the Graduate School of Natural and Applied Sciences

Prof. Dr. Canan Özgen
Director

I certify that this thesis satisfies all the requirements as a thesis for the degree of Doctor of Philosophy.

Prof. Dr. Hüseyin İşçi
Head of Department

This is to certify that we have read this thesis and that in our opinion it is fully adequate, in scope and quality, as a thesis for the degree of Doctor of Philosophy.

Prof. Dr. O. Yavuz Ataman
Supervisor

Examining Committee Members

Prof.Dr. Mehmet DOĞAN (Hacettepe University)

Prof. Dr. O. Yavuz ATAMAN (CHEM, METU)

Prof. Dr. Mürvet VOLKAN (CHEM, METU)

Prof. Dr. İnci G. GÖKMEN (CHEM, METU)

Asst. Prof. Dr. Nusret ERTAŞ (Gazi University)

I hereby declare that all information in this document has been obtained and presented in accordance with academic rules and ethical conduct. I also declare that, as required by these rules and conduct, I have fully cited and referenced all material and results that are not original to this work.

Name, Last name : Oktay CANKUR

Signature :

ABSTRACT

ON-LINE PRECONCENTRATION OF VAPOR FORMING ELEMENTS ON RESISTIVELY HEATED W-COIL PRIOR TO THEIR DETERMINATION BY ATOMIC ABSORPTION SPECTROMETRY

Cankur, Oktay

Ph.D., Department of Chemistry

Supervisor: Prof. Dr. O. Yavuz Ataman

May 2004, 159 Pages

Vapor generation in atomic spectrometry is a well established technique for the determination of elements that can be volatilized by chemical reactions. *In-situ* trapping in graphite furnaces is nowadays one of the most popular methods to increase the sensitivity. In this study, resistively heated W-coil was used as an on-line trap for preconcentration and revolatilization of volatile species of Bi, Cd and Pb. The collected analyte species were revolatilized rapidly and sent to a quartz T-tube atomizer for AAS measurement. Although the nature of revolatilized species of Bi and Pb are not clear, they are probably molecular since they can be transported at least 45 cm without any significant decrease in the peak height values. However, cadmium is revolatilized from the trap surface as atoms.

The experimental parameters were optimized for the highest vapor generation, trapping and volatilization efficiencies. The concentration limits of detection calculated by the 3σ of blank solution were found to be 0.0027, 0.0040 and 0.015 ng/mL for Bi (18 mL), Cd (4.2 mL) and Pb (2 mL), respectively; enhancement factors in the sensitivity were 130, 31 and 20, respectively. These values are comparable with those obtained by *in-situ* trapping in graphite furnaces or even ICP-MS found in the literature or better. Sensitivity can be improved further for Bi and Cd using larger sample volumes, but purification of blank is required for Pb. Certified standard reference materials were analyzed for the assessment of accuracy of developed method.

Keywords: Atomic Absorption Spectrometry, Vapor Generation, On-line Preconcentration, W Trap, Bi, Cd, Pb.

ÖZ

BUHAR OLUŞTURAN ELEMENTLERİN ATOMİK ABSORPSİYON SPEKTROMETRİ İLE TAYİNİNDEN ÖNCE ELEKTRİK AKIMI İLE ISITILAN W-SARMAL ÜZERİNDE HAT ÜSTÜ ÖNZENGİNLEŞTİRİLMESİ

Cankur, Oktay

Ph.D., Kimya Bölümü

Tez danışmanı: Prof. Dr. O. Yavuz Ataman

Mayıs 2004, 159 Sayfa

Atomik spektrometride buhar oluşturma, kimyasal tepkimelerle buhar haline getirilebilen elementlerin tayininde oldukça yerleşmiş ve kabul edilen bir tekniktir. Grafit fırın içerisinde yerinde tuzaklama, duyarlılık artışı sağlamak için günümüzde gözde yöntemlerden biridir. Bu çalışmada, elektrik akımı ile ısıtılan W-sarmal, Bi, Cd ve Pb'nin uçucu bileşiklerinin önzenginleştirilmesi ve tekrar buharlaştırılması için hat üstü tuzak olarak kullanılmıştır. Toplanan analit türleri hızlı bir şekilde buharlaştırılmış ve AAS ölçümü için kuvars T-tüpe gönderilmiştir. Tekrar buharlaştırılan Bi ve Pb bileşiklerinin doğası bilinmemekle birlikte, sinyal alanlarında anlamlı bir düşme olmadan en az 45 cm taşınabildiklerinden muhtemelen moleküler yapıdadırlar. Bunlardan farklı olarak Cd tuzak üzerinden atom olarak buharlaşmaktadır.

Deneysel parametreler en yüksek verimlilikte buhar oluřturma, tuzaklama ve yeniden buharlařtırma iin optimize edilmiřtir. Kr zeltisinin 3σ deęeri baz alınarak hesaplanan gzlenebilirlik sınırları Bi (18 mL), Cd (4.2 mL) ve Pb (2.0 mL) iin sırasıyla 0.0027, 0.0040 ve 0.015 ng/mL olarak hesaplanmıřtır; duyarlılıktaki artıř katsayıları sırasıyla 130, 31 ve 20'dir. Bu deęerler, literatrde bulunan grafit fırında yerinde tuzaklama ve hatta ICP-MS ile elde edilenlerle karřılařtırılabilir veya daha iyidir. Bi ve Cd iin verilen duyarlılıklar daha fazla rnek hacmi kullanılarak daha da geliřtirilebilir, fakat Pb iin kr deęerlerinin dřrlmesi gereklidir. Geliřtirilen yntemin doęruluęunun deęerlendirilmesi iin sertifikalandırılmıř standart referans maddeleri analiz edilmiřtir.

Anahtar Kelimeler: Atomik Absorpsiyon Spektrometri, Buhar Oluřturma, Hat st nzenginleřtirme, W Tuzak, Bi, Cd, Pb.

To my son, Sarp Eren

ACKNOWLEDGEMENTS

I am deeply grateful to Prof. Dr. O Yavuz Ataman for his invaluable and professional guidance. He always supported me by giving valuable suggestions throughout all stages of this thesis. Without our inspiring discussions, this thesis would not have been what it is today.

I would like to acknowledge Asst. Prof. Dr. Nusret Ertaş for his expert advice and constructive comments. He asked me questions that made me think in more depth.

I truly appreciate the members of examination committee for their time and advice.

I am also deeply grateful to my wife, Dilek Cankur, for her unwavering support during the many long days which went into this endeavor. She provided continuous understanding, patience and love.

Sincere thanks are to my friends, Dr. Deniz Korkmaz, Süleyman Z. Can and Dr. Eftade Gaga for sharing the joys and worries in the laboratories. They always encouraged and helped in various ways. I would like to express my special thanks to Dr. Gülay Yılmaz for her unforgettable moral supports, helps and guidance.

I would like to express heartfelt thanks to my parents for financial and infinite moral supports during the studies. I would also extend my thanks to my father-in-law and mother-in-law for their patience and endurance.

This work was financially supported by Middle East Technical University Research Fund through grant BAP 2002-07-02-00-41.

TABLE OF CONTENTS

ABSTRACT	iv
ÖZ	vi
DEDICATION.....	viii
ACKNOWLEDGEMENTS.....	ix
TABLE OF CONTENTS	xi
LIST OF TABLES	xvii
LIST OF FIGURES	xix
LIST OF ABBREVIATIONS	xxiv
CHAPTER	
1. INTRODUCTION	1
1.1 Atomic Absorption Spectrometry	2
1.1.1 Flame AAS	2
1.1.2 Vapor Generation AAS (VGAAS)	3
1.1.2.1 Hydride Generation (HG).....	5
1.1.2.2 Mechanism of Hydride Generation	7
1.1.2.3 Methods of Hydride Generation AAS	9
1.1.2.4 Hydride Forming Elements	11
1.1.2.5 Hydride Generation Efficiency	12

1.1.2.6 Atomization in HGAAS	14
1.1.2.6.1 Atomizers used in HGAAS	14
1.1.2.6.2 Atomization Mechanism	15
1.1.2.7 Interferences in HGAAS	17
1.1.3 Electrothermal AAS	18
1.1.3.1 Graphite Atomizer ETAAS	19
1.1.3.2 Metal Atomizer ETAAS	20
1.2 Preconcentration Methods	21
1.3 <i>In-situ</i> trapping techniques	23
1.4 ETV Techniques	25
1.4.1 ETV with Graphite Vaporizers	26
1.4.2 ETV with Metal Vaporizers	28
1.5 Individual Elements	30
1.5.1 Bismuth	30
1.5.1.1 Importance of Bi	30
1.5.1.2 Determination of Bi	31
1.5.1.3 Determination of Bi by Hydride Generation	32
1.5.2 Cadmium	33
1.5.2.1 Importance of Cd	33
1.5.2.2 Determination of Cd	34
1.5.2.3 Determination of Cd by Hydride Generation	35
1.5.3 Lead	37
1.5.3.1 Importance of Pb	37
1.5.3.2 Determination of Pb	38

1.5.3.3 Determination of Pb by Hydride Generation	40
1.6 The Aim of the Study	43
2. EXPERIMENTAL	44
2.1 Instrumentation	44
2.2 Hydride Generation System	45
2.2.1 Apparatus	45
2.2.2 Atomizer and Atom Cell	49
2.3 Trap System	50
2.4 Reagents	55
2.5 Procedure	56
2.5.1 Bismuth	58
2.5.2 Cadmium	58
2.5.3 Lead	61
2.6 Digestion of Standard Reference Materials	62
3. RESULTS AND DISCUSSION	67
3.1 Selection of Trap	67
3.2 Heating System of W-trap and Temperature Measurements	68
3.3 Composition of Carrier Gas	70
3.4 Conditioning and Life Time of W-Trap	71
3.5 Bismuth	71
3.5.1 Optimization of Hydride Generation Parameters	71
3.5.2 Optimization of Trapping Conditions	73
3.5.2.1 Collection and Revolatilization Temperatures	73
3.5.2.2 Carrier Gas Flow Rates	77

3.5.2.2.1 Argon Flow Rate	77
3.5.2.2.2 Hydrogen Flow Rate	79
3.5.2.3 Stability of Collected Species on the W-Trap	80
3.5.2.4 Effect of Cooling Time after Releasing Stage	80
3.5.2.5 Length of Transport Tubing between W-Trap and Atomizer.....	80
3.5.3 Relation between Collection Volume and Analytical Signal	82
3.5.4 Analytical Signal and Reproducibility	84
3.5.5 Calibration Plot	86
3.5.6 The Analytical Figures of Merit	87
3.5.7 Accuracy of the Method	89
3.6 Cadmium	91
3.6.1 Atom Cell	91
3.6.2 Optimization of Vapor Generation Parameters	92
3.6.2.1 General Considerations in the Vapor Generation of Cd by Tetrahydroborate Reduction	92
3.6.2.2 Concentration of HCl in Sample and Carrier Solution	93
3.6.2.3 Concentrations of NaBH ₄ and NaOH in Reductant Solution ...	96
3.6.2.4 Reaction and Stripping Coil Lengths	99
3.6.2.5 Reaction Temperature	100
3.6.3 Optimization of Trapping Conditions	101
3.6.3.1 Placement of W-coil Trap	101
3.6.3.2 Collection and Revolatilization Temperatures	102
3.6.3.3 Carrier Gas Flow Rate	103

3.6.3.4	Coating with Pt and Ir	105
3.6.3.5	Distance between Tip of Transport Capillary and W-trap	106
3.6.3.6	Stability of Collected Species on the W-Trap	107
3.6.3.7	Effect of Cooling Time after Releasing Stage	108
3.6.3.8	Length of Transport Tubing between GLS and W-Trap	109
3.6.3.9	Distance between W-Trap and Atomizer	111
3.6.4	Relation between Collection Volume and Analytical Signal	112
3.6.5	Analytical Signal and Reproducibility	113
3.6.6	Calibration Plot	114
3.6.7	The Analytical Figures of Merit	116
3.6.8	Accuracy of the Method	118
3.7	Lead	119
3.7.1	Optimization of Hydride Generation Parameters	119
3.7.1.1	Concentrations of HCl and NaBH ₄	119
3.7.1.2	Concentration of Oxidizing Reagent in the Reaction Medium	121
3.7.2	Optimization of Trapping Conditions	124
3.7.2.1	Collection and Revolatilization Temperatures	124
3.7.2.2	Carrier Gas Flow Rate	126
3.7.2.3	Coating with Pd, Pt and Ir	128
3.7.2.4	Distance between W-Trap and Atomizer	130
3.7.2.5	Tandem W-trap Arrangement	131
3.7.3	Relation between Collection Volume and Analytical Signal	131
3.7.4	Analytical Signal and Reproducibility	132

3.7.5 Calibration Plot	133
3.7.6 The Analytical Figures of Merit	134
3.7.7 Accuracy of the Method	137
4. CONCLUSIONS	139
REFERENCES	142
VITA	159

LIST OF TABLES

TABLES

2.1 Instrumental parameters used in the measurements	45
2.2 Hydride generation, trapping and revolatilization conditions for Bi, Cd and Pb in CF mode for W-trap HGAAS	57
2.3 The standard reference materials used for the accuracy check of the methods developed for Bi, Cd and Pb and the concentrations of elements	63
2.4 The temperature program used for the decomposition of standard reference material and applied power values	63
3.1 Analytical figures of merit and enhancement factors for Bi calculated by using peak height of analytical signal	87
3.2 Comparison of the limit of detection and the sample volume of the method with those of others in literature	88
3.3 Results of the analysis of standard reference materials and their certified values (n=3 for each measurement)	89
3.4 Analytical figures of merit and enhancement factors for Cd calculated by using peak height of analytical signal	117
3.5 Comparison of the limit of detection and the sample volume of the method with those of others in literature	117
3.6 Results of the analysis of standard reference materials and their certified values (n=3 for each measurement)	118
3.7 Analytical figures of merit and enhancement factors for Pb calculated by using peak height of analytical signal	136

3.8 Comparison of the limit of detection and the sample volume of the method with those of others in literature	137
3.9 Results of the analysis of standard reference materials and their certified values (n=3 for each measurement)	138

LIST OF FIGURES

FIGURES

1.1 Classification of hydride generation methods	10
2.1 Gas liquid separators used in the experiments: (a) Cylindrical GLS used for Cd; (b) U-type GLS used for Bi and Pb	47
2.2 The experimental set up used for generation of Bi and Pb hydrides	48
2.3 The experimental set up used for generation of volatile Cd atoms	49
2.4 Quartz T-tube atomizer used in the experiments	50
2.5 The dimensions of W-coil traps extracted from bulbs and made in the laboratory	51
2.6 The W-coil placed in the inlet arm of quartz T-tube used for Bi and Pb	52
2.7 The W-coil placed in the inlet arm of quartz T-tube used for Cd	52
2.8 Tandem arrangement of W-coil trap system	54
3.1 Voltage versus temperature of W-coil at different gas flow rates	69
3.2 The effect of oxidation of W-coil on QTA when H ₂ was not used in the carrier gas	71
3.3 Optimization of HCl concentration for BiH ₃ generation. Concentration of Bi was 20 ng/mL and the volume of sample loop was 0.500 mL	72
3.4 Optimization of NaBH ₄ concentration for BiH ₃ generation. Concentration of Bi was 20 ng/mL and the volume of sample loop was 0.500 mL	73
3.5 The effect of collection and release temperatures on analytical signal for 5.0 ng Bi. During the variations of collection and release temperatures, a constant release temperature of 1200 °C and a constant collection temperature of 270 °C, respectively, were employed	75

3.6 Effect of H ₂ flow rate on collection temperature for 5.0 ng Bi. During the variations of collection, a constant release temperature of 1200 °C was employed	76
3.7 Effect of collection Ar flow rate on the peak height of analytical signal for 0.500 mL of 10 ng/mL Bi	78
3.8 Effect of release Ar flow rate on the peak height of analytical signal for 0.500 mL of 10 ng/mL Bi	78
3.9 Effect of H ₂ flow rate in the carrier gas on the analytical signal of 0.500 mL of 10 ng/mL Bi	79
3.10 Analytical signal versus trap-atomizer distance for 0.500 mL of 10 ng/mL Bi (5.0 ng Bi)	82
3.11 Analytical signal versus collection volume for 0.100 ng/mL Bi in 1.0 mol/L HCl; collection temperature, 270 °C; release temperature, 1200 °C	83
3.12 The analytical signals for Bi. Collection at 270 °C and releasing at 1200 °C. a) 36 mL of 0.100 ng/mL Bi (3.6 ng Bi), b) 36 mL of 0.020 ng/mL Bi (0.72 ng Bi)	85
3.13. The calibration plot drawn by using peak height and peak area for 18 mL of aqueous standard solutions of Bi under optimum conditions	86
3.14 Effect of HCl concentration in sample and carrier solutions on the analytical signal of Cd obtained by conventional FI-HGAAS. Carrier solution and sample solution acidities were 0.25 mol/L and 0.15 mol/L HCl, respectively, as the other parameter was varied. 0.500 mL of 1.0 ng/mL Cd was used in the experiments	94
3.15 Effect of HCl concentration in the sample solution on the analytical signal of Cd obtained from W-trap system in CF mode. The signals were obtained by collecting 0.7 mL of 10.0 ng/mL Cd, a total of 7.0 ng Cd.....	95
3.16 Effect of NaBH ₄ concentration on the analytical signal of Cd obtained in conventional FI-HGAAS. The concentrations of HCl were 0.15 and 0.25 mol/L in sample and carrier solutions, respectively. 0.500 mL of 1.0 ng/mL Cd was injected	97
3.17 Effect of NaBH ₄ concentration on the analytical signal of Cd obtained from CF-W-trap system. The signals were obtained by collecting 0.7 mL of 5 ng/mL Cd, a total of 3.5 ng Cd	97

3.18 Effect of NaOH concentration in reductant solution on the analytical signal of Cd obtained in conventional FI-HGAAS. The signals were obtained by collecting 0.500 mL of 1.0 ng/mL Cd in 0.15 mol/L HCl. Carrier acidity was 0.25 mol/L HCl	98
3.19 Effects of reaction and stripping coil lengths on the analytical signal of Cd obtained in conventional FI-HGAAS. Lengths of reaction and stripping coils were 60 and 15 cm, respectively, as the other parameter was varied. The signals were obtained using 0.100 mL of 5.0 ng/mL Cd in 0.15 mol/L HCl. Carrier was 0.25 mol/L HCl	99
3.20 Effect of reaction coil temperature on the analytical signal of Cd obtained in CF-W-trap-HGAAS. The signals were obtained by collecting 0.7 mL of 5.0 ng/mL Cd in 0.2 mol/L HCl	101
3.21 The effect of collection and release temperatures on analytical signal for Cd. During the variations of collection and release temperatures, a constant release temperature of 1000 °C and a constant collection temperature of 150 °C, respectively, were employed. The signals were obtained by collecting 0.7 mL of 5.0 ng/mL Cd in 0.2 mol/L HCl	102
3.22 The effect of collection Ar flow rate in the carrier gas on the signal of W-trap HGAAS; H ₂ flow rate was kept at 150 mL/min. The signals were obtained by collecting 0.7 mL of 5.0 ng/mL Cd in 0.2 mol/L HCl	103
3.23 Effect of carrier Ar flow rate on the peak height of analytical signal of Cd in conventional FI-HGAAS. The signals were obtained using 0.100 mL of 5.0 ng/mL Cd in 0.15 mol/L HCl. Carrier acidity was 0.25 mol/L HCl	104
3.24 The effect of argon flow rate in the carrier gas on the trapping efficiency during collection; H ₂ flow rate was kept at 150 mL/min. The signals were obtained by collecting 0.7 mL of 5.0 ng/mL Cd in 0.2 mol/L HCl	105
3.25 Effect of distance between capillary tip and the W-trap on analytical signal. The signals were obtained by collecting 0.7 mL of 5.0 ng/mL Cd in 0.2 mol/L HCl. Collection and release temperatures were 150 °C and 1000 °C, respectively	107
3.26 Effect of time between collection and release stage on the trap signal of Cd. The signals were obtained by collecting 0.7 mL of 5.0 ng/mL Cd in 0.2 mol/L HCl. Collection and release temperatures were 150 °C and 1000 °C, respectively	108
3.27 Effect of cooling time after each revolatilization stage for Cd. The signals were obtained by collecting 0.7 mL of 5.0 ng/mL Cd in 0.2 mol/L HCl. Collection and release temperatures were 150 °C and 1000 °C, respectively	109

3.28 The effect of length of PTFE transport tubing between GLS and W-trap. The signals were obtained by collecting 0.7 mL of 5.0 ng/mL Cd in 0.2 mol/L HCl. Collection and release temperatures were 150 °C and 1000 °C, respectively.....	110
3.29 The effect of distance between the trap and atomizer on the normalized peak height and peak area signals of Cd	112
3.30 Relationship between the collection volume and the analytical signal for both peak area and peak height using 0.50 ng/mL Cd solution under optimized conditions; the flow rate was 2.1 mL/min for both sample and the reductant	113
3.31 The analytical signals for 4.2 mL of 0.025 ng/mL Cd in 0.2 mol/L HCl. Collection at 150 °C and releasing at 1000 °C. 1.5% (w/v) NaBH ₄ was used	114
3.32 The calibration plot of Cd for both peak height and peak area of the analytical signal obtained by W-coil HGAAS. The collection volume was 4.2 mL and aqueous standard solutions were employed; the flow rate was 2.1 mL/min for both sample and reductant	115
3.33 Effect of sample acidity on Pb signal in conventional FI-HGAAS. The signals were obtained using 0.500 mL of 10.0 ng/mL Pb in 0.5% (w/v) K ₃ Fe(CN) ₆ . NaBH ₄ concentration was 1.0% (w/v)	120
3.34 Effect of NaBH ₄ concentration on Pb signal in conventional FI-HGAAS. The signals were obtained using 0.500 mL of 10.0 ng/mL Pb in 0.06 mol/L HCl and 0.5% (w/v) K ₃ Fe(CN) ₆	121
3.35 Effect of concentration of K ₃ Fe(CN) ₆ on analytical signal in conventional FI-HGAAS. The signals were obtained using 0.500 mL of 10.0 ng/mL Pb in 0.06 mol/L HCl	123
3.36 Effect of nitroso-R salt concentration on analytical signal in conventional FI-HGAAS. The signals were obtained using 0.500 mL of 10.0 ng/mL Pb in 0.06 mol/L HCl	124
3.37 The effect of collection and release temperatures on analytical signal for 5.0 ng Pb. During the variations of collection and release temperatures, a constant release temperature of 1300 °C and a constant collection temperature of 350 °C, respectively, were employed	125
3.38 Effect of collection Ar flow rate on the analytical signal obtained by W-coil HGAAS; H ₂ flow rate was 100 mL/min, release Ar flow rate was 210 mL/min; 0.500 mL of 10 ng/mL Pb was used	127

3.39 Effect of release Ar flow rate on the analytical signal obtained by W-coil HGAAS; H ₂ flow rate was 100 mL/min, release Ar flow rate was 210 mL/min; 0.500 mL of 10 ng/mL Pb was used	127
3.40 The dependence of analytical signal on the collection temperature of Pt coated W-coil for 5.0 ng Pb. During the variations of collection temperature, a constant release temperature of 1300 °C was employed	129
3.41 The effect of distance between the trap and atomizer on both peak height and peak area signals of Pb. 0.500 mL of 5.0 ng/mL Pb was used	130
3.42 Analytical signal versus collection volume obtained by using reagent blank solutions: 0.5% (w/v) K ₃ Fe(CN) ₆ in 0.06 mol/L HCl and 1.0% NaBH ₄ (w/v) (reagent blanks gave a signal equal to that obtained from 0.2 ng/mL Pb, and no Pb was added); collection temperature, 350 °C; release temperature, 1300 °C	132
3.43 The analytical signals for 2.0 mL of 5.0 ng/mL Pb; Collection at 350 °C and releasing at 1300 °C	133
3.44 The calibration plot drawn by using peak height for 2.0 mL of aqueous standard solutions of Pb in 0.5% (w/v) K ₃ Fe(CN) ₆ under optimum conditions (No blank correction was made)	134

LIST OF ABBREVIATIONS

AAS	Atomic Absorption Spectrometry
AES	Atomic Emission Spectrometry
CF	Continuous Flow
CV	Cold Vapor
CVG.....	Chemical Vapor Generation
CVAAS	Cold Vapor Atomic Absorption Spectrometry
EcHG	Electrochemical Hydride Generation
ETAAS	Electrothermal Atomic Absorption Spectrometry
ETV	Electrothermal Vaporizer
FAAS	Flame Atomic Absorption Spectrometry
FEP	Fluorinated Ethylene-Propylene
FI	Flow Injection
GLS	Gas Liquid Separator
HG	Hydride Generation
HGAAS	Hydride Generation Atomic Absorption Spectrometry
i.d.	Inner Diameter
ICP	Inductively Coupled Plasma
LOD	Limit of Detection
MS	Mass Spectrometry
o.d.	Outer Diameter
OES	Optical Emission Spectrometry
QTA	Quartz T-tube Atomizer
RSD	Relative Standard Deviation
VGAAS	Vapor Generation Atomic Absorption Spectrometry

CHAPTER I

INTRODUCTION

The metals and their compounds have important physiological and toxic effects in living systems. While some of them are essential for the biological activities in living systems, the necessity and essentiality of others have not been proven yet. Some heavy metals including Hg, Cd and Pb show toxic effects even at very low concentrations. They have the potential of adverse effects in the biological systems. In addition to environmental and biological considerations, the presence of metals even at trace concentrations may alter the physical characteristics of alloys. Therefore, the determination of traces and ultra-traces of such elements in environmental, biological and metallurgical samples is very important. Since the desired detection levels in such determinations are very low, highly sensitive and precise techniques are needed. In addition the technique must be fast and easy to apply. Atomic absorption spectrometry (AAS) is a well established and extensively used technique for the determination of metals and metalloids in environmental and biological samples for many years. In the last two decades, inductively coupled plasma optical emission spectrometry (ICP-OES) and mass spectrometry (ICP-MS) have become very popular. However, AAS is still the most widely used method since it is relatively inexpensive and easy to apply, and also accessible in most analytical chemistry laboratories.

1.1 Atomic Absorption Spectrometry

Atomic absorption spectrometry is one of the most popular techniques for the determination of trace elements. Due to its high specificity and selectivity as well as relatively simple operation, AAS has preserved its place alongside ICP-OES and ICP-MS. The actual birth of modern AAS was in 1955. Although the publications by Alkemade and Milatz in Netherlands, and Alan Walsh in Australia appeared in the same year, Alan Walsh is generally recognized as the father of modern AAS [1]. About 60 elements can be determined by AAS.

The technique is based on the measurement of selective absorption of light by free atoms created in an atomizer. The main components of an AA spectrometer are: (1) a lamp which emits a beam of light at suitable wavelength to be absorbed selectively by analyte atoms, (2) an atomizer that converts analyte species into gaseous atoms (3) a wavelength selector which selects a bandwidth of desired wavelength (4) a detector that measures the intensity of light. AAS techniques can be classified into several categories depending on the atomization and/or sample introduction procedures followed in order to obtain analytical signal. According to a recent publication, where the characteristics of each are summarized, these are flame AAS (FAAS), electrothermal AAS (ETAAS), vapor generation AAS (VGAAS), and hyphenated AAS techniques where one or more techniques are combined [2]. Usually the sample is dissolved / decomposed in acids or other chemical reagents and then introduced to the atomizer as solutions. In addition, some methods of AAS allow solid and slurry sampling.

1.1.1 Flame AAS

Flame AAS, where flame is used for the atomization of the analyte, is relatively easy to use, accessible and low cost technique; whenever possible it is preferred

over others. The temperature of the flame and thus the atomization efficiency depends on types of fuel and oxidant as well as fuel to oxidant ratio. The analyte must be taken into usually aqueous phase and then introduced to the flame via a nebulizer at a flow rate of 5-10 mL/min. The function of nebulizer is to convert liquid phase into a mist composed of small droplets, called aerosol, by a pressurized gas flow. The larger droplets are not allowed to reach to the flame since they alter the temperature and thus atomization efficiency. The nebulization efficiencies of nebulizers commonly employed in FAAS instruments does not exceed 10%; only this amount of the aspirated solution is converted to aerosol and reaches to the flame. The low efficiency of nebulizers is one of the most important drawbacks of FAAS. High efficiency nebulizers are also available, but the solution flow rates are low, $\mu\text{L}/\text{min}$, which are suitable for highly sensitive techniques such as ICP-MS [3, 4]. The atomization of analyte takes place in the flame as a result of temperature and chemical reactions. The analytical beam of photons to be absorbed by the atoms is forwarded through the flame and the absorption occurs therein. The absorption by the analyte atoms is a function of their concentration in the flame. The need for large sample volume is another limitation of FAAS. In case of limited sample volume micro-injection can be employed but the sensitivity is decreased. The dilution of the analyte species in the flame due to the high velocity of flame gasses, 10-30 L/min, is usually considered as a disadvantage, but if there is no limit of detection problem, it appears to be an advantage when the heavy sample matrix has a significant depression effect on the analytical signal. FAAS often lacks sensitivity at analyte concentrations below 0.1 and 10 $\mu\text{g}/\text{g}$ in liquid and solid samples, respectively.

1.1.2 Vapor Generation AAS (VGAAS)

In vapor generation AAS the analyte is converted to its volatile species by chemical or electrolytic means and then introduced to the atomizer in the gas phase. As a sample introduction method, it offers significant advantages over

conventional nebulization. It is a simple and low cost method providing high sensitivity and low LODs because of high chemical yields and high transport efficiency to the atomizer. It provides analyte separation from the matrix which may become a serious problem during atomization. It enables enrichment of analyte and speciation as well as automation in flow injection (FI) and continuous flow (CF) modes. In some cases, it has fairly high sample throughput rates, typically 40-100 /hour [5, 6].

Hydride generation AAS is currently the most popular vapor generation method which can be applied to the determination of elements which form relatively stable and volatile hydrides [5]. Cold vapor AAS (CVAAS), another method of vapor generation where the analyte is converted to atomic vapor at ambient temperatures, can be applied to determination of Hg and more recently Cd; in fact Cd is first converted to unstable hydride that quickly decomposes to atomic vapor and hydrogen [7]. Investigations were also made on other ways to selectively vaporize analytes. In 1975, Skogerboe et al. [8] vaporized Bi, Cd, Ge, Mo, Pb, Sn, Tl and Zn as their chlorides which are subsequently forwarded to a microwave induced plasma (MIP). Volatilization of Ni as its volatile carbonyl compound had never been exploited for analytical purposes until 1980, when an AAS determination method was described [9]. Brueggemeyer and Caruso [10] determined trace amounts of lead by quartz furnace AAS after converting to its tetramethyl compound. Speciation of lead and methylead ions by chromatographic separation and AAS detection after ethylation with sodium tetraethylborate was described in 1986 [11]. Sturgeon et al. [12] used sodium tetraethylborate for vapor generation and subsequent sequestration of volatile lead species in graphite furnace followed by atomization there. Elements have also been volatilized as their oxides, and chelates such as β -diketonates, dithiocarbamates and trifluoroacetylacetonates [1, 6].

1.1.2.1 Hydride Generation (HG)

Method of hydride generation involves the conversion of analyte in the solution phase to its volatile hydride by chemical or electrochemical reactions. It has been used over 100 years for the determination of arsenic in methods known as Marsh reaction or Gutzeit test [1, 5]. Hydride generation as a method of sample introduction to AAS was used for the first time by Holak in 1969 [13] for the determination of As. In this study, after collecting the generated arsine in a U tube that was immersed in liquid nitrogen, the U tube was brought to room temperature. The evaporated hydride is sent to flame via spray chamber. HGAAS is currently the most popular method for the determination of trace amounts of elements which form volatile covalent hydrides. Although Cd can be determined by CVAAS, it can also be included into the list of hydride forming elements since the acidified solution of Cd reacts with tetrahydroborate to form volatile Cd species, presumably hydride with a very unstable nature.

The complex on-line chemistry involved in the hydride generation process is one of the limitations of HGAAS. Since the oxidation state and the form of the element effects the efficiency of hydride generation, specific sample pretreatment may be required. The chemical interference is sometimes a serious problem during hydride release or atomization. Due to the large number of parameters to be optimized, the possibility of multielement determination is low. Foaming and aerosol formation due to the vigorous reaction between sample and the reductant solution may be a serious problem for the transportation of vapor species to the atomizer due to condensation in the transfer tubings. Dilution of vapor species by the carrier gas can be considered as another disadvantage [5, 6].

For analytical purposes, two different chemical vapor generation methods have been used to generate volatile hydrides. The first one that was used in the earlier stages of HGAAS was metal/acid (usually Zn/HCl) system. Zinc metal in the

forms of granules, tablet, dust or slurry was added to acidified sample solution. Reaction vessels were most frequently flasks equipped with a dosing fitting for the introduction of metal [14, 15]. The metallic zinc reacts with hydronium ion and this is followed by the formation of volatile hydride. The reaction can also be achieved by a flow of acidified sample solution through a Zn column [16]. Other metal acid reactions involved in HG include mixtures of Mg-TiCl₃ reacted with HCl and H₂SO₄ to produce arsine, hydrogen selenide, stibine and bismuthine. Aqueous slurry of Al was also reacted with HCl to generate arsine, hydrogen selenide, stibine [17]. Because of the slow rate of these reactions which results in band broadening in signal shape, a balloon system which functioned to collect reaction products with subsequent rapid expulsion to the atom reservoir was described and frequently used in the early stages of HGAAS [18].

The second type of chemical reaction used in AAS utilizes tetrahydroborate/acid reduction system. The reaction between tetrahydroborate and hydronium ion is a fast reaction. If it is carried under solutions with a pH of less than 1, the tetrahydroborate decomposition is complete within a few microseconds [5, 19]. Although tetrahydroborate reduction to form elemental hydrides had been used for synthetic purposes, the technique was introduced to the atomic spectroscopy in 1972. In the early years, the sodium tetrahydroborate was used in solid form and pellets of it were added to the reaction chamber. Use of tetrahydroborate as aqueous solutions was suggested by Braman et al. [20]. Since then, use of tetrahydroborate dramatically increased in popularity since it offers advantages over metal/acid system. Currently the most commonly sodium, rarely potassium salts of tetrahydroborate are almost exclusively used for hydride generation. Since the reductant dissolved in water is not very stable in the solution phase, usually stabilization is required by increasing the pH of solution by the addition of 0.05-2% sodium or potassium hydroxide [5]. Recently use of aminoboranes and cyanotrihydroborate reagents in HGAAS was investigated and their reactivity towards Hg and hydride forming elements were reported [21].

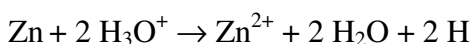
Currently, in most of the studies, the HG reaction is carried out by merging the acidified sample solution with aqueous tetrahydroborate solution. However, rarely the reaction has also been carried out by other means such as employing solid tetrahydroborate. Tian et al. [22] developed a system called movable reduction bed HG in which analyte solution, without acidification, was injected onto a tape on which a premixed potassium tetrahydroborate and a solid organic acid was deposited. Maleki et al. [23] have also used solid sodium tetrahydroborate reductant premixed with tartaric acid for the determination of Pb using sodium peroxodisulfate.

Hydride generation can also be achieved via electrolytic reactions employing an electrochemical cell; which is called electrochemical hydride generation (EcHG). The volatile species are formed on the cathode surface. The most important advantage of EcHG based on the reduction of tetrahydroborate consumption is that analyte concentration in reagent blanks is very low when compared to chemical means. Thus, excellent limit of detection values can be obtained by EcHG [5]. Ding and Sturgeon [24] studied the electrochemical hydride generation and *in-situ* preconcentration of As and Se on Ir-Pd coated graphite tubes and reached the detection limit of over ng/L ranges.

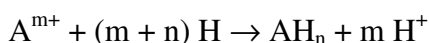
1.1.2.2 Mechanism of Hydride Generation

The mechanism of the hydride generation is still a matter of debate after more than 30 years from its introduction to AAS. The hypotheses on the hydride generation are classified into two classes. The first and widely accepted one is based on the assumption that the effective species in the mechanism is the atomic hydrogen or “nascent hydrogen”. The second class mechanisms are those which are not included in the nascent hydrogen hypothesis. This second class has been termed “non-nascent hydrogen” mechanism [25].

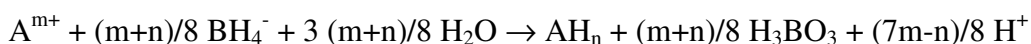
Nascent hydrogen mechanism was firstly suggested by Robbins and Caruso [17] who postulated that when Zn metal or tetrahydroborate reacts with hydronium ion, nascent hydrogen, that is reactive and responsible for the formation of hydride, is formed according the following reactions, respectively:



where H is nascent hydrogen. Then the nascent hydrogen reacts with the analyte for the generation of hydride as follows:



Recently, Laborda et al. [26] strongly criticized the nascent hydrogen mechanism on the base of thermodynamic consideration that neither tetrahydroborate nor Zn would be able to perform the reduction of protons to atomic hydrogen. They concluded that in both chemical and electrochemical hydride generation, no nascent hydrogen has to be involved and the generation of the hydrides can be considered as hydrogenation process. They proposed the following generalized mechanism for the formation of hydride of analyte ion A^{m+} ;



where m and n represent the oxidation state of analyte and coordination number of hydride, respectively.

More recently, D'Ulivo and coworkers studied the generation mechanism to verify the validity of nascent hydrogen mechanism. However, it was concluded that Sn, Sb and Bi hydrides could be generated by the direct action of borane complexes without the need of their decomposition. It was shown that nascent hydrogen

mechanism failed to explain the generation of hydrides in different experimental conditions in a pH range between 4.3 and 12.7 [25].

The electrochemical generation mechanism is considered to take place in at least two sequential events [26]:

1) reduction and deposition of the analyte onto the surface of cathode



2) formation of the hydride from the deposited metal or metalloid



Where H represents a hydrogen atom from an unspecified source (adsorbed H atom, reduced from H_3O^+ or reduced from H_2O).

1.1.2.3 Methods of Hydride Generation AAS

The classification of hydride generation AAS is given in Figure 1. There are two basic hydride generation methods which are direct transfer mode and collection mode. In the former the generated hydride of the analyte released from the solution was directly transported to the atomizer. The direct method is divided into three, namely continuous flow (CF), flow injection (FI) and batch mode. Continuous flow hydride generation method uses the continuous delivery of reductant and acidified sample solution with the help of a constant flow pump and they combine in the reaction coil. Then the released volatile hydride is separated from the liquid phase via a gas liquid separator and sent to the atomizer using a carrier gas. Usually, a stripping coil is employed for the introduction of carrier gas before gas liquid separator in order to achieve efficient separation of vapor species of analyte from the solution phase. This is vital in case of hydrides whose stabilities are low

and solubilities are high in reaction media, or in case of possible interferents present in the solution [5].

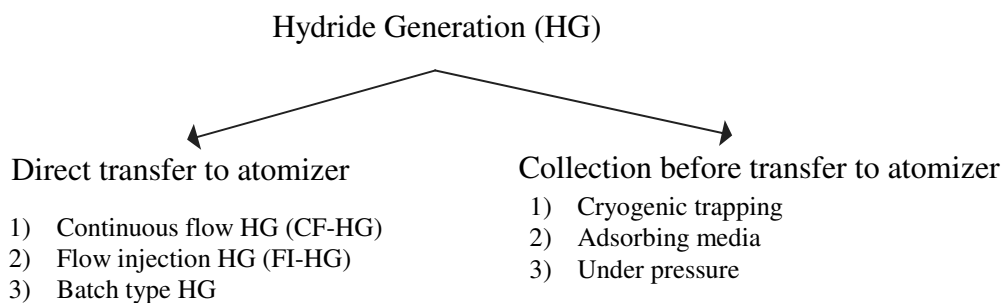


Figure 1.1. Classification of hydride generation methods [5].

In FI mode, which is similar to CF but instead of continuous delivery of analyte solution, a defined volume of sample is injected into a stream of carrier solution that is usually blank. The plug of sample is carried by the carrier and subsequently merged with reductant. In batch mode, a definite amount of reductant solution is added to acidified sample solution rapidly, or vice versa, and the evolved hydride is transported to atomizer by a flow of purge gas.

In the collection before transfer to atomizer, first the generated hydride is trapped in a collection device until the release is complete and then they are sent to the atomizer all at once. The evolved hydride can be trapped in an absorbing media or in a cryogenic trap cooled in liquid nitrogen. Cryogenic trapping is applicable to hydrides which are stable during both trapping and revolatilization. However, all hydrides are not stable for revolatilization after collection. Another way is to collect the evolved hydride under pressure. This method is used much more frequently in the early years since the reduction carried out by Zn/acid systems is slow [18]. Cryogenic trapping is also used today since the analyte vapor is preconcentrated before measurement. Methods employing *in-situ* trapping where

the analyte is trapped in the atomizer are not classified among the collection modes since the hydride leaves the generator uncollected and it is considered as the first stage of atomization [5]. In addition, in the *in-situ* trapping techniques, the hydride is decomposed during collection and thus it is no longer hydride.

1.1.2.4 Hydride Forming Elements

The elements which form volatile hydrides and are usually determined by HGAAS are As, Bi, Ge, Pb, Sb, Se, In, Sn, Te and Tl [5]. Cadmium can also be included in the hydride forming elements since it is converted to volatile species when reacted with sodium tetrahydroborate [27] although the species are not stable [7, 28]. In 1996, it has been shown that volatile species of Cu can be obtained when acidified Cu solution is reacted with sodium tetrahydroborate but not proven to be hydride. [29]. Guo and Guo studied the generation of volatile species of Zn via tetrahydroborate reduction and Sun et al. determined by atomic fluorescence spectrometry (AFS) after hydride generation from surfactant based organized media [30]. The generation of volatile Ni species by the reaction of acidified solution with tetrahydroborate for the first time was reported by Guo and coworkers [31]. More recently, although the nature of volatile species is not known, Ag, Au, Co, Ir, Mn, Pd, Pt, Rh, and Ti were added to the list of elements which form volatile species when reacted with sodium tetrahydroborate [32-36]. The nature of species is thought to be molecular and probably hydride, but remains unknown. It is reported that generated species of transition and noble metals are relatively unstable in solution and are quickly lost during their generation and subsequent transport [36]. For efficient detection, rapid phase separation is necessary [36]. However, it is also proposed for Ag, Cu and Pd that the initially formed species by the reaction with tetrahydroborate are atomic, since the atomic signal with a narrow absorption bandwidth is achieved in the solution phase, and followed by a rapid cluster formation with other atoms [37].

Most of the hydrides detected by HGAAS have very low boiling points and present in the gas phase at ambient temperature. The boiling points of As, Bi, Pb, Sb, Se and Sn hydrides are -62.4, +16.8, -13, +18.4, -41.3 and +52.5 °C, respectively [5]. However, the hydrides of some transition metals are not volatile and present in the solid phase under normal temperature and pressure [38, 39]. The stabilities of volatile hydrides are crucial if collection methods are to be used since revolatilization is necessary. Fujita and Takada [40] studied the stabilities of As, Sb, and Bi and found that although As and Sb hydrides are stable, Bi hydride is not stable even at room temperature. They also calculated the rate constants for the decomposition of gaseous bismuthine and found that its half lives at 0 °C and 40 °C are 14.7 and 2.4 min, respectively. Their results supported the findings of Fernandez [41] who observed that prolonging the collection time for bismuthine in a balloon system resulted in a much poorer limit of detection.

1.1.2.5 Hydride Generation Efficiency

Hydride generation can be considered as a sequential processes including conversion of analyte to its hydride, transfer of volatile hydride to the gas phase in the generator and transportation of released hydride to the atomizer/ionizer. The obtained analytical signal depends on the efficiency of each process. Total hydride generation efficiency is the fraction of analyte transported to the atomizer in the form of hydride [5]:

$$\beta_g = N_o / C_o * V_s$$

Where N_o is the total number analyte atoms transported to the atomizer in the form of hydride, C_o is the concentration in the sample, and V_s is the volume of sample used in the generation process. Since the total process is combination of sequential

steps, the above formula can be written for each step. The hydride release efficiency (β_r) is the fraction of released analyte atoms (N_{released}) in the form of hydride to the total number of analyte atoms in the solution as follows

$$\beta_r = N_{\text{released}} / C_o * V_s$$

In a similar way, hydride transport efficiency (β_t) is the total number of released atoms reaching to the atomizer in the form of hydride to the number of released atoms as hydride:

$$\beta_t = N_o / N_{\text{released}}$$

If a collection method is not employed, the total efficiency is the multiplication of efficiencies of individual steps, Otherwise collection and revolatilization efficiencies must be taken into account.

$$\beta_g = \beta_r * \beta_t$$

Hydride release efficiency depends on the amount of tetrahydroborate, concentration of acid, design of generator, mixing process of reductant with analyte temperature and the kinetics of reaction mechanisms. It is also affected by the purge gas flow rate which is used for stripping of the solution for efficient separation of volatile species from the liquid phase [5]. There are also other parameters affecting release efficiency such as addition of catalytic reagents or creating microenvironments in the solution as in the cases of hydride generation of lead and cadmium, respectively.

Generated hydride is transported to the atomizer by a flow of purge gas. Hydride transport efficiency is critical for the evaluation of total efficiency. Losses of hydride during transportation on the surfaces of generator and transport lines can be a serious problem. Such losses are probably due to decomposition or sorption.

The hydride may be dissolved in water droplets usually present in the gas liquid separator and / or in the condensed water on the surfaces of transfer tubings. The physical properties of the material making up the generator and the transfer lines, such as size, diameter and volume, and also chemical properties may have significant influence on the transport efficiency. An efficient way of minimizing such losses are the silanization of glass surfaces to make it hydrophobic, using the transfer tubings as short as possible, minimizing the surface area that hydride come in contact by using tubings of smaller diameter and relatively small gas liquid separator. In order to minimize the condensation of water vapor, various desiccants have been suggested to remove moisture in gas phase stream. However, they must be used carefully since some hydrides may be trapped on such desiccants. Another way of removing water vapor is to use hygroscopic membranes such as nafion [5].

1.1.2.6 Atomization in HGAAS

1.1.2.6.1 Atomizers used in HGAAS

In the early years of HGAAS, the classical burners were used as atomizers and generated hydride was introduced via nebulizer. Due to strong absorbance of air/acetylene flame especially at short wavelengths, N₂- or Ar- hydrogen entrained flames were used. Later on the use of open ended Vycor glass (95-96% SiO₂) as an absorption tube which was heated externally by a resistance wire was introduced by Chu et al. 1972 [14]. This was the first study where a T-tube was used as atomizer. Later on different quartz T-tube designs were developed.

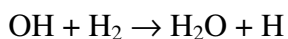
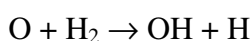
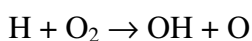
Today, there are three types of atomizers commonly employed for the atomization of hydride [5]:

- 1) inert gas hydrogen diffusion flame,
- 2) quartz tube atomizer
- 3) graphite furnace

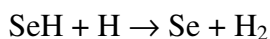
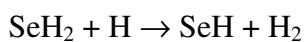
The most commonly employed atomizers in HGAAS are flameless or flame-in-tube quartz T-tube atomizers (QTA) which can be heated externally by air acetylene flame or electrically. Graphite atomizers have also been used in hydride atomization but not extensively used in continuous flow or flow injection systems because of difficulties of coupling HG system to ETAAS. In addition, moderately heated graphite ends are capable of trapping hydride if it is introduced through purge gas. They are used in *in-situ* preconcentration methods and will be discussed later.

1.1.2.6.2 Atomization Mechanism

The temperature achieved by QTA does not exceed 1300 °C which is not sufficient for complete atomization of hydride forming elements. Dědina and Rubeska have made serious effort to elucidate the mechanism involved in the atomization of hydrogen selenide using flame in tube atomizer. They found evidence that the atomization of selenium hydride proceeded via collision with free hydrogen radicals [5]. The proposed mechanism for the formation of hydrogen radicals in flame in tube atomizer is as follows:

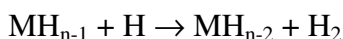
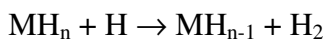


According to their hypothesis, the atomization proceeds most probably via the interaction of hydride with H radicals as exemplified by selenium hydride as follows:

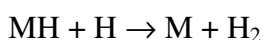


Dědina have shown that the atomization in flame-in-tube atomizers and externally heated atomizers are identical. The only difference is the formation of hydrogen radicals [42]. Later, investigations were focused on the atomization of mainly hydrides of Se, As and Sb. Although radicalic mechanism has not been proven, the results of experiments have been interpreted without problems using that theory [43].

Welz and Melcher [44] investigated the effect of O₂ on atomization of arsine and some other hydrides and reported that hydrogen is essential for the atomization of arsine. The atomization of gaseous hydrides in a heated quartz cell is caused by collision with H radicals which are generated by a reaction with O₂ at elevated temperatures. The effect of temperature is more if the O₂ concentration is very low. In the absence of H₂ although arsine is decomposed in a quartz cell it is not atomized. They have also demonstrated that the surface characteristics also play important role in atomization via generation of H radicals by unsaturated oxygen atoms at the surface. They generalized the atomization mechanism as follows:



:



In 1997, Johansson et al. [45] investigated the spatial distribution of lead atoms along the cross-section of QTA to elucidate the mechanism of alkyllead. They found that the diameter of the quartz atom cell is important for the distribution of atoms. Furthermore, H₂ and CO are found to be equally efficient in promoting the atom process. Therefore it has been suggested that in reducing environment, hydrogen radicals are not essential for atomization of alkyllead and the atomization is a thermal process.

In 1999, a direct method for the detection of hydrogen radicals in an analytical H₂/O₂ flame was developed and the decline and consumption of hydrogen radicals by As species introduced into the flame were monitored by electron spin resonance (ESR). It was the first study for the observation of H radicals in the flame and the experimental results supported the atomization mechanism by H radicals [46].

1.1.2.7 Interferences in HGAAS

The separation of analyte from matrix by hydride generation provides spectral interference free measurements. Although some molecular emissions may be observed, these are few, no line interferences occur at all [5]. Non-spectral interferences may appear in solution phase or in gaseous phase. Liquid phase interferences are caused by the interfering species in the sample solution. Interferent may affect the rate of hydride generation or decrease the release efficiency. If the interferent is volatilized together with analyte, it may affect the analytical signal during transportation or in the atomizer. The most frequently encountered and extensively studied interference is matrix interferences due to inorganic compounds. The basic mechanisms of these interferences are categorized by Dědina and Tsalev [5]. The ionic analyte may react with the ionic interferent or the newly formed compound by the reaction of interferent and reductant. Another possibility is that, the generated hydride may be captured by

the ionic interferent or the compound by the reaction of interferent and reductant. The last way of interference in the liquid phase is the consumption of reductant by the interferent so much that the remaining reductant would not be sufficient for the effective reduction of analyte.

Significant interferences are observed in the presence of strong oxidants, transition and noble metals and the other hydride forming elements. The interferences by the transition and noble metals are the mostly pronounced and thus extensively studied ones. Dilution of sample solution partly minimizes the interference but the sensitivity is degraded [5]. The interferent ion may be separated from the solution using appropriate methods [47, 48]. Masking agents, which bind interferent to a non-reactive form, are effective to remove both hydride-ion and hydride-product interferences [49].

1.1.3 Electrothermal AAS

Electrothermal AAS, due to its high sensitivity and specificity, is one of the most promising methods for the determination of trace elements. In this technique, usually the graphite tube and rarely metal atomizers which are heated electrically to high temperatures, serve as atomizers. Metals such as W, Mo and Ta, have also been used as atomizers for many years but not been widely commercialized yet. Since ETAAS allows gas, solution, slurry or solid sample introduction, it is widely used in the analysis of environmental and biological samples. After the sample is dried, an ashing procedure is applied to remove matrix for interference-free atomization, the temperature increased rapidly by applying a high voltage to both ends of the sample cuvette and the atomization is achieved.

1.1.3.1 Graphite Atomizer ETAAS

L'vov was the first person who used an electrically heated furnace for the atomization and published his works in 1959 [1]. The temperature can be increased up to 2900 °C at a rate of 2-4 °C/ms. Since the nebulization is eliminated and residence time of the atoms in the graphite tube are longer than FAAS, the sensitivity is usually about 2-3 orders of magnitude higher than that obtained by FAAS.

Matrix interferences are usually the main problem encountered in GFAAS due to small dilution of sample matrix during atomization. Thus the ashing step is one of the most critical steps in ETAAS. The purpose of ashing is to remove most of the constituents injected without losing analyte; i.e. to leave the analyte at the atomization step with a minimum of matrix elements. Another important consideration is *isoformation*; all the analyte species in the sample must be turned into the same form before atomization. During the determination of volatile elements, chemical interferences often occur in graphite furnaces due to co-volatilization of the analyte with matrix constituents in the ashing step. In those cases, usually matrix modification by the addition of chemical modifiers such as MgNO₃, Ni(NO₃)₂, Ir, platinum group metals (PGM) and carbide forming elements such as W, Zr is required [1]. The purposes of matrix modification are 1) to decrease analyte volatility to prevent losses of analyte during pyrolysis, 2) to volatilize matrix elements to prevent interferences during atomization, 3) transformation of all chemical forms of analyte into one form to atomize them at once (*isoformation*) [50]. High cost of instrument when compared to FAAS is the other disadvantage of this technique since it requires a complex and powerful heating system. Consumables such as graphite tubes are also cost effective. The technique has rather poor speciation capability and low sample throughput. When compared to metal atomizers, GF-ETAAS has the disadvantage of requirement of an external cooling system after each atomization. In last two decades, ETAAS

systems have been used as ETV devices for the sample introduction systems prior to other determination techniques such as ICP-AES and ICP-MS.

1.1.3.2 Metal Atomizer ETAAS

Although the most common atomizer in ETAAS is graphite tube, the limitations such as need for a high power supply and difficulties in the determination of elements that form refractory oxides and carbides, have led to the development of many metal atomizers [51]. Among the metal atomizers, tungsten has been the predominant atomizer. In recent years, tungsten coils or tubes have been used as an alternative atomizer to the graphite tube in the determination of elements by ETAAS [52, 53]. Their use has been extended to ETAES, ETA-LEAFS as atomizer and ICP-AES as vaporizer [54, 55]. The W devices used in atomic spectrometry as atomizers or vaporizers are summarized in a recent review [51]. The other metals used as atomizer in ETAAS are tantalum [56], molybdenum [57] and platinum [58].

Tungsten has the highest melting point (3410 ± 20 °C) among the elements in the periodic table [59]. In addition, it has good electrical conductivity and may be formed into different shapes reproducibly. Tungsten atomizers or vaporizers are designed in different shapes including wire, ribbon, boat, foil, tube or coil. Among them tungsten coil and tube are the most commonly used form of the metal. The metal is relatively inexpensive and commonly used as filaments in ordinary electrical bulbs. Beside these, tungsten is relatively inert, stable in air and water, and resistant to high concentrations of common acids such as hydrochloric, sulfuric and nitric acids under normal temperature and pressure [51].

The main advantages of W coil atomizer over graphite atomizer is that it needs a relatively simple power supply compared to rather complicated and bulky power

system used to heat high mass graphite rapidly [51]. Besides, it enables the determination of elements that form refractory oxides and carbides [1]. In addition, the rate of heating for W-coil (30 K/ms) is about 10 times faster than that of graphite tubes (2-4 K/ms) [60]. Another advantage is the adaptability to portable instrumentation [61]. It does not need an extra cooling system that is a requirement for GF ETAAS, the cooling by purge gas is enough. These properties provide an advantage of alternative atomizer to graphite atomizers or vaporizers in ETAAS. However, at high temperatures, tungsten is easily oxidized in the presence of O₂ and a reducing environment is required. In order to prevent oxidation, the metal is purged with a mixture of hydrogen and argon during the atomization or vaporization of analyte [51].

A temperature of 3300 °C, which is high enough for the efficient atomization of most of elements, can be reached by a simple commercial W coil by applying a current of 10 A. Tungsten atomizers can be used for the determination of all the elements that have been determined by GFAAS except Mo which can present as impurity in the W metal [51]. Recently, W coil atomizer has been employed for the atomization of hydrides. Ribeiro et al. utilized W coil atomizer placed in quartz T-tube for the atomization of Bi and As that were introduced as their hydrides [62, 63].

1.2 Preconcentration Methods

The detection of ultra-trace amounts of analyte in samples requires high sensitivity and low limits of detection which can not be attained by using ordinary techniques. The analyses of samples where the analyte concentration is low and the matrix have a depression effect on analytical signal require preconcentration and / or matrix separation methods. In preconcentration methods the analyte in a defined volume of sample was concentrated before the achievement of analytical signal.

The preconcentration can be applied directly to the sample prior to determination step or just before achievement of analytical during the determination. The most popular preconcentration methods from liquid phase are evaporation of solvent, liquid phase extraction, solid phase extraction and ion exchange; these can be applied on line or off line. In these classical methods, the analyte in large volumes of sample are collected on an adsorbing media or extracted to another phase and then dissolved or back-extracted into a small volume of solvent. The preconcentration factor is simply the ratio of volume being collected to final volume if the recovery is 100%.

The electrodeposition on high melting point metals has also been used for both preconcentration and then atomization in a number of investigations. The use of W wire for electrochemical deposition and then ETAAS determination was proposed by Lund and Larsen for the first time [64] and applied for the determination of Cd in sea water [65]. Then they replaced W wire with Pt wire for the determination of Cd in urine samples [66]. In these methods metal wires served as the atomizer. Czobik and Matoušek [67] used W wire for the electrodeposition and subsequently placed in graphite furnace atomizer for the determination of Ag, Cd, Cu, Pb and Zn. Wolff et al. [68] reached a detection limit of pg/g level for Cd, Cu, Pb and Zn using a tungsten wire for electrodeposition and subsequent atomization in graphite rod atomizer. Recently, Barbosa et al. [69] developed a method of *in-situ* and on-line electrochemical preconcentration on W-coil for the determination of Pb by ETAAS. In another study, a Mg-W cell was used for the electrochemical deposition of Bi on W wire and the atomization from the electrode surface inserted into graphite furnace [70].

Cryogenic trapping is widely used for preconcentration of gaseous analyte species and have been used extensively in HGAAS studies. Nowadays the most popular preconcentration method for volatile hydrides is *in-situ* trapping in atomizers. In recent years this method has appeared to be a powerful preconcentration method

since it provides significant enhancement in relative detection power and the sensitivity. In addition to atomizers, the volatile species have also been collected on ETV devices for subsequent detection by other detection systems than AAS.

1.3 *In-situ* Trapping Techniques

In-situ trapping are nowadays one of the most popular preconcentration methods for the determination of elements that can be volatilized by vapor generation methods. The most common one is the preconcentration graphite tubes. The graphite tube is used for the thermal decomposition of volatile hydride and trapping analyte species in the tube thereby affecting a clean separation from the matrix before atomization as well as preconcentration [71]. In this technique, the advantages of both vapor generation and graphite furnace ETAAS are combined [6]. The analyte is separated from the matrix by vapor generation and detected by a powerful ETAAS. The advantages provide enhancement in the relative detection power over conventional batch or continuous HGAAS. The effectiveness of the method depends on the hydride generation, transportation and the collection efficiency. There is large number of reports on the successful application of this method for the determination hydride forming elements [71].

The method of collection of vaporized analyte species in atomizer and the subsequent atomization was described first described by Drasch et al. [5]. He used commercial graphite furnaces as a trapping medium and also as the atomization cell. Lee was the first to utilize this technique in the form as practiced today on carbon rod atomizer [72]. He showed that 72 % of the generated Bi was captured in the graphite rod atomizer; 85% of which is collected on the supporting electrode; only 15% of the collected amount is in the carbon rod cell. Sturgeon et al. found that the generated stibine is trapped on partially scrapped pyrolytic graphite tube, with an efficiency of 84 % [73].

In-situ trapping in graphite tubes suffer from a number of disadvantages including need for a well developed porous graphite structure, high deposition temperatures for some elements (As, Sn) and little chance of multielement detection due to different hydride generation and collection conditions. The trapping efficiency of graphite tube can be increased by coating the graphite surface by carbide forming elements [74] or platinum group elements (PGM) [75] since the analytes are trapped on those surfaces by chemical interactions. The coating material can be applied as a mixture as well as alone. Usually the trapping on such coated surfaces requires lower trapping temperatures. Use of coating material may also enables multi-element determination; using appropriate coating material, more than one element can be collected under the same conditions.

Sturgeon et al. compared the stabilization effects of platinum group metals (PGM) for As Sb Se Bi and Sn, and mentioned that the effect of PGMs is catalytic decomposition due to their affinity for H₂ and Pd has the most stabilizing effect over others [75]. Li et al. also stated that coating with Pd significantly increases the trapping efficiency and reduces the trapping temperature for As Sb, Se [76] and Bi, Ge and Te [77]. However Pd as a coating material is not permanent and must be injected before each collection atomization cycle.

In contrast to Pd coating which must be repeated before each trapping, Ir coating is stable if the temperature does not exceed 2300 °C. Carbide forming elements such as tungsten and zirconium also increase the trapping efficiency in the graphite furnace. Liao and Haug studied the trapping efficiency of graphite tubes coated with carbide forming elements (Zr, Nb, Ta, W) and noble metals (Ir, Ir/Mg, Pd/Ir) for Se, Te [78], and As, Sb and Bi [79]. They showed that Ir/Mg coated tubes traps Se and Te better than Ir coated tubes. Because of high sensitivity and better long term stability, Zr-coated graphite tubes are recommended for the trapping and concentration of As, Se and Bi. Tsalev et al. [74] evaluated the performance

characteristics of Ir-Zr- and Ir-W- treated platforms in an automated FI-HG-ETAAS system and found that Ir-Zr treated platforms are more suitable than those treated with Ir-W for trapping hydrides. Beside increase in trapping efficiency and higher sensitivity, the use of modifiers provide simultaneous multielement determination with a multichannel spectrometer. Garboś et al. [80] developed a method for the determination of As and Se by trapping their hydrides and detection with a multichannel AAS simultaneously; resulted in doubled sample throughput. Murphy et al. [81] used Ir coating for the simultaneous determination of Bi and Se after preconcentration on Ir coated graphite tube.

Although there are many reports on *in-situ* trapping in graphite tubes, use of W atomizer for *in-situ* trapping of volatile analyte species have appeared in limited number of studies. In a recent work, Dočekal and Marek [82] studied the trapping hydrides of Se and As in a tungsten tube atomizer and showed that when coated with Pt, Ir or Re, the trapping efficiency of tungsten atomizer increases significantly. The most efficient trapping approaching to 100% was observed at trapping temperatures of 100-200 °C when the W tube was treated with Pt. The collection temperature on Ir and Re coated tubes was as high as 700-900 °C and the trapping efficiency was only 10%. In another study, Rh coated W coil atomizer was also used for *in-situ* trapping of selenium hydride [83].

1.4 ETV Techniques

Scientists have been interested in developing better sample introduction methods for spectroscopic techniques in order to achieve highest efficiency. Various methods have been used as sample introduction techniques to the atomization or ionization sources. The most common method is pneumatic nebulization. Different designs of nebulizers have been discussed and each type presents different advantages and limitations [3, 4]. In addition, hydride generation and liquid

chromatography have also been used as sample introduction methods for ICP-OES and ICP-MS as well as AAS. Although transport efficiency of hydride generation approaches to 100%, it can be applied to a limited number of elements that form volatile hydride. Laser ablation (LA) has also been employed for the introduction of solid materials to high temperature ionization sources.

In recent years, ETV has become an important tool for the sample introduction to independent detection systems especially for ICP-AES or ICP-MS. In ETV the sample was introduced to the measurement unit by vaporization in ETV device. It provides effective matrix removal and high transport efficiency. Its main concern is in plasma spectrometry since matrix problems appeared commonly in plasma spectrometry such as change in plasma conditions and isobaric interferences due to the plasma gas and concomitant elements. The advantages of ETV making it an attractive tool for sample introduction method to the ICP-OES or ICP-MS are summarized in ref [84, 85]. The sample introduction efficiencies are increased and thus required sample volume is minimized. Matrix and isobaric interferences due to the elements are reduced by applying appropriate sample pretreatment procedures. The rate of sample introduction can be achieved by varying the heating rate of ETV device. In addition, solid or slurry sampling is possible with ETV. The direct production of an analytical signal from a solid sample offers a number of important advantages resulting from the elimination of dissolution step; short analysis time, less contamination risk, enhanced sensitivity and limit of detection smaller amount of sample and no need to use hazardous chemicals [86]. The most widely used one is the graphite tubes. Metal atomizers have also been employed in ETV methods.

1.4.1 ETV with Graphite Vaporizers

Graphite furnaces used in GF-ETAAS are the predominant types of ETV devices [87]. Electrothermal vaporization on GF as a sample introduction method have

been studied and used for more than 20 years. The main disadvantage of this method is the losses of analyte during transportation to the detection system by a carrier gas. It was clear even early stages that the mass transport is not quantitative and significant fraction of analyte did not reach to the measurement system [88]. The appearance of nonlinear calibration curves obtained was an indication of losses during transportation. Schäffer and Krivan showed that the majority of analyte losses occurred due to condensation on the colder ends of the graphite tube, end cones and the interface between ETV and detection system. [89].

Kantor first used the theoretical prediction of analyte vapor from the ETV to the plasma [90]. The efficiency is dependent on the formation of stable nuclei of size exceeding critical diameter. For higher analyte masses the critical diameter decreased and the transport efficiency increased. It is assumed that the presence of particles acting as condensation and adsorption nuclei can enhance the transport efficiency.

Studies on the improvement of transport efficiency have been focused on the use of carriers. In order to increase transport efficiency, various modifiers were added to the sample in the graphite tube and the transport efficiencies increased when nanograms of samples are co-vaporized with micrograms of added modifiers. The suggested modifiers include palladium, carbon, sodium chloride and magnesium nitrate [91]. The use of halogenation by halocarbons added to the sample matrix has also been investigated and found to be effective to assist the vaporization of low volatility analytes. However they have the adverse affects of low atomization efficiency in low temperature sources and isobaric interferences in ICP-MS [87].

ETV devices can also be used as a trap device for hydride preconcentration. Uggerud and Lund [92] used ETV-ICP-MS following *in-situ* trapping of the hydrides of Sb and As on Ir and Pd modified graphite furnaces. Matusiewicz and Koprás applied ETV-MIP-OES method for the simultaneous determination of

hydride forming elements and Hg after *in-situ* trapping on modified graphite tubes [93]. Chang and Jiang developed a method for the determination of Bi by ETV-ICP-MS after preconcentration of its hydride on platinum coated graphite tube [94]. Matoušek et al. investigated the mechanism of trapping and desorption of volatile hydrides and mercury in modified graphite furnace and detection by ICP-MS [95]. It has been found that the adsorption of arsine on Pd-Ir was interpreted in terms of initial physisorption followed by chemisorption.

1.4.2 ETV with Metal Vaporizers

Besides the graphite furnace, tungsten vaporizers commonly in the form of boat and coil have been used as ETV devices for liquid, solid and slurry sampling for the sample introduction to independent sources as reviewed in a recent paper [51]. Two main advantages of W over graphite in the area of ETV-ICP-MS are the elimination of isobaric interferences due to the presence of carbon in the plasma e.g. ^{52}Cr and $^{40}\text{Ar}^{12}\text{C}$, and restrictions to vaporization temperatures below 2600 °C [51]. In 1988 some rare earth elements were determined by W-coil ETV-ICP-OES and it was found that the sampling efficiency and thus the detection power were improved by two orders of magnitude when compared to nebulization ICP-OES [96]. Barth et al. determined 15 trace elements in silicon carbide, silicon dioxide and silicon nitride using W-coil ETV-ICP-OES [55]. They coated the W coil with W-carbide to reduce the ablation of tungsten during vaporization and reported the transport losses of the elements that ranged between 7% for La and 54% for Cu. Levine and Wagner determined 10 elements in peach leaves and oyster tissue samples using an ETV-ICP system employing a CCD detector. Their LOD values are at picogram levels [97]. Shibata et al. used liquid sampling W furnace ETV-ICP-MS for the determination of 14 rare earth elements; obtained limit of detection values are at lower femtogram ranges for 20 µl sampling amounts corresponding 0.1-0.6 ng/L in solution [98]. Hauptkorn et al. used slurry sampling

ETV-ICP-MS for the detection of 14 elements in high purity quartz and reached a detection limit of 2 ng/g levels for Li and U [99].

It has been shown that by applying a temperature program for W-coil ETV device some spectral interferences may be eliminated and low resolution miniature CCD spectrometer can be used to achieve similar LODs compared to those by traditional large monochromator ICP-AES [54].

Okamoto et al. developed a method of W boat-ETV-ICP-MS and applied successfully for the determination of Pb in biological and rock samples [100, 101].

The use of W coil as an ETV for the sample introduction to AAS is rather rare when compared to ICP-MS detection. Bruhn used the method for the detection of elements with low atomization temperatures. The attained LODs were 100, 6, 80, 50 and 2 pg for Bi, Cd, Pb, Tl and Zn respectively [102].

The use of metal vaporizers for the preconcentration of hydrides is relatively new and few studies appeared in recent years. Osama [103] used Pt coil for the sequestration of volatile Cd species. Then the collected species were vaporized by heating Pt coil and transported to unheated quartz T-tube atomizer for AAS detection; high sensitivity and low limit of detection close to ETAAS values were obtained. The use of W coil as an ETV for trapping hydrides and then transportation to AAS, that is a part of this thesis, was described for the first time and published in 2002 [104]. Very recently, Dočekal et al. used Mo foil strip for trapping As and Se hydrides and subsequent electrothermal volatilization to flame for AAS detection [105]. They reported that the trapping temperature for the analytes are significantly higher than that of reported for W coil atomizer. Guo and Gou [106] used gold wire placed in the inlet arm of a quartz T-tube as a trapping medium for selenium hydride. In addition to Au, some other metals in the form of wire, foil or strip were also tested but these attempts were not successful except Ta

which is not preferred since it became very cracky due to the reaction with H₂ used for the transportation of volatile species. In this study, differing from the others, the trapping material was heated externally with a Ni-Cr wire so that the transient signal was completed in about 12 s.

1.5 Individual Elements

1.5.1 Bismuth

1.5.1.1 Importance of Bi

In recent years, Bi became an important element due to its chemical and physical properties. The earliest use of Bi compounds in medicine appears to have been in the middle ages. In 1786, it was administrated first for the treatment of dyspepsia. In 1889, it was discovered that Bi might be useful as an antisyphilitic agent [107]. In modern pharmacy, it has been used for clinical and medical purposes for about 70 years for the treatment of syphilis. Since then, its pharmaceutical uses expanded to antacids, peptic ulcer treatments and topical dermatological creams [1, 108]. Recently, the effectiveness of Bi has been attributed to its antibactericidal action against helicobacter pylori which was discovered in 1983 and may well initiate the ulcer formation by excreting acid [109].

Bismuth has also been used in metallurgy, iron casting, electrochemistry, plastics and pigments, lubricants and cartridges [110]. The presence of trace amounts of Bi may influence several characteristics of different metallurgical materials affecting physical, mechanical and magnetic properties depending on its concentration and the composition of the material [62]. The presence of the metal in alloys even at

very low concentrations changes the characteristics of the metal. Bismuth promotes iron carbide stabilization during the solidification process when added to steels. On the other hand, even small amounts of this element may produce a decrease in hot ductility, workability and cause the rupture of alloys and steels [111].

A number of toxic effects in human and animal have been attributed to Bi compounds such as osteoarthropathy, hepatitis and neuropathology [70], encephalopathy and nephrotoxicity [112]. In a recent study, it has been shown that oral dosing with Bi compound is followed by Bi entering the nervous system of mice with a particular predilection for motor neurons and it has been suggested that Bi needs to be included in the list of potential toxins that enter motor neurons [113].

Due to low abundance of Bi in the Earth's crust, about 0.00002% and limited absorption and its poor solubility compounds, the determination of Bi in environmental and biological matrices require sensitive techniques. Furthermore, since the usual level of Bi in biological and geological materials are $\mu\text{g/g}$ or ng/mL , usually the separation and preconcentration methods are required.

1.5.1.2 Determination of Bi

The techniques mostly used among the applications for trace Bi determination are ICP-MS, ICP-AES and ETAAS. Schramel et al. determined Bi in urine with a LOD of 5 ng/L [114]. Li et al. described a sensitive method of determination by direct injection nebulization ICP-MS [115]. Moyano et al. used FI-ICP-AES with ultrasonic nebulization for the determination of bismuth in urine samples after column preconcentration [116]. Burguera et al. [108] and da Silva et al. [117] used on-line separation and preconcentration methods for bismuth and then determined by ETAAS.

1.5.1.3 Determination of Bi by Hydride Generation

Hydride generation method combined with AAS is currently one of the best methods for the determination of Bi in different matrices. The application HGAAS method goes back to early 70's. In 1973, Pollock and West developed a method of metal reduction procedure using TeCl_3 / Mg for the determination of Bi and obtained a LOD of 3.2 ng for 15 mL sample volume; first the hydride was collected in a pressure chamber and then send to flame via auxiliary air channel [118]. In the same year, Fernandez employed solid NaBH_4 pellets for the reduction of Bi using both collection in a balloon reservoir and achieved LODs of 5 ng for 20 mL sample volume, respectively [41]. Fleming and Ide [119] applied the method of HG using solid NaBH_4 and obtained an LOD of 1 μg Bi/g in steel. They investigated the interferences of some elements and reported that although Ni, Mo, Cu and Co did interfere in the absence of iron, the presence of iron eliminated the interference. Bedard and Kerbyson [120] used pressure concentration method for the determination of bismuth by hydride generation by eliminating the Cu interference by lanthanum hydroxide coprecipitation and reported that the collection time should not be very long due to the unstable nature of bismuthine at room temperature. Vanloo et al. [121] showed that Bi can be determined in steel and cast iron at $\mu\text{g/g}$ level accurately by HGAAS using aqueous sodium tetrahydroborate as reductant and heated QTA as atomizer. In 1982 Aöstrom [122] developed an FIA system with a quartz atomizer where the analyte solution of 0.700 mL was injected into a continuous flowing stream of HCl solution. Under the best conditions, a limit of detection of 0.08 ng/mL was obtained. Cadore and Baccan suggested use of thiourea-KI for the minimization of interference from some trace elements [111]. Moyano et al. [123] used an on line column preconcentration and hydride generation ICP-AES method for the determination in urine.

Atomic fluorescence and plasma atomic emission spectrometries have also been employed for the detection of volatilized Bi species. Feng and Fu [48] determined Bi and 4 more hydride forming elements in nickel metal by HGAFS after coprecipitation with lanthanum hydroxide. They reported that five elements can be coprecipitated quantitatively and separated from nickel matrix.

In recent years the studies have been focused on the development of *in-situ* preconcentration methods for the determination of Bi. Matusiewicz et al. [124] obtained a detection limit of 0.020 ng/mL Bi for a sample volume of 5 mL by using HG-ETAAS with *in-situ* preconcentration in graphite tube. Murphy et al. [125] developed a multielement detection method for the hydride forming elements including Bi after *in-situ* collection on Ir treated graphite tubes. A limit of detection of 40 ng Bi/L was achieved for 0.500 mL sample volume. Chang and Jiang [94] used vapor generation graphite furnace ETV-ICP-MS for the determination of Bi and obtained a detection limit of 0.003 ng/mL Bi for 2 mL sample volume.

1.5.2 Cadmium

1.5.2.1 Importance of Cd

Cadmium occurs as a constituent of lead and zinc ores, from which it can be extracted as a byproduct [126]. It is one of the rarer metals which makes up about 0.00005% of the Earth's crust. It is distributed on the land as a consequence of emissions from industrial and waste incineration plants, and coal fired power plants. Concentrations of Cd as high as 500 mg/kg have been reported in soils near mines and smelters. About one third of the cadmium production is used in

manufacture of batteries, paints, plastics, and in metal plating processes. It is also used as an anticorrosive element for some metals [1, 127].

The toxic nature of Cd was revealed in 1900 and its compounds are also known to be toxic. The essentiality has not been proved yet for the adult human body which contains about 30 mg of Cd. It is a highly cumulative poisonous metal with an estimated biological half life of 20-30 years in humans. About half of body burden of Cd is found in the liver and kidney. It affects several enzymes in the body [126]. Cadmium can cause high blood pressure, kidney damage and sterility among males. Long term exposure can cause bones to become brittle. It was reported that in the 1950's, about 100 people died in Japan due to Cd poisoning caused by the consumption of rice grown on the Cd contaminated soil. Since carcinogenic potential is expected, Cd and a number of its compounds are included the list of elements whose concentration must be controlled at the workplace [1, 127].

1.5.2.2 Determination of Cd

Cadmium can be easily determined by air/acetylene flame with a characteristic concentration of 0.02 mg/L [1]. Because of high toxicity of this element at low concentrations, more sensitive techniques are required at trace and ultra-trace determinations in environmental and biological samples.

ETAAS is one of the most powerful methods for the determination of Cd at sub ng/mL level. The greatest difficulty in the determination by GFAAS is the high volatility of Cd. Use of modifiers such as Pd, Ir, Mg and some ammonium salts have been suggested to provide efficient removal of matrix prior to atomization. Lückner et al. used solid sampling ETAAS for the determination of Cd in kidney [128]. ETAAS with W coil atomizers have also been employed for the determination of Cd in mussels [129], in hair and blood [130]. Hirano et al.

developed an FI on-line preconcentration GF-ETAAS method for Cd by collecting on a imminodiacetate type resin and reached a detection limit of 0.2 ng/L using 12 mL sample volume [131].

1.5.2.3 Determination of Cd by Hydride Generation

The first report on the preparation of very unstable cadmium hydride appeared in 1951; cadmium hydride was synthesized in an organic medium at $-78.5\text{ }^{\circ}\text{C}$ at which no evidence was observed for the decomposition [39]. In 1989, D'Ulivo and Chen [132] demonstrated that Cd can be determined by AAS after vapor generation in aqueous solution by using sodium tetraethylborate. In the same year, the determination of Cd using HGAAS and heated QTA was reported for the first time by Cacho et al. [27]. The volatile species, probably hydride, were generated in an organic media. The rate of hydride generation can be increased by the addition of diethyldithiocarbamate (DDTC) and increasing temperature. After 4 years, Valdés-Hevia et al. [133] proposed a method for the hydride generation with sodium tetrahydroborate and ICP-AES detection; limit of detection attained was 1 ng/mL. Ebdon et al. [134] used atomic fluorescence spectrometry for ultra-trace detection of volatile Cd species generated by the reaction with tetraethylborate.

In 1995, two independent groups showed that the generated volatile species by the reaction with sodium tetrahydroborate are unstable and decomposes quickly at room temperature [7, 28]. Decomposition yields free atomic Cd vapor which can be determined by using an unheated atomizer similar to the one used for the determination of Hg by CVAAS [7, 28]. The sensitivity of cold vapor system is found to be higher than that of heated QTA since the residence time of the atomic species in the atomizer is less in heated QTA due to thermal expansion [7].

Literature data reveal much inconsistency and contradictory statements for hydride generation conditions of Cd, probably because of the inherent instability of its hydride and difficulties with generation, stripping off solution and transportation of volatile species to the atom cell. The generation process, efficiency of hydride release and the transport processes are highly sensitive. Usually high concentrations of NaBH₄ are required and the concentration of HCl is very critical [135]. The design of GLS is also critical and the sensitivity is much more effected when compared to other hydride forming elements (HFEs). It is reported that even no signal was obtained using conventional U type GLS. [136]. Feng et al. investigated the effect of surface of GLS and showed that when Ryton (a sulfur containing polymer) GLS was used, the atomic Cd species are adsorbed by S containing groups and no signal was obtained when the atomizer was at room temperature [137].

Guo and Guo [138] investigated the effect of some organic reagents, mainly nitrogen and sulfur containing ones on the hydride generation efficiency and found that the addition of 1% (w/v) thiourea and 1 µg/mL Co results in a significant enhancement in the fluorescence signal in the HGAFS determination of Cd. The enhancement in the signal was explained by the catalytic effect of these species in the hydride generation reaction. Hwang and Jiang [139] used VG-ICP-MS for the determination of Cd and found increased sensitivity when thiourea and cobalt were added as catalysts and supported findings of Guo and Guo. It was suggested that use of didodecyldimethylammonium bromide (DDAB) vesicles improve hydride generation efficiency for Cd and a 5 fold decrease was obtained in the LOD by ICP-AES [133]. In another study, 10 µg/mL Ni when added together with 1 % thiourea increased signal and reduced some metal interferences [136].

In recent years, the studies are focused on the *in-situ* trapping of volatile Cd species in graphite tubes and successful applications were carried out. Infante et al. showed that the Pd is an efficient coating material and increases the trapping

efficiency for the volatile species generated in vesicular media created by DDAB [140]. The same group compared the trapping efficiency of uncoated and Zr-, W- and Pd-coated graphite tubes and found that the Pd coating is superior to others offering enhanced LOD and precision [141].

Bermajo-Barrera et al. investigated the effects of different metals on the generation of volatile species and found that Ga, Si and Co increase the analytical signal. They also mentioned that by using Ir coated tubes and Ga as the catalyst, a characteristic mass of 3 pg and a limit of detection of 4 ng/L can be obtained [142].

In a more recent study by Lampugnani et al. [135], it is reported that none of the above mentioned catalytic species did enhance the analytical signal. Furthermore, it is noted that the addition of DDAB brought entailed problems with system washing between runs. It was also demonstrated that permanent coating with Zr-Ir and W-Ir was effective and straightforward for *in-situ* trapping in graphite tubes.

1.5.3 Lead

1.5.3.1 Importance of Pb

Lead is one of the rarer elements whose abundance in the Earth's crust is only 0.0018% [1]. Because of its low melting point and malleable properties, Pb is one of the metals used widely in early ages. Its use goes back to ancient Egyptians. Lead ranks fifth behind iron, copper, aluminum and zinc in industrial production of metals. About half of the lead is used for the manufacture of lead storage batteries. A quarter is used for chemicals such as tetraethyl lead and other organolead compounds. Other uses include solders, bearings, cable covers,

ammunition, plumbing, pigments and caulking [1, 126]. Lead compounds are also widely used as anti-knocking additives in gasoline. Lead chromate is a strong yellow pigment extensively used in yellow paints for road markers and as ingredient in many green paint and colored plastics [1].

Lead is a common atmospheric pollutant though much less so now since the use of leaded gasoline is being reduced. Anthropogenic emissions such as those from combustion of fossil fuels, waste incinerators and industrial emissions cause higher levels of metal pollutants including lead in the urban environment [143]. The absorption through the respiratory track is the most common route of human exposure. The greatest danger of pulmonary exposure comes from inhalation of very small particles of lead oxide and lead carbonates, halides, phosphates and sulfates. Lead can also enter into body by ingestion and resorption through the skin. Children are more sensitive to toxic effects of lead because they absorb more from soil and dust than adults absorb. Acute lead poisoning results in dysfunction in the kidneys, reproductive systems, liver, brain and central nervous system, resulting sickness or death [144, 145]. Of all the compounds, the trialkylated forms have the strongest neurotoxic effect for mammals. The recommended clinical test for assessment of exposure is the determination of lead in blood [1].

1.5.3.2 Determination of Pb

AAS is the most frequently used method for the determination of lead. It can be determined in the air acetylene flame largely free of interferences. Since it is highly toxic and often be determined in very low concentrations, limit of detection of 0.01 mg/L that can be achievable by FAAS is often inadequate. More sensitive methods are required [1].

Graphite furnace ETAAS is one of the most powerful and widely used techniques for direct determination of lead in blood [146]. Interferences that are partly dependent on the high volatility of Pb and on the influence of concomitants are eliminated with proper use of stabilized temperature platform furnace (STPF) [1]. The Pd-Mg modifier was found to be the best one which allows a pyrolysis temperature of 1200-1400 °C. However addition of modifier also increases the atomization temperature [1]. Correira et al. [147] obtained a detection limit of 9.3 pg using $\text{NH}_4\text{H}_2\text{PO}_4 + \text{Mg}(\text{NO}_3)_2$ mixed modifier allowing an ash temperature of 750 °C in the determination of lead in foodstuffs.

Tungsten coil ETAAS was also employed for the determination of Pb. Parsons et al. determined Pb in blood by using a W filament atomizer [148]. Rhodium was investigated as a permanent modifier for the atomization of Pb from biological fluids by W filament ETAAS. It has been found that Rh not only stabilizes Pb but also extends the life time of W coil from 60-70 to over 300 firings [149]. Wagner et al. [52] developed a method for the multielement determination employing an ETAAS with W coil atomizer. Four elements could be determined simultaneously by a CCD spectrometer using near line background correction. In another study the tungsten boat was used as boat digestion vessel and electrothermal vaporizer, and then the detection was carried out by ICP-MS; achieved a detection limit of 5.2 pg of Pb corresponding to 10.2 ng/g in solid sample [100].

Czobik and Matoušek [67] used a preconcentration method of electrodeposition of lead from aqueous solution on W wire. Then they inserted the W-coil into graphite furnace and obtained the analytical signal. The characteristic concentration of lead was 0.15 µg/L for 5 min electrodeposition. Barbosa et al. used electrochemical on-line preconcentration method. However in their system the W coil served as both trapping medium and atomizer [69].

1.5.3.3 Determination of Pb by Hydride Generation

Lead can be determined by HGAAS but has some difficulties with the hydride formation. Lead hydride PbH_4 is unstable at room temperature and has a boiling point of approximately -13°C [5]. Thompson and Thomerson published the first report on lead hydride generation for analytical purposes by the reaction of acidified sample solution with sodium tetrahydroborate, but the efficiency was poor [150].

The generation efficiency of plumbane by direct reaction of acidified solution with tetrahydroborate is very low presumably because of the very low redox potential of the $\text{Pb}^{2+} / \text{PbH}_4$ pair. Use of oxidizing agents such as dichromate or hydrogen peroxide increased the generation efficiency presumably by the formation of meta-stable Pb(IV) whose reduction is thought to be easier than that of +2 valance state [5]. A linear relationship was observed between the logarithm of absorbance and the redox potential of oxidants [5]. A variety of oxidizing agents were tried in order to increase efficiency. In 1976, Fleming and Ide [119] reported that use of $\text{K}_2\text{Cr}_2\text{O}_7$ -tartaric acid reaction medium increases the generation efficiency significantly. They also noted that more $\text{K}_2\text{Cr}_2\text{O}_7$ is required in the presence of iron and it must be added to the analyte solution just before the measurement. Use of H_2O_2 in nitric or perchloric acid was suggested by Vijan and Wood [151]. Jin and Taga [47] compared hydride generation efficiencies and the selectivity of three different media, and found that peroxodisulfate-nitric acid was the most efficient medium for PbH_4 generation among $\text{K}_2\text{Cr}_2\text{O}_7$ -malic acid, HNO_3 - H_2O_2 and $(\text{NH}_4)_2\text{S}_2\text{O}_8$ - HNO_3 but it gave high blank values and poor selectivity; more effected by concomitant elements. In 1985, Thao and Zhou proposed a method of plumbane generation using $\text{K}_3\text{Fe(CN)}_6$ - HCl medium and achieved a detection limit of $0.37 \mu\text{g/L}$ in food samples [152]. Li et al. [153] obtained the most sensitive hydride generation in 0.3% w/v oxalic acid and 3% w/v $(\text{NH}_4)_2\text{Ce(NO}_3)_6$ among

other media however the concentration of tetrahydroborate as potassium salt needed was very high, 8% (w/v).

Use of nitroso-R salt (1-nitroso-2-naphthol-3,6-disulfonic acid, disodium salt) was suggested by Zhang et al. [154]. They found improved sensitivity compared to those obtained using peroxodisulphate, dichromate or hydrogen peroxide as oxidants. It was proposed that the mechanism of reaction involved the oxidation of lead(II) to lead (IV) while chelated with nitroso-R salt. Chen et al. investigated a series of 22 organic chelating reagents including nitroso-R salt. 1-(2-pyridylazo)-2-naphthol-6-sulfonic acid (PAN-S) was also found to be as effective as nitroso-R salt although it is not an oxidizing agent [155]. The increase in the efficiency was explained by the formation of a chelate between Pb(II) and PAN-S rather than the formation of metastable Pb(IV) formation. The use of persulfate as oxidizing agent in FI HG of Pb was reported by Samanta and Chakraborti [156].

Although potassium hexacyanoferrate(III) is a mild oxidizing agent ($E^\circ = 0.36 \text{ V}$) when compared to other reagents H_2O_2 ($E^\circ = 1.78 \text{ V}$), potassium dichromate ($E^\circ = 1.33 \text{ V}$) and $(\text{NH}_4)_2\text{S}_2\text{O}_8$ ($E^\circ = 2.01 \text{ V}$) it is found to be more effective in the hydride generation of lead [157-159]. Therefore, the efficacy of hexacyanoferrate suggests that a mechanism other than oxidation is occurring to generate plumbane generation similar to the case of PAN-S.

The HG technique has also been coupled with plasma spectrometry for the determination of lead. In 1981, Ikeda et al. [160] used HCl- H_2O_2 medium for the generation of plumbane and then detected by ICP-OES. High blank signal equivalent to that of 2 ng/mL Pb was observed. Li et al. [161] determined Pb by HG-ICP-MS using oxalic acid-ammonium cerium nitrate-sodium tetrahydroborate system having a detection limit of 7 ng/L. They mentioned that some interferences were minimized with the help of masking effect of oxalic acid. Chen et al. [162]

who also reported the masking effect of oxalic acid against the interferences employed potassium hexacyanoferrate (III) medium and ICP-MS detection system.

In-situ trapping techniques were successfully applied for the determination of lead after hydride generation. Bermejo-Barrera et al. [163] investigated the effect of Ir, Zr, and W as coating materials for graphite tube and found that Ir is better when compared to others and effective trapping was achieved at room temperature, 20 °C. They used HCl/H₂O₂ medium for HG and obtained a detection limit of 60 ng/L with 0.500 mL sample volume. Tyson et al. [159] used hexacyanoferrate and obtained a detection limit of 0.03 µg/L with purified hexacyanoferrate after *in-situ* trapping on Ir coated L'vov platform at 300 °C.

According to research results obtained in our laboratory, silica is also capable of trapping hydrides when heated to moderate temperatures. It has been shown that the silica surface can be used as a trapping medium for the determination of Pb and thus significant enhancement in the sensitivity and detection limit was achieved [164].

Besides hydride generation, ethylation was also used for the generation of volatile Pb species. Rapsomanikis et al. [11] described the speciation of dimethyl and alkyllead species using chromatographic separation and then detection by AAS after ethylation with sodium tetraethylborate. Sturgeon et al. [12] used sodium tetraethylborate for the generation of tetraethyl lead and then determined using ETAAS after preconcentration in graphite tube heated to 400 °C. They reached a detection limit of 1 ng/L.

1.6 The Aim of the Study

The determination of metals at trace and ultra-trace levels is important in environmental, biological and metallurgical samples because of their toxic effects or critical concentration ranges. The sensitivity that is attainable by FAAS, conventional HGAAS and even ETAAS sometimes may not be enough for such analyses. Although ICP-MS systems offer high sensitivity and very low detection limits, they suffer from interferences due to high solid contents. Furthermore these instruments are not accessible in all laboratories due to high costs and also high expense of its consumables. Therefore alternative methods which are accessible, easy to use, providing high sensitivity and low limits of detection with a minimal cost of both instrumentation and consumables are needed.

Hydride generation combined with atomic absorption or emission spectrometry is a powerful method for the determination methods for hydride forming elements. The sequestration of hydride forming elements on heated graphite surfaces is a widely used technique for common hydride forming elements. In recent years, metal atomizers, mostly coiled W, has gained its importance against the graphite atomizer.

The purpose of this study is to develop on-line preconcentration methods for the determination of hydride forming elements. The method involves the separation of analytes, Bi, Pb and Cd from sample matrix as their volatile species by chemical vapor generation. Volatile species are preconcentrated on heated W-coil followed by revolatilization and transportation to quartz T-tube. The developed method is simple to apply. Due to its low cost, it can be applied in any instrumental analysis laboratory having a simple FAAS instrument.

CHAPTER II

EXPERIMENTAL

2.1 Instrumentation

A Philips Pye Unicam (Cambridge, UK) PU9200 atomic absorption spectrometer equipped with deuterium background correction system was used for absorbance measurements. The instrumental parameters for the elements investigated are given in Table 2.1. The hood of spectrometer was connected to an Elicent AXC 315/A (maximum suction rate is 1300 m³/h) channel fan equipped with an Elicent (Lonato, Italy) speed regulator. Quartz T-tube either heated by stoichiometric air/acetylene flame for Bi and Pb or kept at room temperature for Cd was used as atomizer or atom cell, respectively, in the measurements.

For the decomposition of standard reference materials, a Milestone Ethos Plus microwave oven was used. The digestion programs were based on temperature control according to the recommendations of manufacturer with some adaptations.

Table 2.1 Instrumental parameters used in the measurements.

Instrumental parameter	Bi	Cd	Pb
Hollow cathode lamp	Photron or Philips	Narva or Pye Unicam	Philips
Wavelength of measurement, nm	223.1	228.8	217.0
Lamp current, mA	8 or 10	5 or 6	8
Spectral bandwidth, nm	0.5	0.5	0.5
Atomizer	Flame-heated quartz T-tube	Unheated quartz T-tube	Flame-heated quartz T-tube

2.2 Hydride Generation System

2.2.1 Apparatus

The experiments were carried out in both continuous flow (CF) and flow injection (FI) mode using Gilson Minipuls 3 (Villers Le Bell, France) 4-channel peristaltic pumps. In FI mode, a Rheodyne Model 5020 6-port injection valve (CA, USA) was used for the injection of analyte solution into carrier solution stream. For the pumping of analyte and reductant solutions, blue-blue or red-red color coded Ismatec Tygon peristaltic pump tubings (Germany) were employed. In order to remove the waste solution from cylindrical gas liquid separator, purple-purple color coded tygon tubings were utilized.

Tubings that were made of polytetrafluoroethylene (PTFE) (0.8 mm i.d. and 1.4 mm o.d.) and supplied from Cole Parmer (USA) were used for the transportation of solutions. The reaction and stripping coils were also made from the same PTFE tubing in different lengths. The 3-way or 4-way connectors used for merging of the analyte, reductant and carrier gas streams were all made of PTFE and supplied from Cole Parmer.

The carrier gas which was used for stripping of solutions and transportation of volatile species to trap and to atomizer was Ar (99.95%) that was supplied from Oksan (Ankara). During the trap studies, where W-coil was used as trap, H₂ (Oksan) was added to the carrier gas. The flow rates of Ar and H₂ in the carrier gas were measured and controlled by two separate rotameters obtained from Cole Parmer.

For the separation of gaseous analyte species from the liquid phase, a gas liquid separator (GLS) was used. Two different GLS designs, whose schematic diagrams and dimensions were given in Figure 2.1, were employed in the measurements; a home-made U-type GLS for Bi and Pb and a cylindrical GLS with a smaller inner volume similar to that proposed by Matoušek et al. [165] for Cd. The inner volumes of them were approximately 20 mL and 3 mL, respectively. In U-type GLS, the liquid part of the reaction products was forced to waste by gravity. In cylindrical type GLS, waste solution was removed by a second peristaltic pump and the solution level inside was kept at minimum.

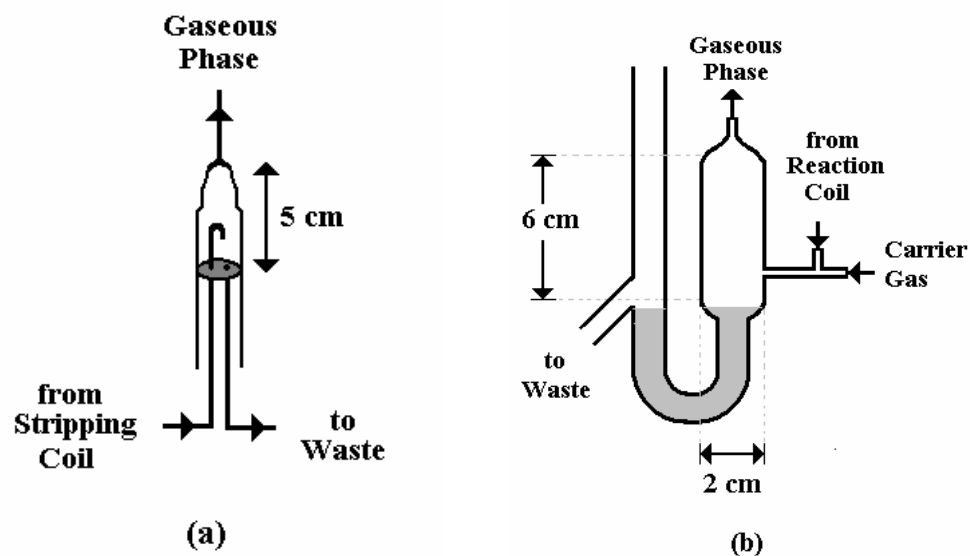


Figure 2.1 Gas liquid separators used in the experiments: (a) Cylindrical GLS used for Cd; (b) U-type GLS used for Bi and Pb.

The generated volatile species of Bi and Pb were transported from gas liquid separator to the atomizer by using Tygon tubing (3.1 mm i.d., Cole Parmer Instrument Co., USA). For volatile Cd species, the transport tubing was made of PTFE (0.8 mm i.d., 1.4 mm o.d.) between GLS and the atom cell. The transport tubings were kept as short as possible in order to prevent losses of volatile species during transportation. In the experiments, where cylindrical GLS was used, the tip of PTFE capillary was inserted into inlet arm and the tubing was kept as close as possible to the junction point of horizontal arm of quartz T-tube. In trap experiments, it was directed onto the W-trap through a distance of 0.5 cm.

In the trap experiments where the trap was separated from quartz T-tube, the released species were transported through tygon tubing (3.1 mm i.d.). For Cd, PTFE (4 mm i.d.) and fluorinated ethylene propylene (FEP) coated tygon tubings (6 mm i.d.) were also utilized.

The experimental set up for hydride generation of Bi and Pb was slightly different than that of Cd. Their respective schematic diagrams are given in Figure 2.2 and 2.3. In CF mode, the analyte and the reductant solutions were pumped continuously by the peristaltic pump. In FI mode, instead of analyte solution, only a carrier solution was pumped but the analyte solution was injected into carrier stream. A reaction coil was needed for all the elements. The lengths of reaction coils employed for the generation of bismuthine and plumbane were 15 and 30 cm, respectively. For Bi and Pb, no stripping coil was used other than a 2 cm length of glass connection where the carrier was introduced into flowing stream at the entrance of U-type GLS. For Cd the length of reaction coil was 60 cm and this figure strongly depended on the length of stripping coil. The length of stripping coil was 15 cm for Cd; however, the same sensitivity was obtained when the length was 120 cm without a reaction coil. In some experiments instead of employing a reaction coil, this configuration was also used.

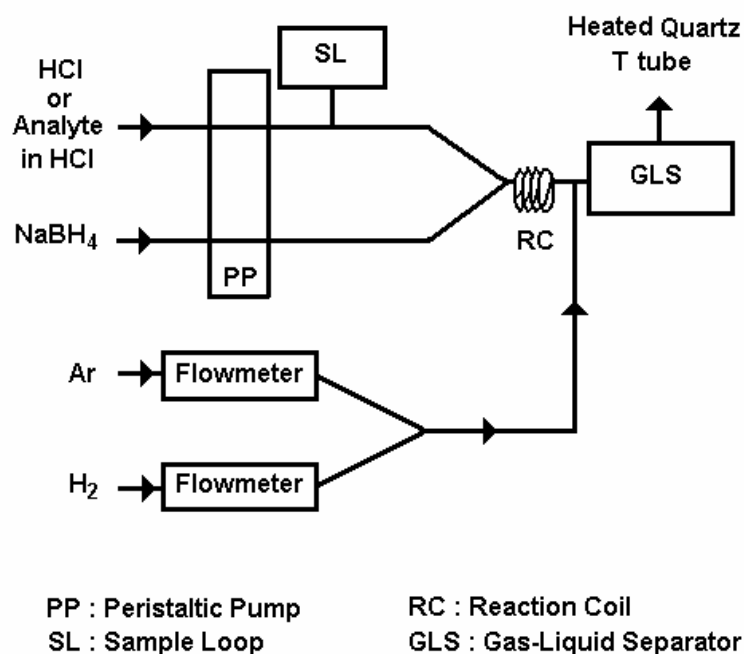


Figure 2.2 The experimental set up used for generation of Bi and Pb hydrides.

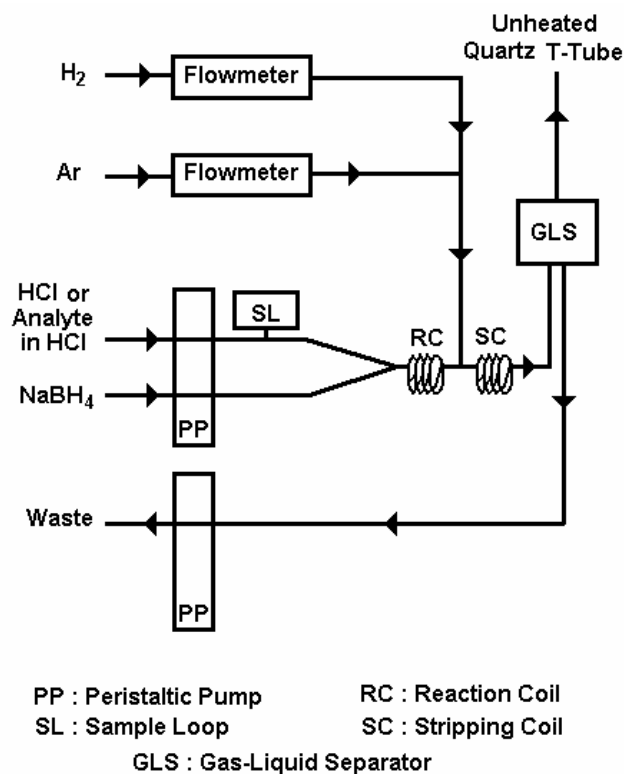


Figure 2.3 The experimental set up used for generation of volatile Cd species.

2.2.2 Atomizer and Atom Cell

A quartz T-tube atomizer commonly used as atomizer in hydride generation methods was either heated externally on a stoichiometric air acetylene flame for Bi and Pb or kept at room temperature for Cd served as the atomizer and atom cell, respectively; its dimensions are indicated in Figure 2.4. The ends of quartz T-tube used at room temperature for Cd were not covered with any windows.

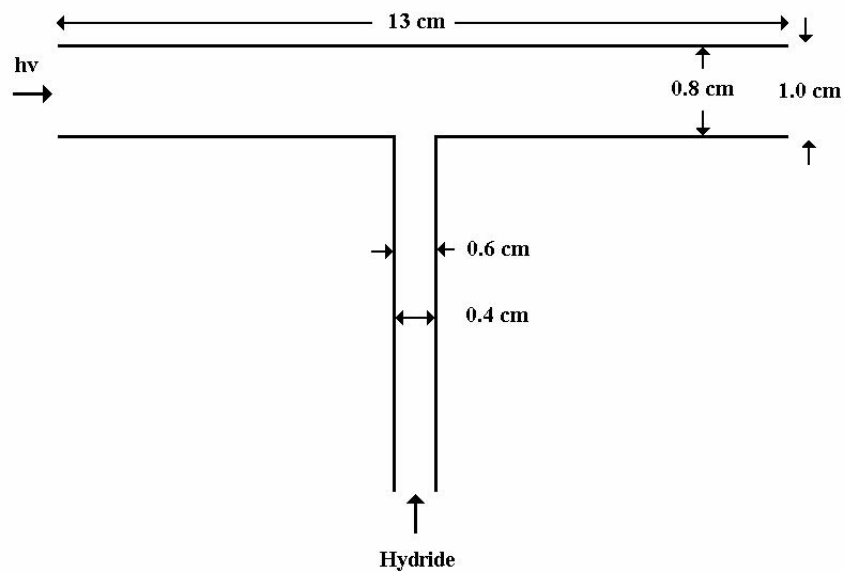
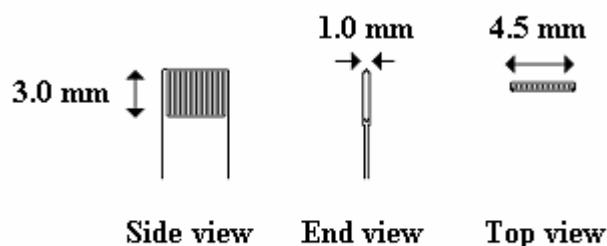


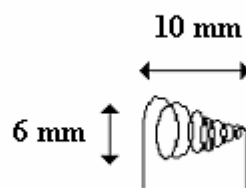
Figure 2.4 Quartz T-tube atomizer used in the experiments.

2.3 Trap System

In the preliminary studies, the trap was made up from commercially available nickel-chromium and tungsten wires. About 15 cm of wire was coiled into a conical shape such that it would supply maximum cross-sectional and thus trapping surface area, and could be heated without breakage. Then, W-coil filament extracted from a 15 V, 150 W projector bulb (Halogen Photo Optic Lamp Xenophot, Osram, Germany) was used as trap. The dimensions of both home-made and commercially handled W-coil traps are given in Figure 2.5. This type of commercially available W-coil has been commonly employed in ETAAS with metal atomizers. It is easily handled and inexpensive. In addition, it supplies larger surface area for the trapping when compared to that was designed in the laboratory.



W-coil extracted from projector bulb



W-coil made in laboratory

Figure 2.5 The dimensions of W-coil traps extracted from bulbs and made in the laboratory

The W-coil was placed in the inlet arm of QTA. It was inserted into the inlet arm of quartz T-tube through a small slot in a tilted position so that it would supply maximum crosssectional area for maximum trapping efficiency. The schematic diagram of trap system and its electrical connections are given in Figure 2.6 and 2.7, for Bi and Pb, and Cd, respectively. The distance between the horizontal arm and the trap was 5.0 cm for Bi and Pb since the quartz T-tube was externally heated by flame. Since unheated QTA was employed in Cd studies, it was possible to place the trap very near to the junction point of inlet arm and horizontal arm. During cold vapor studies, this distance was approximately 1 cm. The coil was fixed and sealed from the outside by using a temperature resistant alumina based powder material. The powder Al_2O_3 was mixed with sodium silicate solution, both of which were obtained from Tetcis (Ankara) and a viscous slurry was obtained. After inserting the coil into its place, the location of insertion was covered with

this slurry and dried at room temperature for at least 2 days. The isolation of W-coil was important in order to prevent oxygen entering to the system which caused deterioration of the W-coil by oxidation and also affected the trapping-revolatilization performance.

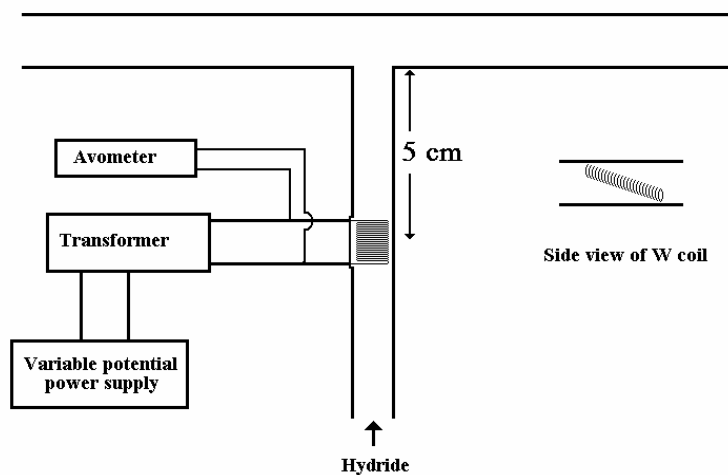


Figure 2.6 The W-coil placed in the inlet arm of quartz T-tube used for Bi and Pb.

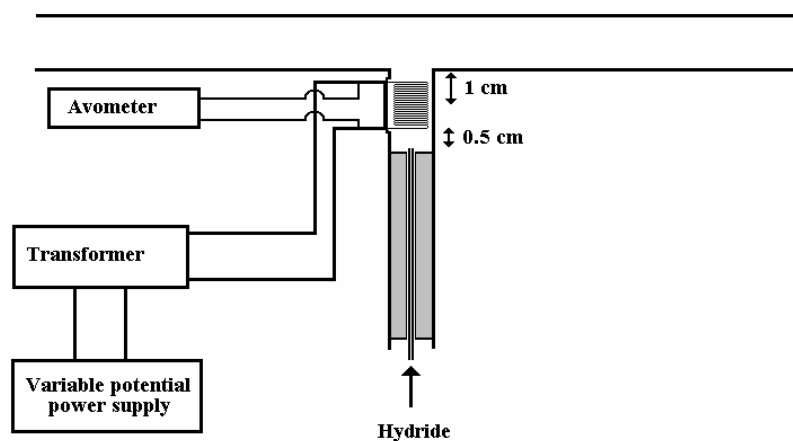


Figure 2.7 The W-coil placed in the inlet arm of quartz T-tube used for Cd.

The resistive heating of W-coil was achieved by applying an alternating voltage by using a transformer and a power supply which was connected to wall electricity (220 V a.c.) through a power switch as shown in Figures 2.6 and 2.7. The electrodes of coil were connected to 0-8 V output of transformer (available input voltages were 110 and 220; and output voltages were 5, 8, 12 and 18 V) which was connected to the wall electricity through a variable voltage power supply (input voltage 220; output voltage, adjustable between 0-220). The voltage was varied by the variable potential power supply. Therefore with this system, a potential between 0 and 8 V could be applied to the coil. If higher temperatures was to be used, the connections of the coil was altered to the 0-12 V output voltage of the transformer. The applied voltage and its accuracy was checked by using a ampere-volt-ohm meter which was connected to power cables at the junction point of W-coil as shown in the figures.

For the measurement of W-coil temperature, a Ni-Cr thermocouple which was capable of measuring temperatures up to 1200 °C was used. The central part of coil was heated more than the ends. The temperature measurements were carried out by contacting the tip of the thermocouple to the center of the coil, at different gas composition and flow rates. The approximate release temperatures that can not be measured by the thermocouple were estimated by the extrapolation of the graph between applied voltage and measured temperature, as long as it was not very high; since the relationship between applied voltage and the temperature was nearly linear between the applied voltages of 4 V and 6 V [166].

In order to investigate the distance that the released species could be transported, the trap was removed from the quartz T-tube and placed in a piece of quartz tube that has the same inner diameter with the inlet arm of T-tube. The distance between trap and the inlet arm of atomizer or atom cell was varied using Tygon tubing. In these experiments both the peak height and the peak area values were

recorded. This would also give an idea about the released species whether they are atomic or molecular.

In order to investigate the trapping efficiency, a tandem arrangement of two W-coil traps was used; one of them was in QTA and the other was a separate one. This arrangement, shown in Figure 2.8 was also used for the investigation of nature of released species from the trap. The temperature of each W-coil was controlled independently. By this arrangement untrapped species passing through the first coil could be trapped on the second one, while both the first and second traps were in collection mode. In addition, while the first trap was used in releasing mode and the second one was in collection mode, the revolatilized species from the first coil could be trapped on the second coil.

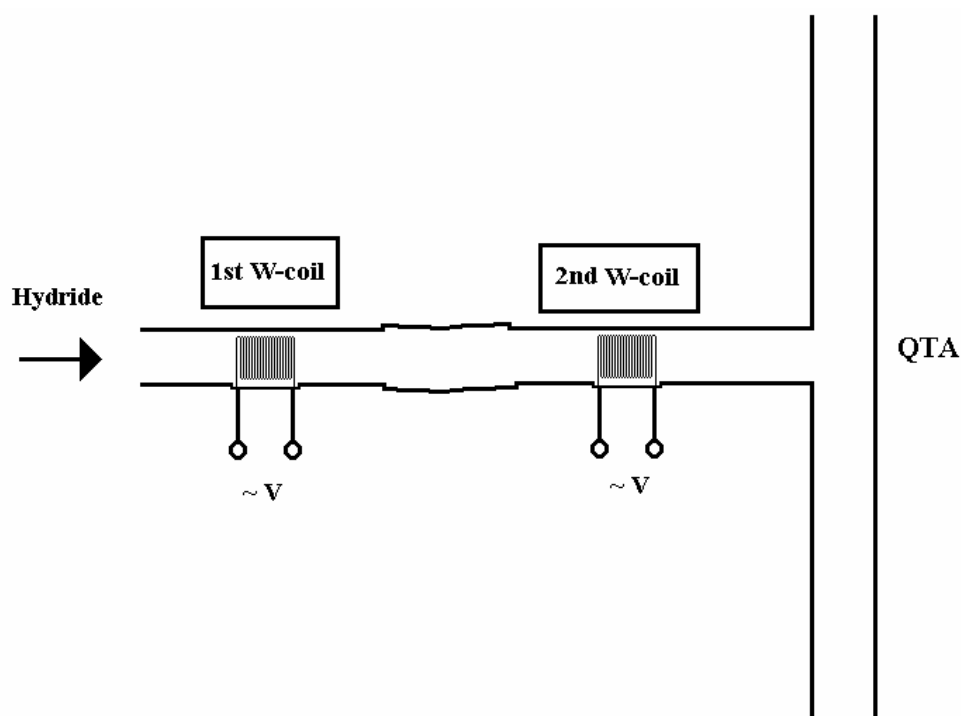


Figure 2.8 Tandem arrangement of W-coil trap system.

2.4 Reagents

All the reagents used were at least analytical reagent grade. Dilutions were made using 18 M Ω -cm deionized water obtained from a Millipore (Molsheim, France) Milli-Q water purification system which was fed by Millipore Elix 5 electrodeionization system.

The working solutions of Bi, Cd and Pb were prepared by making necessary dilutions from their standard stock solutions; 10000 mg/L Bi (Titrisol, Merck), 1010 mg/L Pb (Aldrich), 100 mg/L Cd, (Leeman Labs Inc. Plasma-Pure, USA) and 1000 mg/L Cd (Ultra Scientific).

For the acidification of analyte solutions, analytical grade 37% (w/w) HCl (Merck) was used. Reductant solutions were prepared daily from powder sodium tetrahydroborate(III) (Merck, min. 96% purity). For the stabilization of NaBH₄ solution, NaOH (Carlo Erba, Milano, Italy) was used. Analytical grade 65% (w/w) HNO₃ (Carlo Erba, Italy), 37% (w/w) HCl and 38-40% (w/w) HF (Merck) were used for the decomposition and digestion of geological reference materials.

Solutions of 0.5% (w/w) potassium hexacyanoferrate (III), K₃Fe(CN)₆ was prepared from analytical grade salt with a minimum purity of 99% (w/w) (Merck). Due to its low stability in the aqueous phase, the solutions were prepared daily. Nitroso-R salt (Aldrich) and 35% (w/w) H₂O₂ (Merck) was also used as the reaction medium for the generation of lead hydride.

The coating of W-coil was achieved by injecting aliquots of Pd, Ir, and Pt from their corresponding 1000 mg/L solutions (BDH, UK). Injections were made by using an adjustable volume micropipette (Transferpette).

2.5 Procedure

The hydride generation conditions were carried out in conventional FI mode by injecting a definite amount of analyte solution into the carrier solution stream. However, the optimized values were also verified in the trap mode where mostly a CF sampling was employed. In CF mode the solutions of sample and reductant were pumped at a constant flow rate by the peristaltic pump. The generated volatile species of analyte were transported to W-coil which was previously heated to collection temperature. After the hydride evolution and preconcentration was complete, all the collected analyte species were revolatilized at once by increasing the trap temperature rapidly to revolatilization temperature. The collection volume and thus time was determined by the element and its concentration in the sample solution. The optimum hydride generation, trapping and releasing conditions were summarized in Table 2.2.

The details of procedure for each element are given in the following sections. Since the trap signals are transient and very sharp, the integrated absorbance values were highly affected by the lamp noise and the very slight drifts in the base line caused large errors in peak area values. In most cases the peak height values are the basis of the measurements. In some experiments where the lamp noise was low, peak area values have also been used by keeping the integration time as short as 2-3 s. Therefore, in most cases the optimizations were based on the measurement of peak height and the integrated absorbance values were rarely taken into account. The residence time of the atoms were highly affected by the release gas flow rate which was optimized with respect to peak height. The signal obtained by each release was the basis for optimization of collection and release temperatures. During the collection temperature optimizations, the continuous signal created by untrapped species during collection was also followed. All the experimental parameters were optimized by changing one variable at a time. While optimizing one parameter, the others were kept at their optimum value. Multi-cycling method was employed.

Table 2.2 Hydride generation, trapping and revolatilization conditions for Bi, Cd and Pb in CF mode for W-trap HGAAS.

Parameter	Bi	Cd	Pb
Concentration of HCl in sample solution, mol/L	1.0	0.2	0.06
Concentration of NaBH₄ in reductant solution, % (w/v)	0.5	1.5	1.0
Concentration of NaOH in reductant solution, % (w/v)	0.2	0.15	0.2
Flow rate of sample and reductant, mL/min	6.0	2.1	6.0
Length of reaction coil, cm	15	60	30
Length of stripping coil, cm	2	15	2
Gas liquid separator	U-type	Cylindrical type	U-type
Collection Ar flow rate, mL/min	75	270	210
Collection H₂ flow rate, mL/min	70	150	100
Release Ar flow rate, mL/min	500	270	210
Release H₂ flow rate, mL/min	70	150	100
Collection trap temperature, °C	270	150	350
Release trap temperature, °C	1200	1000	1300

2.5.1 Bismuth

In FI mode 1.0 mol/L HCl was used as carrier. The optimum HCl and NaBH₄ concentrations were determined in conventional FI mode by using 0.500 mL sample loop and 10.0 ng/mL Bi in 1.0 mol/L HCl solution without the W-coil trap. During this studies the carrier gas was only Ar and no H₂ was added. The reductant and the carrier (analyte in CF) solutions were pumped at a flow rate of 6.0 mL/min.

The trapping and release temperatures were optimized using FI mode by injecting 0.500 mL of 10.0 ng/mL Bi in 1.0 mol/L HCl. The bismuthine generated was transferred to quartz T-tube through a tygon tubing using a carrier gas mixture composed of H₂ and Ar at flow rates of 70 and 75 mL/min, respectively. The transferred bismuthine was trapped on W-coil placed in the inlet arm of the quartz T-tube; the W-coil was previously heated to 270 °C. After on-line preconcentration on the W-coil, the Ar flow rate in the carrier gas was increased to 500 mL/min, the H₂ flow rate was kept at 70 mL/min, and then the analyte was released by increasing the trap temperature rapidly to 1200 °C. The residence-time of analyte species on the light-path was very short and the transient signal was obtained in less than 0.5 s.

The effect of distance between trap and atomizer was investigated by varying the length of the transfer tubing between 10 cm and 200 cm. Tygon tubing (3.1 mm i.d.) was used for the transportation of released species from the surface.

2.5.2 Cadmium

In all the experiments including conventional HG and preconcentration on W-coil, the flame was turned off and the measurements were conducted using the quartz T-tube at room temperature. The ends of atom cell were not covered with windows.

Use of an atom cell with quartz windows commonly used for CV Hg studies was also investigated. In addition to atom cell that was different for Bi and Pb, a cylindrical GLS was used for Cd and the waste was removed by a second peristaltic pump. Furthermore the volatile species of Cd were transported to the atomizer or to trap through a PTFE tubing (0.8 mm i.d.) that was inserted into the inlet arm of QTA and thus minimization of possible losses on the inner walls of quartz inlet arm was assured. The distance between the tip of PTFE transport tubing and the W-coil was 0.5 cm in order to prevent damaging of the tip at the release stage.

The careful optimization of experimental parameters was required in order to obtain reproducible analytical signals. Conventional FI-HGAAS method was used for these optimizations. However, the sample acidity was also investigated for CF mode using W-trap HGAAS. The optimization of sodium tetrahydroborate was carried out in FI mode using both conventional and W-trap system. The concentration of NaOH in NaBH₄ solution was also investigated by conventional FI-HGAAS.

The reaction and stripping coils lengths were optimized in FI mode by injecting a definite volume of Cd solution without the W-coil trap. The lengths of reaction and stripping coils were found to be dependent on each other. In some experiments the reaction coil was removed and a relatively longer stripping coil, 120 cm, was used since the same sensitivity was obtained in this case.

Optimum trap and release temperatures were determined in CF mode by introducing the solutions for a period of time. The optimizations were based on the signal obtained after each release. The trapping was carried out at 150 °C. After vapor generation was complete, the trap temperature was increased to 1000 °C and the transient signal was obtained in less than 1 s. The peak height of the analytical signal was taken into account for these optimizations. The optimum gas flow rates

for collection and release steps were found to be the same with each other. Thus, similar to Pb experiments, gas flow rates were kept constant and not varied between collection and revolatilization stages.

The effect of distances between GLS and W-trap, tip of transfer tubing and W-coil, and also trap and atom cell was investigated by varying the length of tubings. The stability of the trapped species was investigated by varying the time interval between collection and release stages. The effect of cooling time after each release step was also investigated.

The effect of reaction temperature on the analytical signal was investigated by immersing the reaction coil in a water bath placed on a hot plate whose temperature was varied between 0 °C and 98 °C. Cooling was achieved by putting ice pieces into water bath. The temperature of water bath was measured using a thermocouple and a thermometer inserted into water. These experiments were carried out in both conventional FI-HGAAS and W-trap-HGAAS. Since the evaporation of water was high as the temperature of reaction coil increased, inner surfaces of GLS, transfer tubings and quartz T-tube was dried by passing Ar at a flow rate of 1 L/min between the injections until the water drops on the surfaces were removed completely.

The effects of coating with Ir and Pt on the collection efficiency were investigated by coating the W-coil separately with 100 µg of each element by subsequent injections of 25 µL from their 1000 mg/L stock solution. The injection was repeated 4 times by applying a drying step under H₂ environment between each injection. At the end, the coil temperature was increased to 1300 °C to reduce the coatings into metallic form. The optimization of collection and release temperatures were investigated for coated traps.

The tandem arrangement of consecutively coupled W-coil traps was used for the investigation of trapping efficiency and the nature of the released species from the trap surface. The volatile species that were not trapped on the first coil were tried to be trapped on the second one by injecting the analyte into the system by keeping both of the coils at collection temperature. The nature of released species from the first trap was investigated by trying to collect them on the second trap; during the releasing stage for the first trap, the second trap was kept at collection temperature.

2.5.3 Lead

The working Pb solutions were prepared in potassium hexacyanoferrate(III) $K_3Fe(CN)_6$. The optimum concentrations of HCl, $NaBH_4$ and $K_3Fe(CN)_6$ were determined in conventional FI mode utilizing a 0.500 mL sample loop and 10 ng/mL Pb solution. In these experiments the carrier gas was Ar and the carrier solution was 0.5% (w/w) $K_3Fe(CN)_6$ prepared in 0.06 mol/L HCl. The effects of nitroso-R salt and H_2O_2 on the generation of plumbane were also investigated under the same conditions by preparing the analyte solution in these reagents.

Optimum collection and release temperatures for lead were determined in CF mode using 10.0 ng/mL Pb solution in 0.06 mol/L HCl and 0.5% (w/w) $K_3Fe(CN)_6$. The sample and the carrier solutions were pumped at a constant flow rate for 20 s and the generated plumbane was collected on the trap. The optimizations were based on the signal obtained for each release. The trapping temperature was 350 °C. After vapor generation was completed, the trap temperature was rapidly increased to 1300 °C and a transient signal was obtained. The optimum gas flow of collection step was the same as that of release step. Thus, there was no need to change the carrier gas flow rate between collection and volatilization stages.

The effects of coating with Ir, Pd and Pt on the collection efficiency were investigated by coating the W-coil with 100 µg of each element separately by subsequent injections of 25 µL from their 1000 mg/L stock solution. The injection was repeated 4 times applying a drying step, under H₂ environment between each injection. At the end, the coil temperature was increased to 1300 °C to reduce the coatings into metallic form (under H₂ environment).

The effect of distance between the trap and the atomizer was investigated by varying the length of the transfer tubing between 10 cm and 45 cm.

The consecutively coupled W-coil traps were used for the investigation of trapping efficiency and the nature of the released species from the trap surface. The volatile species that were not trapped on the first coil was tried to be trapped on the second one by injecting the analyte into the system by keeping both of the coils at collection temperature. The nature of released species from the first trap was investigated by trying to keep them on the second trap; during the releasing stage for the first trap, the second trap was kept at collection temperature.

2.6 Digestion of Standard Reference Materials

The accuracy of the methods developed for Bi, Cd and Pb was checked by the analysis of various environmental certified standard reference materials (SRM) that have different matrices. The SRMs and the concentration of elements in them were summarized in Table 2.3. Microwave digestion program employed for the decomposition and digestion of solid standard reference materials was given in Table 2.4. The program was based on the temperature control.

Table 2.3 The standard reference materials used for the accuracy check of the methods developed for Bi, Cd and Pb and the concentrations of elements

Analyte	Standard Reference Material	Concentration of analyte
Bi	GSJ Rock Reference Material JR-1	0.51 $\mu\text{g/g}$
	GSJ Rock Reference Material JR-2	0.65 $\mu\text{g/g}$
	Trace Metals in Drinking Water CRM-TMDW (Lot # 818921)	10.00 \pm 0.05 $\mu\text{g/L}$
Cd	NIST SRM 1573a Tomato Leaves	1.52 \pm 0.04 $\mu\text{g/g}$
	NIST SRM 1566b Oyster Tissue	2.48 \pm 0.08 $\mu\text{g/g}$
	CRM 403 Trace Elements in Sea Water	0.175 \pm 0.018 nmol/kg
Pb	NIST SRM 278 Obsidian Rock	16.4 \pm 0.2 $\mu\text{g/g}$
	Ultra Scientific Metals on Soil/Sediment #4	95.3 \pm 5.3 $\mu\text{g/g}$

Table 2.4 The temperature program^a used for the decomposition of standard reference material and applied power values^b

Step	Bi^c			Cd^d			Pb^e		
	T, °C	t, min	P, W	T, °C	t, min	P, W	T, °C	t, min	P, W
1	150	3	500	180	5	1000	100	5	700
2	210	3	700	180	5	1000	180	10	800
3	240	3	800	200	5	1000	190	5	900
4	240	20	800	200	5	1000	190	30	1000

^a Indicated temperatures are the temperatures reached at the end of that step

^b Indicated power values are the maximum power applied in that step

^c GSJ JR-1 and GSJ JR-2

^d NIST SRM1566b Oyster Tissue and NIST SRM 1573a Tomato Leaves

^e Metals on Soil/Sediment and NIST SRM 278 Obsidian Rock

For Bi two geological reference materials GSJ JR-1 and GSJ JR-2 supplied from Geological Survey of Japan were digested in microwave oven. Each geological standard reference material was analyzed in three parallel replicates, which were prepared by decomposing approximately 0.150 - 0.200 g of solid material using an acid mixture of 3.0 mL of 40% (w/w) HF and 5.0 mL of 65% (w/w) HNO₃. The microwave program applied was given in Table 2.4. After complete decomposition, the clear solutions were transferred to polyethylene volumetric flasks and diluted to 50 mL with 1.0 mol/L HCl. Two different procedures were applied for the measurements. In the first one (P1), 2.0 mL from the diluted solution was injected to the system through injection valve using 2.0 mL sample loop. In the second one (P2), first the solution was further diluted 10 times with 1.0 mol/L HCl and 18 mL of resulting solution was pumped to the reaction coil in CF mode. In addition to geological SRM, Trace Metals in Drinking Water CRM-TMDW supplied from High Purity Standards (Charleston, USA) was also analyzed. For this purpose, 1.0 mL of water sample was diluted to 100 mL with 1.0 mol/L HCl and the resulting solution was analyzed directly. For the analysis of water reference material, a sampling volume of 36 mL was used for the measurements.

For the verification of method for Cd three different certified reference materials were used. NIST SRM 1566b Oyster Tissue and NIST SRM 1573a Tomato Leaves were decomposed and digested in microwave oven by using the program given in Table 2.4. The analyses were conducted by using three replicates for each certified reference materials. In the decomposition of oyster tissue, 5 mL of 65% (w/w) HNO₃ were added onto 0.250 g portion of oyster tissue. For tomato leaves in addition to 5 mL (w/w) HNO₃, 0.5 mL of 40% (w/w) HF was added onto 0.250 g of tomato leaves. After the material was decomposed by applying the microwave oven program given in Table 2.4, clear solutions were diluted to 50.0 mL with deionized water using volumetric flasks made of glass and polyethylene for oyster tissue and tomato leaves, respectively, and transferred to polyethylene bottles. Due

to strong matrix interferences, standard addition method was applied for the determination of Cd in tomato leaves; a 25 fold dilution was made for the minimization of matrix interferences by diluting them with 0.2 mol/L HCl. An aliquot of 2.1 mL (corresponds to 1.0 min collection time) of diluted solution was pumped to the generation system in CF mode and the generated volatile Cd species were collected on the trap. Spiked solutions were also injected in the same manner. In the analysis of oyster tissue SRM, the digests were further diluted 200 times with 0.2 mol/L HCl which allowed the use of direct calibration method with a collection period of 2.0 min that corresponds to a collection volume of 4.2 mL. The analysis of CRM 403 Trace Elements in Sea Water was carried out without any digestion procedure. Water sample was acidified with HCl and injected into HG system in CF mode. The collection volume was 4.2 mL and the direct calibration method was applied for the analysis of sea water SRM.

The accuracy of the method developed for Pb was demonstrated by analyzing two different standard reference materials, Metals on Soil/Sediment #4 (Ultra Scientific) and NIST SRM 278 Obsidian Rock standard reference materials. The SRMs were decomposed in microwave oven employing the temperature program given in Table 2.4. A 0.100 g portion of soil/sediment was decomposed using 4.0 mL of 65% (w/w) HNO₃, 2.5 mL of 37% (w/w) HCl and 0.75 mL of 40% (w/w) HF. For the decomposition of obsidian rock material 5.0 mL of 65% (w/w) HNO₃, 5.0 mL of 37% (w/w) HF and 2.0 mL of deionized water were added onto accurately weighed sample. The SRMs were analyzed in three replicates. After their complete decomposition, they were transferred to PTFE beakers and evaporated to dryness. The residue was dissolved and diluted to 100 mL using 0.06 mol/L HCl. Then they were transferred to polyethylene bottles for the measurements. During the measurements, the digests of soil/sediment SRM were diluted 100 times with 0.5% (w/w) potassium hexacyanoferrate(III) in 0.06 mol/L HCl solution. In the analysis of obsidian rock digests, the solutions were further diluted 25 times; the final solution was 0.5% (w/w) potassium hexacyanoferrate

and 0.06 mol/L in HCl. The samples were analyzed by FI-W-coil-HGAAS using 0.5 mL sample loop. In these experiments the carrier solution was 0.06 mol/L HCl. No interferences were observed from the matrix elements. Both analyses were carried out by direct calibration method.

CHAPTER III

RESULTS AND DISCUSSION

3.1 Selection of Trap

In the preliminary experiments Pt, W and Ni-Cr wires were tested as trap material. These materials were selected such that all can be heated resistively and thus the trapped species would be revolatilized rapidly. At the beginning of experiments, traps were made in the laboratory by coiling them in such a shape that could be placed in the inlet arm of quartz T-tube and supply maximum cross-sectional area. Although Pt is soft metal for making it in different shapes easily, its melting point is relatively low, 1769 °C [59], and becomes soft at about 1400-1500 °C. Therefore it is not convenient for the elements that require higher temperatures for volatilization. Ni-Cr wire can also be heated up to similar temperatures as Pt. Regarding the temperatures that can be reached, W has the advantage of having the highest melting point, 3410 ± 20 °C [59], among the elements in the periodic table. It can be heated up to temperatures as high as 3200 °C which is high enough to vaporize and even atomize most of the analyte compounds [51]. Another advantage is its inertness to most of acids and chemical reagents. Tungsten also has the disadvantage of being hard and that it can be easily broken during coiling process. The experiments showed that it is also capable of trapping volatile species of Bi, Cd and Pb when heated to moderate temperatures.

At initial experiments, where the traps were made from Pt, Ni-Cr and W wires by coiling them into desired geometry, successful results were obtained by Ni-Cr traps used for the sequestration of bismuthine. However, it was not easy to reproducibly make Ni-Cr traps both in resistance and physical shape thus recalibration of temperature and applied voltage was necessary. Furthermore the hardness of W made the coiling process difficult since it could be broken easily during shaping process. However, it is inexpensive and can be obtained easily by extracting from ordinary projector bulbs in different shapes and electrical properties. Having observed that W-coil trapped bismuthine efficiently, it was selected as the trap material since it offered some advantages over other metals. Coiled W filament was preferred since its geometry was suitable to be placed in the inlet arm of quartz T-tube which was commonly used as atomizer in HGAAS techniques. In addition to its geometry, this type of filament has been the most widely used one employed in ETAAS with metal atomizers [51, 52, 53]. The coil was placed into the inlet arm of quartz T-tube in tilted position so that it would provide maximum cross-sectional area for efficient trapping. The dimensions of the coil extracted from bulbs and that made in the laboratory were given in the experimental section.

3.2 Heating System of W-trap and Temperature Measurements

The temperature measurements were done by using a thermocouple by bringing its tip in contact with W-coil. Since the tip was coated with a ceramic material, the contact did not create any problems during the temperature measurements. The temperature profile of the coil was not uniform along the coil. The measurements were done at the center of the coil which was the most heated part. The coil temperature as a function of applied voltage was given in Figure 3.1. The temperature of coil was found to be approximately linearly correlated with the applied temperature between 0-4 V as shown in the figure. The temperature of the coil was slightly affected by the purge gas especially when it contains H₂. This

cooling effect was due to higher thermal conductivity of H₂, $446 \cdot 10^{-6}$ (cal/s·cm)(°C/cm) at 26.7 °C, which is approximately 10 times higher than that of Ar, $43 \cdot 10^{-6}$ (cal/s·cm)(°C/cm) [59]. The cooling effect of H₂ was clear especially at higher temperatures. During the experiments, the temperature of the coil was controlled by the voltage applied by a transformer and a variable potential power supply. By the aging, if inadequate H₂ was supplied or O₂ entered to the system, the central part of the coil that was the most heated and oxidized region became thinner and thus electrical and thermal characteristics changed. In this case, the temperature was recalibrated against voltage.

The peak height was strongly dependent on rate of heating at releasing step for the coil; higher heating rates caused sharper signals. Thus the coil must have been heated as fast as possible at the releasing stage in order to obtain sharp and reproducible signals. For this purpose a power switch was connected in front of variable potential power supply. At the releasing stage, first the power switch was kept in off position and the potential was adjusted to the desired release voltage on variable potential power supply and then the power switch was turned on. Thus the heating was very fast since the voltage was applied at once.

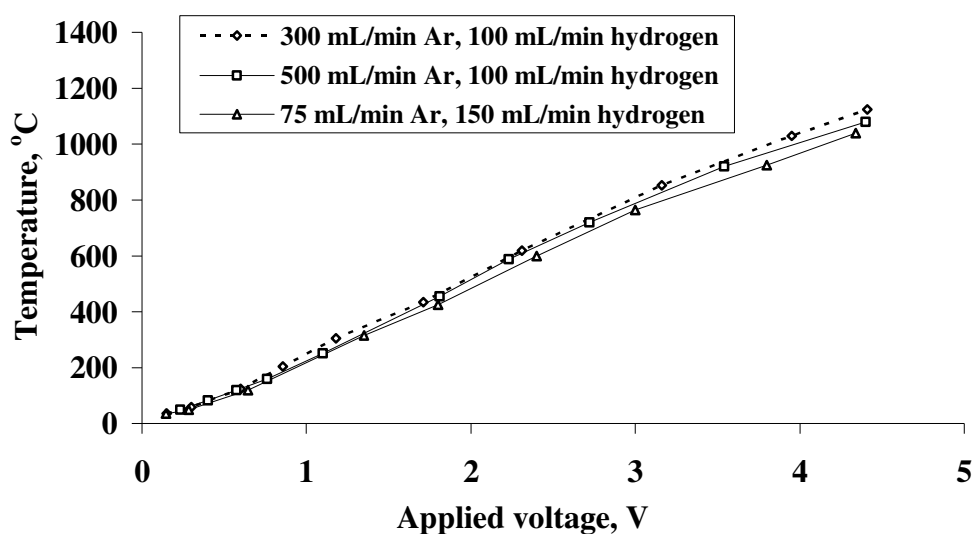


Figure 3.1 Voltage versus temperature of W-coil at different gas flow rates.

3.3 Composition of Carrier Gas

In the conventional HGAAS studies the carrier gas was only pure Ar. However since W was easily oxidized when heated to the higher temperatures in the presence of traces of O₂, it was necessary to create a reducing environment in order to minimize its oxidation. In the preliminary stages of trap experiments, only Ar gas was used as the carrier gas; in this case the horizontal arm of quartz T-tube as well as the inlet arm was gradually but definitely covered with a blue to brown opaque layer as shown in Figure 3.2. These colored layers possibly indicated the formation of WO₂ (brown), W₂O₅ (blue) and W₄O₁₁ (blue) [59]; the last two compounds with higher oxygen content were deposited further away from the T-junction of quartz atomizer, where the O₂ diffusion was higher. The addition of H₂ into the carrier gas eliminated the background absorption; this was accompanied by significant reduction in colored oxide formation. Although H₂ was formed during HG process, the amount produced was not sufficient to prevent the W-coil from being oxidized during collection. The formation of such oxides depended on the reagent flow rate, collection time (sample volume) and the strength of HG reaction determined by the concentrations of HCl and NaBH₄. The higher the flow rate and the concentrations of reductant and HCl, the more vigorous the reaction was; thus higher amount of aerosol and water vapor reached to trap. This was resulted in an increase in the oxidation. The sampling time was also found to be correlated with the oxidation of coil. For example sampling volumes higher than 40 mL (for Bi) resulted in an increase in the background signal due to oxidation of W-coil; however, the signal magnitude was not affected significantly. Nevertheless, the increase in background should be interpreted as a sign of W-coil being oxidized; in this case, an increase in the percentage of H₂ in carrier gas eliminated the background signal, protecting the W-coil from being oxidized. The oxidation definitely reduces the life time of W-coil. Therefore, choice of H₂ flow rate depended on these factors and it was selected such that the oxidation was kept as minimum.



Figure 3.2 The effect of oxidation of W-coil on QTA when H_2 was not used in the carrier gas

3.4 Conditioning and Life Time of W-Trap

The total efficiency of a fresh W-coil was relatively low and at the beginning an initial conditioning period with 10-30 firings was required to have a stable analytical signal. The requirement of the conditioning may be explained by the impurities present on the coil or the surface characteristics of new coil. As mentioned in the previous section, the life time of the coil was determined by the oxidation of W-coil. For prolonged use, the coil life was inversely proportional to working volume; the larger volumes causes the oxidation of W-coil more and this resulted in the shortening of the W-coil life. Each coil can be used for at least 2000 firings but the life time strongly depended on the factors that caused oxidation.

3.5 Bismuth

3.5.1 Optimization of Hydride Generation Parameters

The acidified solution of bismuth reacts with tetrahydroborate conveniently to form bismuthine, BiH_3 . Since it is relatively stable and the boiling point is low ($17^\circ C$) [5], it can be separated from the solution efficiently using a U-type GLS. The

reaction coil was selected as 15 cm. The length of stripping coil was 2 cm. The optimum values of concentrations of HCl and NaBH₄ were determined by conventional flow injection method (no W-coil on the way) by injecting 0.500 mL of 20 ng/mL Bi. During the optimization of sample acidity, the carrier Ar flow rate was 500 mL/min and the flow rates of solutions were 6 mL/min. The effect of HCl concentration in the analyte solution was given in Figure 3.3. In these experiments 1.0 mol/L HCl was used as the carrier solution. A sharp increase in the analytical signal was observed between 0 and 0.10 mol/L. Between 0.10 and 1.0 mol/L the signal increased slightly and reached a plateau. Thus, optimum HCl concentration in the sample solution was selected as 1.0 mol/L.

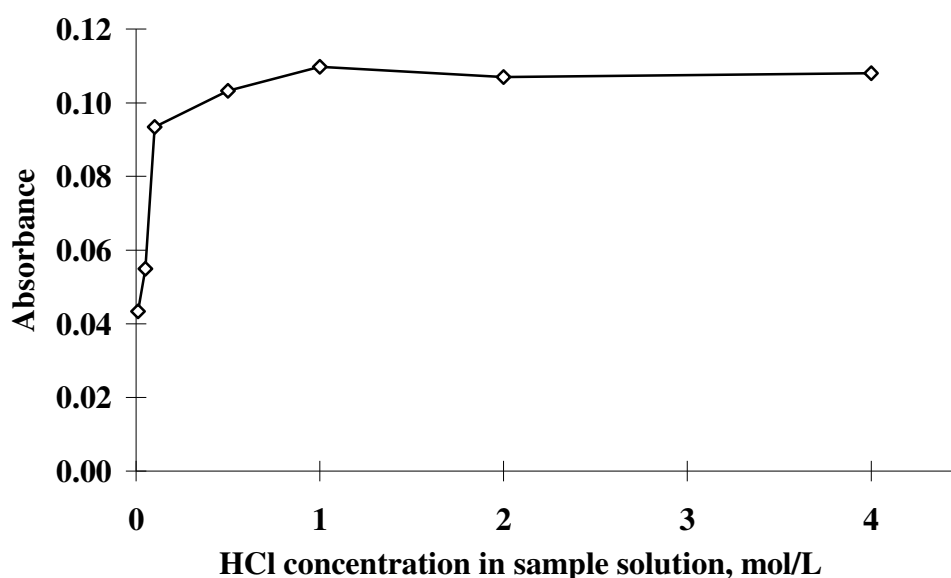


Figure 3.3 Optimization of HCl concentration for BiH₃ generation. Concentration of Bi was 20 ng/mL and the volume of sample loop was 0.500 mL.

The optimization of NaBH₄ concentration was also performed under the same conditions that were used in the optimization of HCl. For the stabilization, the solutions of NaBH₄ were prepared in 0.2% (w/v) NaOH whose concentration was not examined. The optimization plot of analytical signal versus reductant

concentration is given in Figure 3.4. The analytical signal increased gradually up to a concentration of 0.5% (w/v) NaBH₄. A further increase in the concentration was resulted in a decrease in the analytical signal probably due to the dilution of analyte species in the gas stream by the H₂ generated in excess. Therefore a concentration of 0.5% (w/v) was found to be the optimum concentration of NaBH₄ for bismuthine generation.

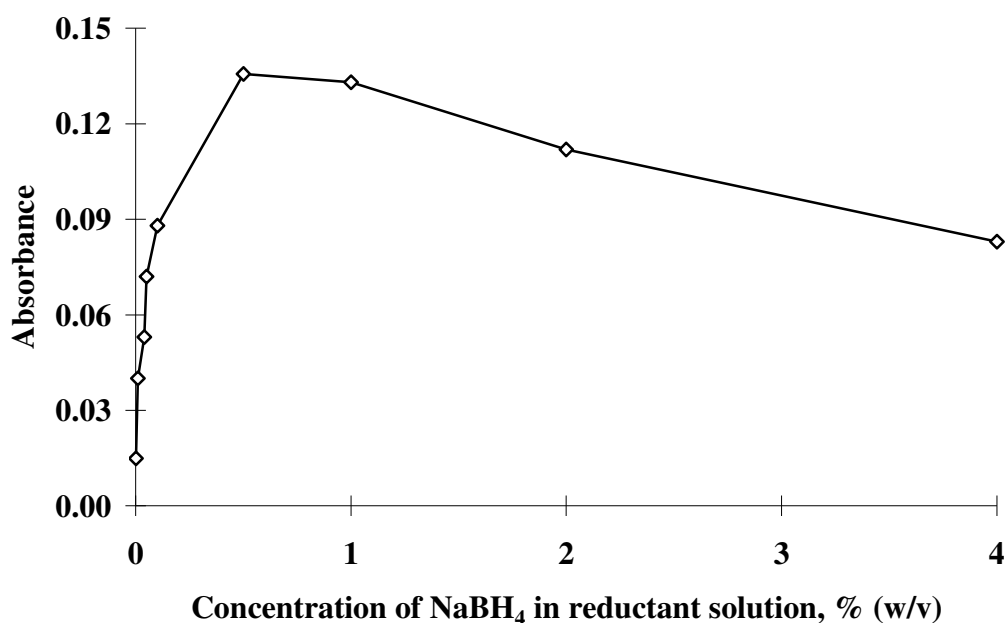


Figure 3.4 Optimization of NaBH₄ concentration for BiH₃ generation. Concentration of Bi was 20 ng/mL and the volume of sample loop was 0.500 mL.

3.5.2 Optimization of Trapping Conditions

3.5.2.1 Collection and Revolatilization Temperatures

The decrease in the analytical signal was an indication of trapping when the W-coil, placed between hydride generator and the atomizer, was being heated

gradually. The estimation of the trapping temperature was made by observing the degree of decrease in the continuous signal. However it was not possible to decide about the collection temperature just by observing the continuous signal since the decrease might also be due to loss of analyte on the heated parts other than the trap itself. Later on, it was observed that quartz was also capable of trapping bismuthine when heated to moderate temperatures by W-coil. Therefore, in order to estimate the temperature at which maximum trapping was achieved by W-coil traps, always the signals obtained after each revolatilization were taken into account. The dependence of analytical signal on collection temperature together with release temperature was given in Figure 3.5. The optimum collection temperature range for bismuthine was rather narrow and reaches to maximum at 270 °C; for higher temperature values, a sharp decrease was observed in the trapping efficiency due to loss of analyte during collection stage. The distance between the trap and the flame was only 5 cm and the trap was unavoidably heated slightly by the flame. Although all of the trapped Bi species can be revolatilized from the surface at 350 °C without any memory effect in the next run, a temperature of 1200 °C was necessary for rapid revolatilization so that the use of peak height in signals was justified. The peak height of analytical signal obtained by a release temperature of 350 °C was low due to slower rate of revolatilization and thus the broadening of the analytical signal was observed. Until 900 °C the signal increased slowly by an increase in the release temperature and a plateau was reached at 1000 °C. A release temperature of 1200 °C was selected since no significant increase was obtained in the analytical signal at higher temperatures.

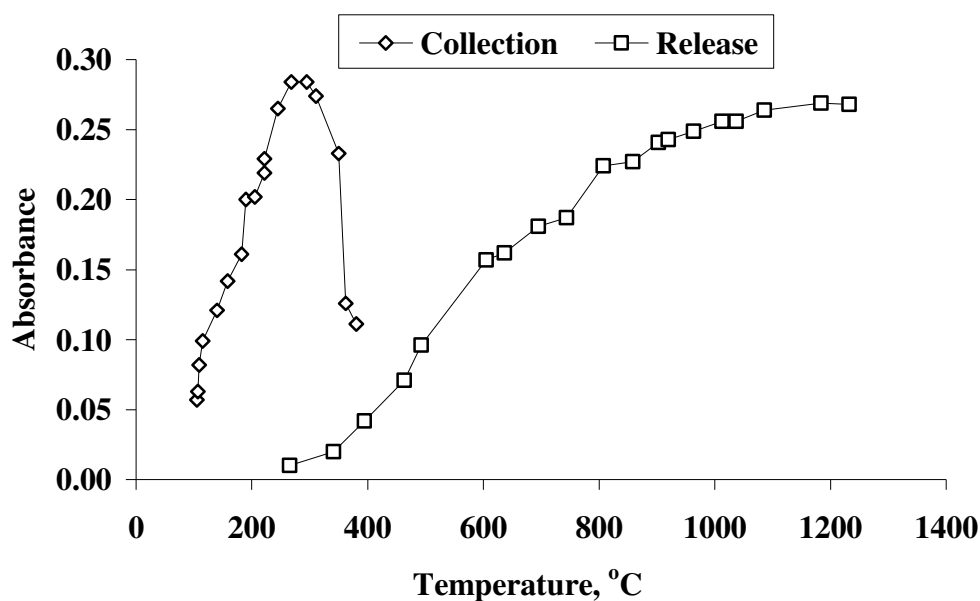


Figure 3.5 The effect of collection and release temperatures on analytical signal for 5.0 ng Bi. During the variations of collection and release temperatures, a constant release temperature of 1200 °C and a constant collection temperature of 270 °C, respectively, were employed.

It has been reported [164] that quartz alone can also be used as a trap for volatilized Pb species; therefore, the rapid electrical heating of W-coil for a short time (1-2 s) in our case was an advantage to assure only the signal from tungsten moiety was analytically measured. Any interference from the collection and releasing of volatile Bi species on the quartz surface may be a problem especially if the heating were affected by external means. It was also observed that if higher collection temperature was used so that the quartz was also heated, the bismuthine was also trapped on the walls of quartz around W-coil. In those cases, if a higher release temperature was used, a second peak next to the analytical signal was appeared. In our case, no such interference was observed as electrical heating of W-coil was used which provide fast heating in a short time.

Since the thermal conductivity of H₂ is higher than that of Ar, the change of temperature of coil at higher flow rates of H₂ is expected to be larger and the decrease in the analytical signal could be more significant. Therefore the effect of H₂ flow rate on the collection temperature was also investigated and the relevant graph is given in Figure 3.6. As it is seen from the figure, the trapping efficiency was slightly higher if no hydrogen was used during collection stage but the difference is not significant. Furthermore, the optimum range of collection temperature at no H₂ condition was rather wider than that at flow rate of 70 mL/min.

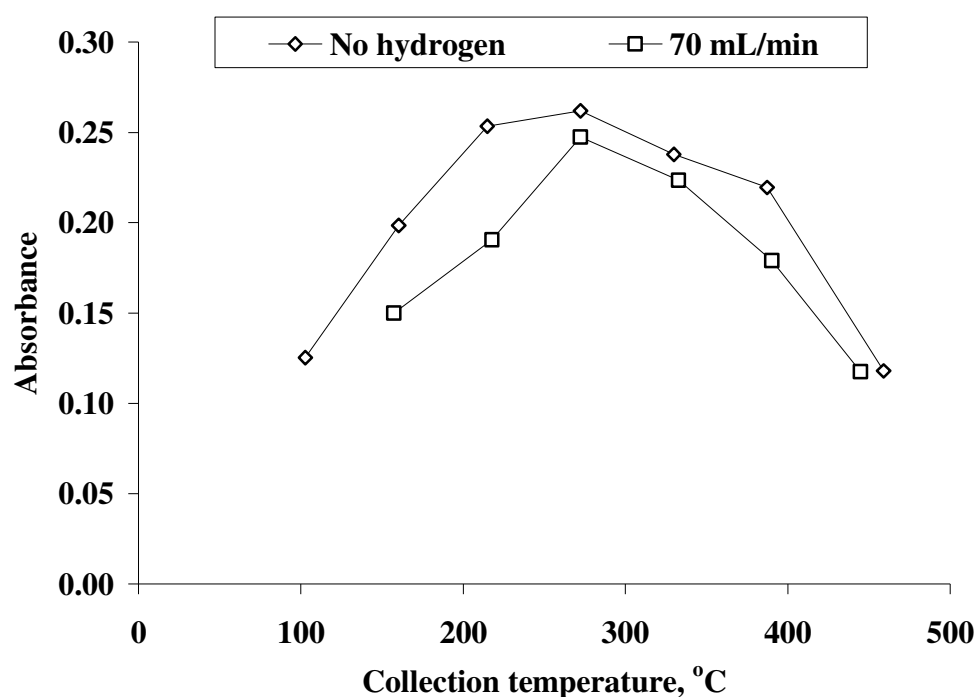


Figure 3.6 The effect of H₂ flow rate on collection temperature for 5.0 ng Bi. During the variations of collection, a constant release temperature of 1200 °C was employed.

3.5.2.2 Carrier Gas Flow Rates

3.5.2.2.1 Argon Flow Rate

The optimum Ar flow rates for collection and release stages were determined in FI mode and optimization graphs were given in Figure 3.7 and 3.8, respectively. During these measurements, only Ar flow rate was varied for the determination of optimum carrier gas flow rate for collection and release steps while H₂ flow rate was kept constant at a flow rate of 70 mL/min for both collection and release steps; the lower flow rates of H₂ caused the oxidation of W-coil and resulted in relatively higher background absorption as discussed in previous section. It was clear that the efficiency of collection increased at lower flow rates of Ar. When the Ar flow rate was decreased from 75 mL/min to 50 mL/min, the trapping efficiency increased by only 5%. Although the trapping efficiency could be increased by using lower carrier flow rates, the optimum Ar flow rate at collection stage was chosen as 75 mL/min in order not to increase the percentage of H₂ in the carrier gas mixture for safety reasons. Hydrogen flow rate could not be decreased at the same rate as Ar flow rate since the lower flow rates resulted increased oxidation of W-coil.

For the releasing stage, the optimum Ar flow rate was selected as 500 mL/min. The slower Ar flow rates for releasing stage caused peak broadening and decrease in the peak height of analytical signal. The decrease in the peak height was more pronounced when the release Ar flow rate was decreased as compared to an increase in the Ar flow rate. At the releasing stage, Ar flow rates higher than 500 mL/min did not cause any significant change in signal shape up to 1000 mL/min. However the peak height decreased approximately 10% at 1000 mL/min. It can be concluded that the re-volatilization of Bi species from the W-coil was a rapid process and could be achieved when the target temperature of coil is 1200 °C. At extreme release Ar flow rates the analytical signal become smaller due to reduced residence time and dilution of analyte species in the horizontal arm.

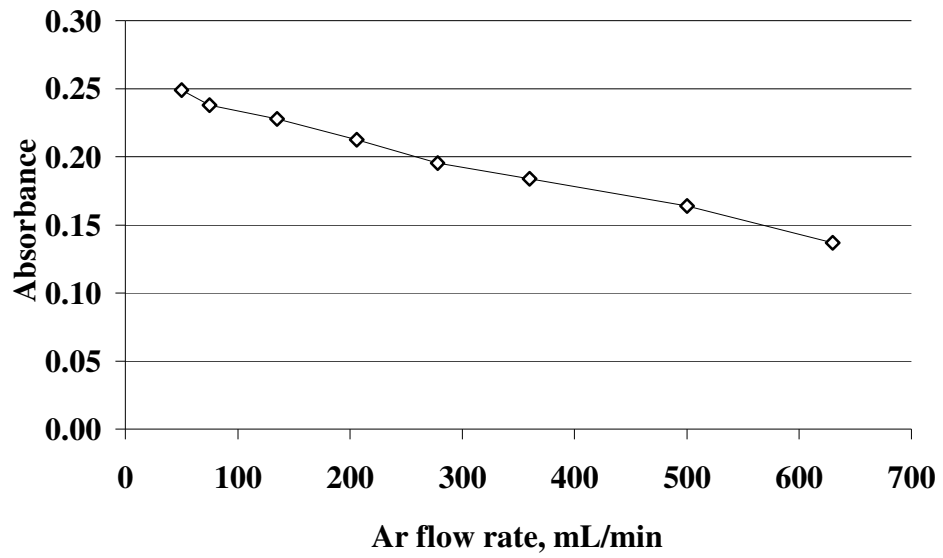


Figure 3.7 Effect of collection Ar flow rate on the peak height of analytical signal for 0.500 mL of 10 ng/mL Bi.

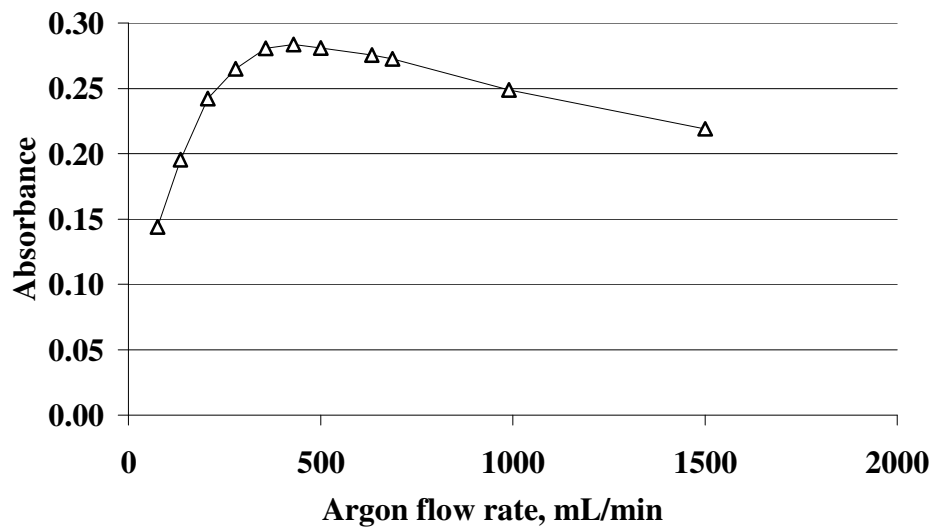


Figure 3.8 Effect of release Ar flow rate on the peak height of analytical signal for 0.500 mL of 10 ng/mL Bi.

3.5.2.2.2 Hydrogen Flow Rate

The effect of H₂ on the collection efficiency was investigated by varying its flow rate during collection while keeping the Ar flow rate constant. The plot of analytical signal versus H₂ flow rate was given in Figure 3.9. It was observed that H₂ which was introduced in the carrier gas did not affect the trapping mechanism as expected since there was generated H₂ already by hydride generation reaction. The slight decrease in the analytical signal at higher flow rates was considered to be the consequence of carrier or cooling effect of hydrogen since the temperature was also effected by the hydrogen flow rate and the trapping temperature was critical for Bi. The effect was also seemed to be not significant during release stage where its flow could not be decreased as for collection since the coil was oxidized and background absorption increased significantly.

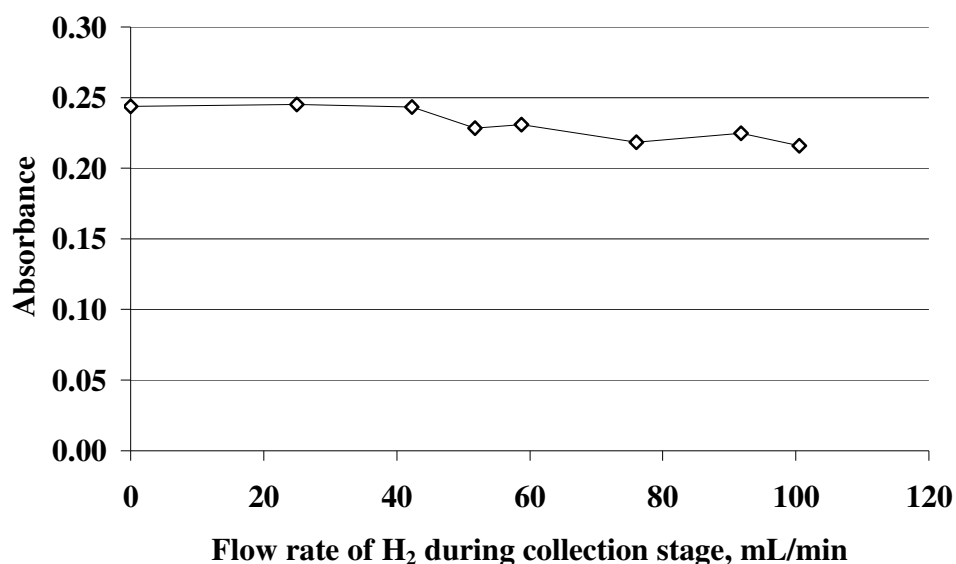


Figure 3.9 Effect of H₂ flow rate in the carrier gas on the analytical signal of 0.500 mL of 10 ng/mL Bi.

3.5.2.3 Stability of Collected Species on the W-Trap

The stability of the trapped species of Bi was investigated by varying the time interval between collection and release stages; the trap was kept unheated in this interval and the carrier gas at its optimum value for releasing step was passed through the HG system. When the time interval between collection and revolatilization stages was varied from 0.5 to 15 minutes, no significant change was observed in the peak height of analytical signal. The trapped Bi species were stable on the coil for at least 15 minutes if the coil was kept unheated.

3.5.2.4 Effect of Cooling Time after Releasing Stage

The effect of cooling time was investigated to see whether there was a need of cooling after each release or there should be an activation stage for the next collection. One of the main advantages of W-coil over graphite cuvette in ETAAS is that it does not need an external cooling system and the coil can be effectively cooled down by the purge gas as its size is small. In the developed methodology, the coil was cooled only by the carrier gas at the flow rates used for transportation of revolatilized species. The results also show that there was no need to wait for cooling and also activation of the surface of W-coil for the next collection. Once the collected species were released from the surface of W-coil, next collection process could be started immediately. Therefore the total analysis period was reduced significantly and was determined mostly by the collection time since the releasing step was completed in a few seconds.

3.5.2.5 Length of Transport Tubing between W-Trap and Atomizer

Although the nature of species released from the W-coil surface was unidentified, it is believed that they were mostly molecular. While volatile species are being

trapped in graphite tubes, first the hydride is decomposed and then analyte species was trapped [71]. Revolatilized analyte species might be atomic or molecular other than hydride. It was expected that if they were atomic, they could not be transported to long distances without being adsorbed on the surface of transport tubings and there should be a decrease in the analytical signal. For the investigation of nature of revolatilized species, they were transported to QTA held at room temperature. In addition, the length of transport tubing between trap and the heated QTA was varied.

When they were sent to an unheated quartz T-tube at a distance of 5 cm, no atomic signal was obtained when 1200 °C was employed for releasing process; the analyte concentration was at ng/mL range. Thus, the revolatilized species were probably not atomic or initially atomic but immediately converted to molecular species after volatilization.

When the distance between W-coil and the junction point of quartz T-tube atomizer heated by the flame was 2-3 cm, the temperature of coil was elevated to 350-400 °C by the flame. At this temperature, the trapped species were not stable on the coil surface and thus sensitivity and reproducibility was degraded. The W-trap was placed further away from the quartz T-tube after separating it in order to investigate the transport ability of released Bi species to long distances. The W-coil trap was separated from quartz T-tube and placed into a piece of quartz tube identical in size to the inlet arm of quartz T-tube atomizer. The length of tygon transport tubing between the trap and atomizer was varied between 10 cm and 200 cm. The change in both peak height and peak area of the analytical signal was given in Figure 3.10. When the transport length was increased to 200 cm, peak height signal was decreased to 28% of its value obtained at 10 cm. If the peak area was considered, the analytical signal was decreased to 76 % of that obtained at 10 cm, which indicates significant peak broadening. The decrease in the analytical signal was mostly due to dilution of volatile analyte species during transportation since the peak height was much more affected than peak area. Furthermore, it was

also observed that as the length of transport tubing was increased from 10 cm to 200 cm, the analytical signal was tailed and the base-width of the signal increased from 0.4 s to 0.8 s. Rather efficient transport properties of the released species indicate that they are probably molecular and the W-coil trap can be used as an ETV device for sample introduction for the determination of Bi by ICP-OES or ICP-MS, as well as by quartz T-tube atomizer.

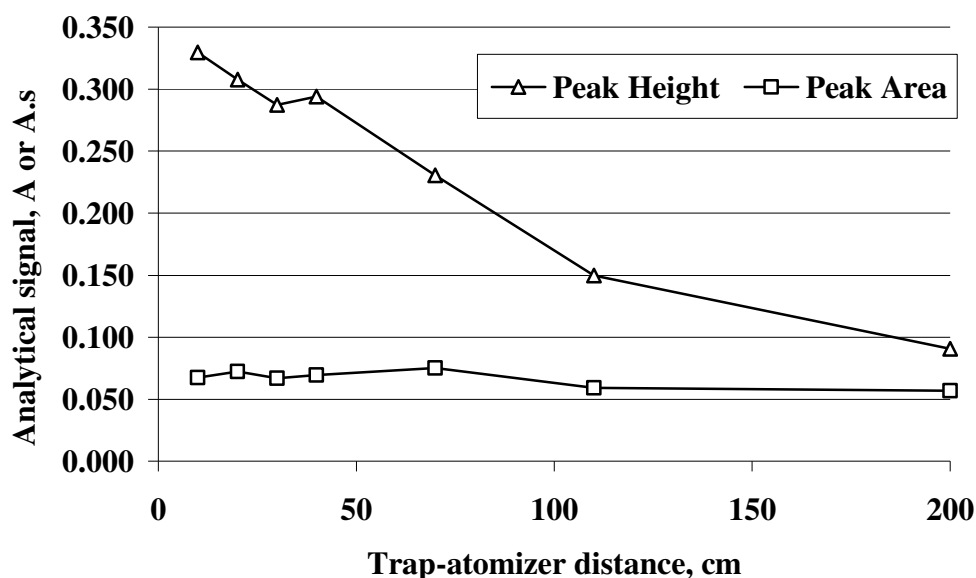


Figure 3.10 Analytical signal versus trap-atomizer distance for 0.500 mL of 10 ng/mL Bi (5.0 ng Bi).

3.5.3 Relation between Collection Volume and Analytical Signal

The relation between the analytical signal and the collection volume was investigated using a 0.100 ng/mL Bi solution in CF mode; the results were displayed in Figure 3.11. The analytical signal increased linearly with collection volume and the linearity was verified between 6.0 and 60 mL with a squared correlation coefficient of 0.998. Under the experimental condition, it took 10 minutes to collect 60 mL of sample. Since the analysis time increased, the

collection volume was not increased further. The linearity of the plot showing sample volume versus analytical signal was also demonstrated for smaller sample volumes (not shown here), ranging in 0.500 to 6.5 mL for 0.50 ng/mL of analyte solution in FI mode with a better correlation coefficient; the equation of the best line was $y = 0.0372x + 0.0034$ ($R^2 = 0.999$).

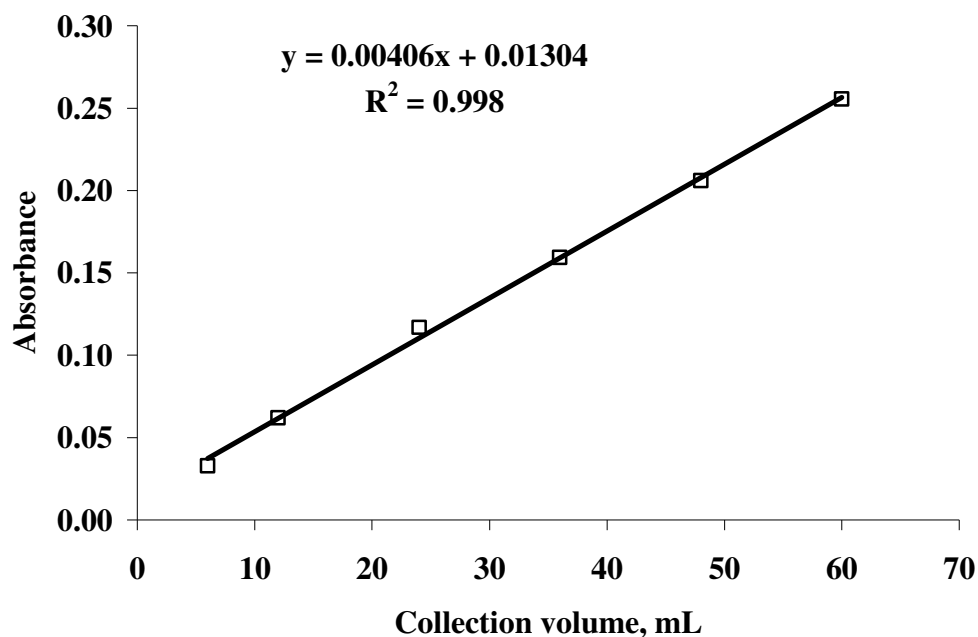


Figure 3.11 Analytical signal versus collection volume for 0.100 ng/mL Bi in 1.0 mol/L HCl; collection temperature, 270 °C; release temperature, 1200 °C.

The blank signal started to become significant when the injection volume was increased to 25 ml. The concentration of Bi in the reagent blank was found to be 0.0056 ng/mL. In this study, no purification process was applied to reagents. If the reagents blank values are reduced, the sample collection volume can be increased up to at least 60 mL since the linearity is conserved. The option of high sampling volume is advantageous in case of strong interferences in the sample, since the dilution of sample is a way of decreasing chemical interference in the hydride generation [5]. Higher collection volumes can be employed after diluting the

sample solution; instead of injecting 1 mL of sample solution, a volume of 10 mL could be injected after diluting it 10 times with blank solution. This was not shown for Bi since there was no such interference but proven for Cd in the analysis of SRMs for the accuracy check.

The choice of collection volume was determined by the concentration of analyte in the sample solution and by the matrix interferences encountered. The sampling rate was also depended on the collection volume. It is better to choose appropriate sampling volume by considering these factors. The collection volume was 18 mL (3 min collection) for the analysis of geological SRMs and 36 mL (6 min collection) for drinking water SRM.

3.5.4 Analytical Signal and Reproducibility

The analytical signal obtained from 36 mL of 0.100 ng/mL Bi (3.6 ng Bi) and that obtained from 36 mL of 0.020 ng/mL Bi (0.72 ng Bi) were shown in Figure 3.12, respectively. An increase of five-fold in concentration results in approximately five times increase in the analytical signal. The base-width of analytical signal is almost the same for both 6.5 mL of 0.500 ng/mL Bi (not shown here) and 36 mL of 0.020 ng/mL and does not depend on the analyte concentration or sample volume.

The replicate measurements of 0.010 ng/mL gave 5.8% and 3.2% RSD (based on peak height) for 18 mL (n=13) and 36 mL (n=7), respectively. The overall reproducibility of the peak height signal obtained in the linear range varied between 2-6% for RSD values. On the other hand, since the residence time of the analyte species was very short on the light path, the low integrated absorbance values were affected significantly by the lamp noise. Although the integration time was chosen as 1.5 s in order to minimize the effect of lamp noise on peak area values, the integrated absorbance values obtained from 0.010 ng/mL gave 27% and

13% RSD for 18 mL (n=13) and 36 mL (n=7), respectively; therefore use of peak height was preferred. However the peak area was also found to be well correlated with the concentration.

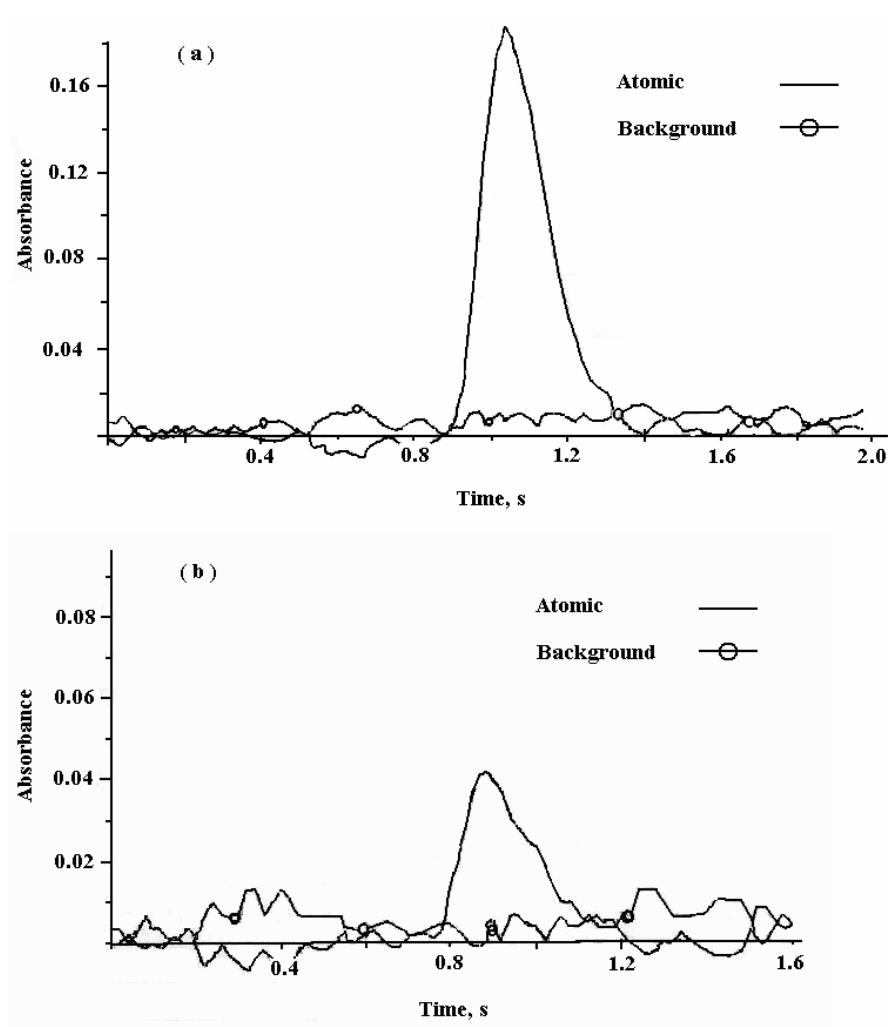


Figure 3.12 The analytical signals for Bi. Collection at 270 °C and releasing at 1200 °C. a) 36 mL of 0.100 ng/mL Bi (3.6 ng Bi), b) 36 mL of 0.020 ng/mL Bi (0.72 ng Bi)

3.5.5 Calibration Plot

The calibration plot drawn by using peak height and peak area for 18 mL of aqueous standard solutions was given in Figure 3.12. It was found that the plot was linear between the concentrations of 0.030 ng/mL and 0.500 ng/mL Bi when drawn for peak height of the analytical signal with a collection volume of 18 mL sample volume (3 min collection). Above this concentration, a slight deviation from the linearity was observed. The peak area was also found to be linearly correlated with the concentration, but the precision of the measurements was poor. The calibration plot for 6.5 mL and 36 mL collection volume was also linear between 0.5 and 2 ng/mL ($y = 0.2917x + 0.0327$ and $R^2 = 0.988$) and 0.020 ng/mL and 0.500 ng/mL ($y = 1.4213x + 0.0116$ and $R^2 = 0.998$), respectively.

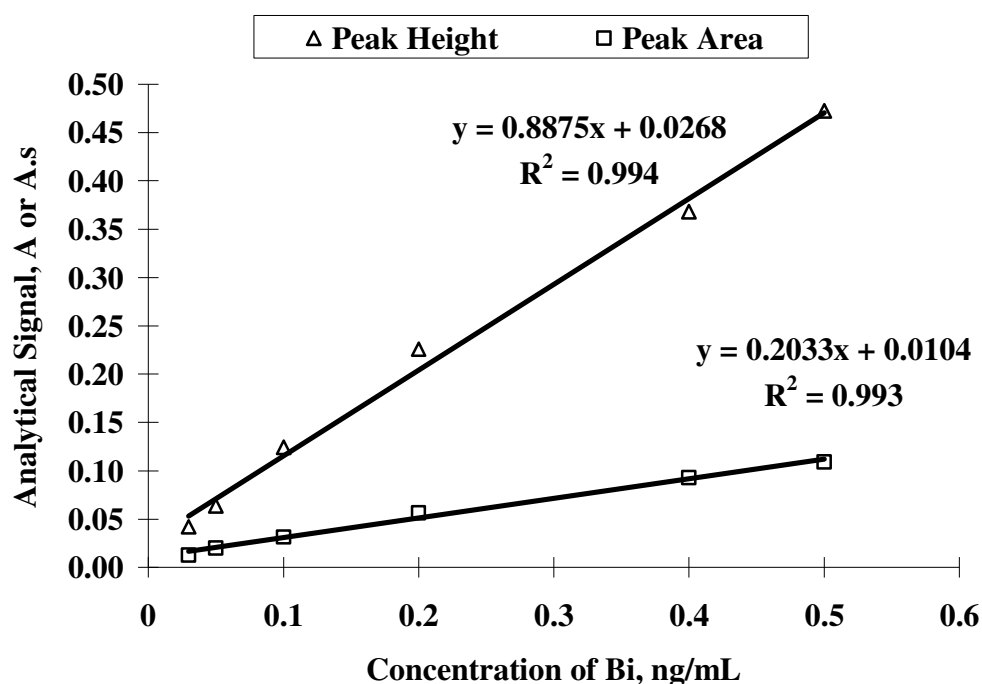


Figure 3.13 The calibration plot drawn by using peak height and peak area for 18 mL of aqueous standard solutions of Bi under optimum conditions.

3.5.6 The Analytical Figures of Merit

The analytical figures of merit of the method, which were calculated by using the peak height values of analytical signal, were given in Table 3.1. The enhancement factor in limit of detection (3σ) which was calculated by using 0.0156 ng/mL (including blank value which contains 0.0056 ng/mL Bi) is found to be 150 for 18 mL collection volume (for 36 mL it is 270) when compared to conventional FI-HGAAS. The characteristic concentration for 18 mL sample volume is calculated as 0.0023 ng/mL (per 0.00436 absorbance unit corresponding to 1% absorption) which was 130 times lower as compared to conventional FI-HGAAS. When peak area was used for these parameters the results were not as satisfactory as peak height values since obtained signals were so sharp that integrated absorbance values were numerically small and were affected by the lamp noise thus the %RSD values increased. The reagent blank value was another limitation for further improvement in the analytical figures of merit for the new technique. No purification method was applied in order to reduce blank values.

The total efficiency of W trap for collection and revolatilization of Bi species were calculated using the peak area values obtained under the same carrier gas flow rates. During these calculations the total efficiency of conventional HGAAS was assumed to be 100%. The total efficiency of W-trap was found to be 23%.

Table 3.1 Analytical figures of merit and enhancement factors for Bi calculated by using peak height of analytical signal.

	FI-HGAAS ^a	W-Trap HGAAS ^b	Enhancement Factor
Limit of detection, ng/mL	0.410	0.0027	150
Characteristic concentration, ng/mL	0.290	0.0023	130

a The parameters were calculated by 10 replicate measurements of 0.500 mL of 1.0 ng/mL Bi solution.

b The parameters were calculated by 10 replicate measurements of 18 mL of 0.010 ng/mL Bi solution.

The limit of detection of the developed method is compared with the literature values in Table 3.2. As seen on the table, the concentration limit of detection value is comparable with the others or better. Although absolute limits of detection of MS systems are better than that of the method presented here, their use is prohibited by high cost and they are not available in most laboratories. The main advantage of W-coil HGAAS is that it can be applied inexpensively in all laboratories having a simple AAS instrument. The time required for the analysis depends on the collection time. When Bi concentration in the sample solution is in the low ng/mL range, approximately 30 s was enough for both collection and the measurement of analytical signal. If the concentration is in the pg/mL range, 3-5 minutes are enough for both collection and measurement of analytical signal. No memory effect was encountered in the experiments.

Table 3.2 Comparison of the limit of detection and the sample volume of the method with those of others in literature.

Method	Concentration LOD, ng/mL	Absolute LOD, pg	Sample Volume, mL	Reference Number
W-Trap HGAAS	0.0027	49	18	This study
Precipitation ETAAS	0.016	8	0.5	108
Electrodeposition ETAAS	0.0078	78	10	70
Direct Injection Nebulization ICP-MS	0.0097	0.19	0.020	115
Microcolumn Preconcentration FI-ICP-AES	0.030	3000	100	116
<i>In-situ</i> trapping HG-ETAAS	0.020	100	5	124
<i>In-situ</i> trapping ETV-ICP-MS	0.003	6	2	94

3.5.7 Accuracy of the Method

The accuracy of the method was tested using a certified reference material CRM, Trace Metals in Drinking Water (Cat No CRM-TMDW Lot # 818921) supplied from High Purity Standards (Charleston, USA) and geological standard reference materials of GSJ (Geological Survey of Japan) JR-1 and JR-2. Determination in CRM-TMDW was carried out by diluting 1.0 mL of CRM to 100 mL with 1.0 mol/L HCl, resulting in a solution of approximately 0.1 ng/ mL in Bi. For the analysis of water reference material the sampling volume was selected as 36 mL for both standards and sample. The analysis was performed by direct calibration method.

The geological standard reference materials were analyzed by two different procedures; by direct injection of digested solutions (P1) and the analysis of solutions after further dilution (P2). In both cases no adverse effect was observed in any glass or quartz part of the system because of the presence of unconsumed HF remaining from the dissolution procedure. The results (n=3 for each analysis) given in Table 3.3 were in good agreement with the certified values. The t-test was applied to results assuming the certified values are the true values. The results passed the t-test at 95% confidence level. Aqueous standard solutions were used for the calibration plots; standard addition method was not needed or used.

Table 3.3 Results of the analysis of standard reference materials and their certified values (n=3 for each measurement)

SRM	P 1 ^a	P 2 ^b	Certified Value
GSJ JR-1 (µg/g)	0.51 ± 0.02	0.53 ± 0.03	0.51
GSJ JR-2 (µg/g)	0.62 ± 0.02	0.64 ± 0.01	0.65
CRM-TMDW (µg/L)	-	10.3 ± 1.5	10

a Sample solution was analyzed directly without further dilution

b Sample solution was diluted and then analyzed; for GSJ reference materials, the solutions were further diluted 10 times with 1.0 mol/L HCl; for TMDW, the solution was diluted 100 times with 1.0 mol/L HCl

In hydride generation studies the transition metals interferes with the analyte and usually negatively. These metals also react with sodium tetrahydroborate and reduced to their hydrides or metallic forms. If there are high amounts of transition metal in the analyte solution, inside of GLS, reaction and stripping coil and also the transfer tubing between GLS and atomizer become dark gray which is due to the formation of metallic particulates. The interferences expected from the transition metals were not investigated. The effect is usually measured as the interferent/analyte ratio. However, regardless of the interferent/analyte ratio, the concentration of interferent is also important. In other words, although the ratio is same in two solutions, the interference may not be observed in solution where both analyte and interferent concentration is low. The preconcentration method offer advantage of dilution of analyte solution if the interferent concentration is high. Only the interference effect of copper that is one of the most interfering elements was investigated by preparing the analyte in solution containing different concentrations of Cu. The interference was observed when the concentration of Cu in the analyte solution exceeds 2 $\mu\text{g/mL}$ and the Bi concentration was 10 ng/mL (interferent/analyte ratio was 200).

The interferences expected from the transition metals were not investigated. However analyzed solutions from P1 for geological reference materials contained high amounts of Si (10^6 times Bi), Al (10^5 times Bi), Fe (10^4 times Bi), Ti (10^3 times Bi), Ca (10^4 times Bi), Mn (10^3 times Bi) and Mg (10^3 times Bi), which did not cause any matrix interference; the values in the parenthesis are the ratios by weight . The water standard reference material contained high amounts of Ca, Mg, Na, K, Sr, Al, Fe, As and Zn whose concentrations (by mass of species) are 3500, 900, 600, 250, 25, 12, 10, 8 and 7 times higher than the Bi concentration, respectively. The fact that there was no need for standard additions to obtain accurate results strongly supports the absence of interferences.

It should be noted that high sensitivity of our method is an advantage regarding interferences. For example, although the mass ratio of interferent to analyte was 1000 in both our work (for the geological reference materials GSJ JR-1 and GSJ JR-2) and elsewhere [167] for Mn, we observed no interference while a signal decrease of 15% was reported by Burns et al. [167]. However, it should also be noted that in our case Bi concentration in final sample solutions was about 0.20 ng/mL, while the same value was reported as 500 ng/mL by Burns et al. [167]; therefore corresponding interferent mass in our case is much lower although interferent/analyte ratio was same in both studies. The similar trend was also reported in another study [70] where although the same ratio was 10000 and no interference was observed; the concentration of Bi was reported as 0.5 ng/mL. It is also well known that Cu is an interferent in HGAAS determination of Bi. During the determination of Bi in geological SRM samples, Cu/Bi mass ratio was only 3; no interference effect was observed. Elsewhere, a signal reduction of 37% [70] was reported when the same mass ratio was 10000; 77% and 100% signal reduction were reported for Cu/Bi mass ratio values of 20 and 200, respectively [167]. Therefore in case of high Cu concentrations interference should be expected.

3.6 Cadmium

3.6.1 Atom Cell

Since the generated volatile species, presumably cadmium hydride, are unstable and quickly decompose to the atomic Cd vapor and H₂ [7], there was no need for externally heated quartz T-tube atomizer. Therefore unheated quartz T-tube could be used as atom cell for Cd throughout the experiments. Furthermore, heating the QTA resulted in a decrease in the analytical signal due to the lowered residence

time of Cd atoms in the cell because of thermal expansion of gases at elevated temperatures. When the QTA was heated by air/acetylene flame, the analytical signal was decreased approximately by one half. This observation was consistent with the findings of Sanz-Medel et al. [7]. Therefore, during Cd studies the quartz T-tube was not heated and kept at room temperature. The ends of T-tube were not covered with quartz plates as in the case of Hg in CV. When both ends were covered, the analytical signal decreased slightly. This reduction was probably due to the absorption of stable Cd atoms outside the quartz T-tube when they left the horizontal arm at both ends. When the ends were covered, the pathlength was reduced as compared to the case with no windows. The change in the signal magnitude was also related with the exhaustion hood flow rate and the movements of air around the cell [168].

3.6.2 Optimization of Vapor Generation Parameters

3.6.2.1 General Considerations in the Vapor Generation of Cd by Tetrahydroborate Reduction

In the literature there are different conditions of vapor generation which are not consistent with each other [135]. When compared to other hydride forming elements, the generation of volatile species of Cd by the reduction with NaBH_4 is rather problematic mostly due to instability of cadmium hydride. The instability of CdH_2 was explained by substantial differences in the electronegativities of Cd and H atoms and less pronounced covalent character of the bond [135]. The rather less covalent character makes the VG reaction incomplete and there remains ionic Cd species in the GLS which may subsequently be converted to its hydride in next runs. Therefore, it was mentioned in the same report that there should be more than one set of optimum conditions for Cd for efficient VG. It requires careful control of acidity of both analyte and the carrier solutions since the concentrations

are very critical and the optimum ranges are very narrow. For common hydride forming elements, such as As and Se, the acidities of sample and the carrier solutions are not very critical and usually they are the same. However, this is not valid for Cd for which the optimum HCl concentration in sample solution is usually different from that in the carrier solution.

It was observed that the presence of O₂ in the carrier gas (Ar) strongly decreases the analytical signal. The presence of 1% O₂ in the stripping gas decreased the analytical signal to about one third of the original signal. This may be attributed to inefficient hydride generation: probably in the presence of O₂ some of the Cd could not be converted to hydride but instead its oxide is produced which is not volatile and quickly decomposes in the reaction medium. Use of H₂ alone as the carrier gas did not change the analytical signal.

Lampugnani et al. [135] summarized the literature data on the vapor generation of Cd by tetrahydroborate reduction. The optimum conditions showed significant variations from one study to another. Usually high concentrations of tetrahydroborate were utilized (3-5% (w/v) as Na or K salts). The concentration of HCl was usually in between 0.2-0.5 mol/L in CF or FI mode [135].

3.6.2.2 Concentration of HCl in Sample and Carrier Solution

The optimum acid concentration in the sample and the carrier solution was determined by FI-HGAAS and were interrelated; depending on the former, the optimum value of latter changes. When using univariate approach, multi-cycling was necessary to find the optimum value. The optimization plots of sample and the carrier acidity for FI-HGAAS were shown in Figure 3.14.

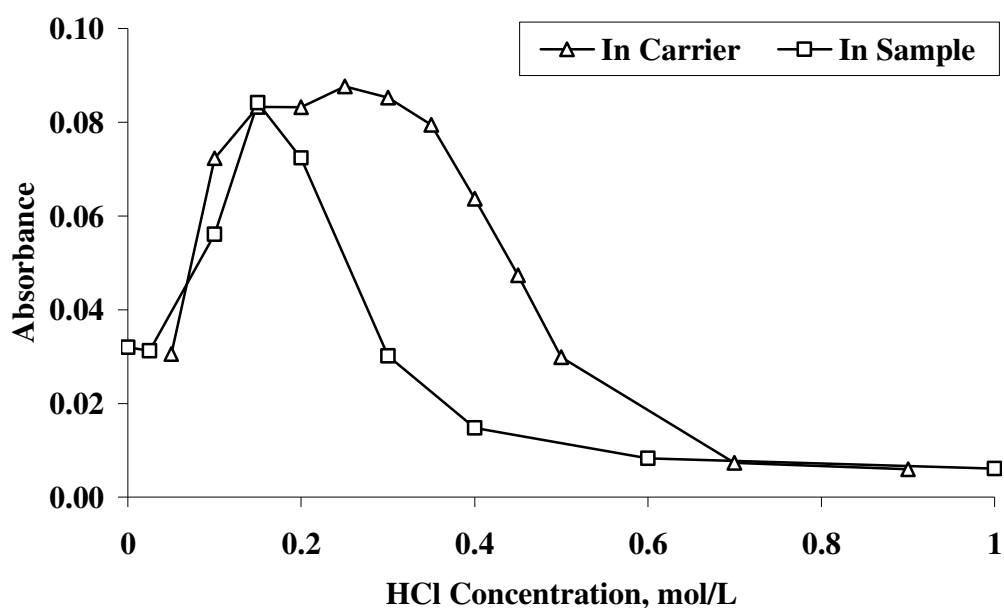


Figure 3.14 Effect of HCl concentration in sample and carrier solutions on the analytical signal of Cd obtained by conventional FI-HGAAS. Carrier solution and sample solution acidities were 0.25 mol/L and 0.15 mol/L HCl, respectively, as the other parameter was varied. 0.500 mL of 1.0 ng/mL Cd was used in the experiments.

The optimum concentration of HCl in the carrier solution was investigated by keeping the HCl concentration in analyte solution at 0.15 mol/L. As it is seen, the analytical signal did not change significantly when the concentration of HCl in the carrier was in between 0.15 and 0.35 mol/L. However, since the signal obtained with 0.25 mol/L HCl was slightly higher and located at the midpoint of the plateau, this value was selected as the optimum HCl concentration in carrier solution in FI studies. The optimization of sample acidity was carried out by keeping the carrier concentration at its optimum value, 0.25 mol/L. The sample acidity was found to be more critical and slight variations resulted in a significant change in the analytical signal. Therefore a concentration of 0.15 mol/L was found to be optimum HCl concentration in sample solution. Almost no signal could be obtained when the concentration of HCl in either solution exceeds 0.8 mol/L.

Therefore, in FI-HGAAS the concentration of HCl in both solutions, especially in sample solution must be carefully controlled.

The effect of sample acidity was also investigated in CF mode, since the trapping experiments were conducted in this mode. These experiments were conducted under trapping conditions. First, the generated species were trapped and then released from the trap. The optimization graph was given in Figure 3.15 for both peak height and peak area. The acidity of sample solution was again found to be critical. Maximum signal was achieved when the concentration was 0.2 mol/L. Therefore the solutions of Cd were prepared in 0.2 mol/L HCl in CF W-trap HGAAS experiments.

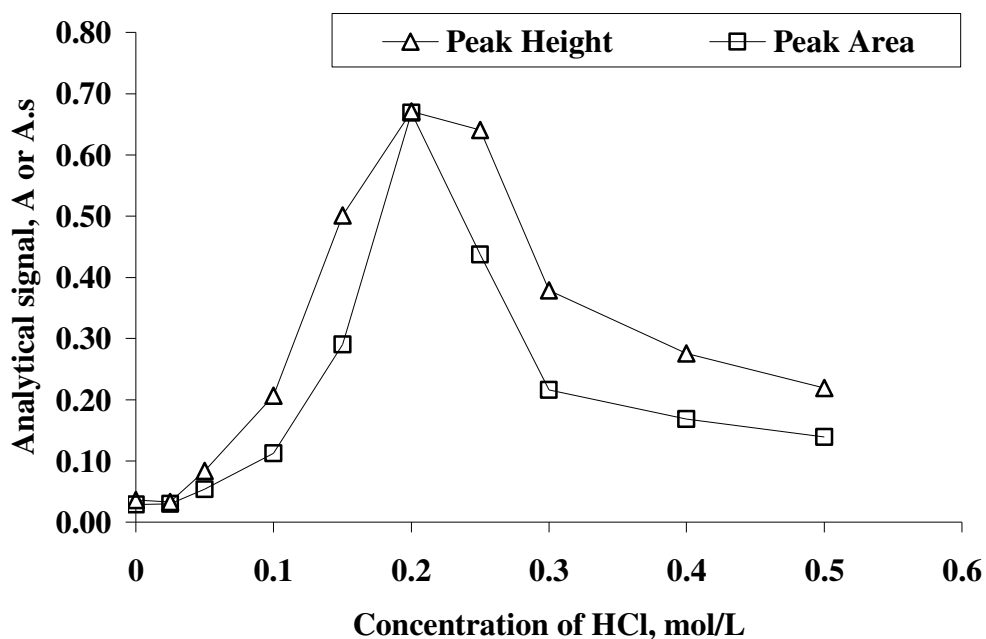


Figure 3.15 Effect of HCl concentration in the sample solution on the analytical signal of Cd obtained from W-trap system in CF mode. The signals were obtained by collecting 0.7 mL of 10.0 ng/mL Cd, a total of 7.0 ng Cd.

3.6.2.3 Concentrations of NaBH₄ and NaOH in Reductant Solution

The effect of reductant concentration was investigated both in FI mode using conventional HG, and in CF using trap system. The change in the analytical signal with respect to reductant concentration for FI-HGAAS (without trap) was given in Figure 3.16. It was observed that the signal increases up to a concentration of 1.2% (w/v) and then decreased. The decrease can be explained by the dilution effect since more H₂ was generated at higher concentrations of reductant. In CF-W-trap-HGAAS, such decline was not observed since the analytical signal was obtained after preconcentration. The relevant graph was given in Figure 3.17. The signal increased with increasing reductant concentration and stayed almost constant after 1.5% (w/v) up to 3% (w/v). A slight increase in the signal was not found to be significant and 1.5% (w/v) was selected as the optimum value. When compared to literature values, 3-5% (w/v) [135], the optimum concentration of tetrahydroborate was significantly lower. This may be attributed to the use of small volume GLS and lower flow rates of solutions. In the preliminary studies, U-type GLS was used and the optimum concentration of reductant was found to be higher than that found here; the analytical signal increased up to a concentration of 3% (w/v) NaBH₄.

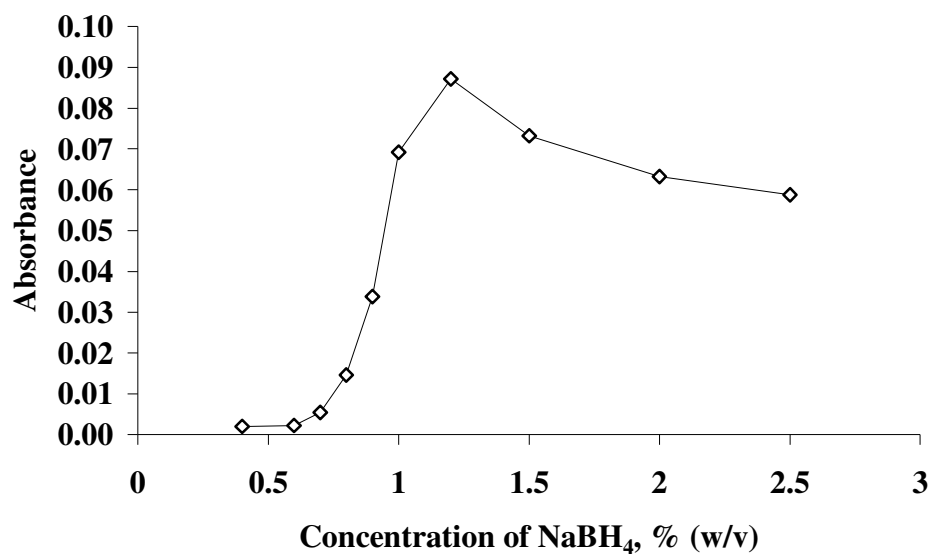


Figure 3.16 Effect of NaBH₄ concentration on the analytical signal of Cd obtained in conventional FI-HGAAS. The concentrations of HCl were 0.15 and 0.25 mol/L in sample and carrier solutions, respectively. 0.500 mL of 1.0 ng/mL Cd was injected.

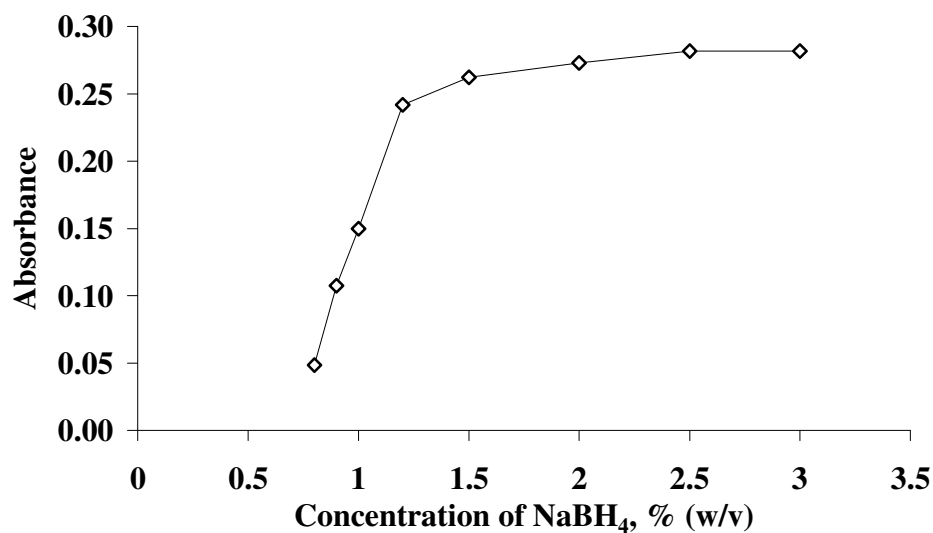


Figure 3.17 Effect of NaBH₄ concentration on the analytical signal of Cd obtained from CF-W-trap system. The signals were obtained by collecting 0.7 mL of 5 ng/mL Cd, a total of 3.5 ng Cd.

Concentration of NaOH used for the stabilization of NaBH₄ was also found to have a significant effect on the analytical signal. Its concentration was optimized in FI mode by conventional HGAAS. The variation in the analytical signal as a function of NaOH concentration was given in Figure 3.18. The highest HG efficiency was obtained when the concentration of NaOH was between 0.1 and 0.2% (w/v) so 0.15% (w/v) was selected as the optimum concentration.

Although the molarity of NaOH in NaBH₄ was about ten times lower than that of HCl in the sample solution, it has a significant effect on the hydride generation efficiency. When both solutions were merged, the pH of the reaction solution was determined by concentrations of HCl and NaOH. Since Cd is susceptible to change in the concentration of HCl in the sample solution, the concentration of NaOH in the reductant solution affected the HG efficiency. The pH of the reaction and also the equilibrium in the gas liquid separator was so critical that during the experiments when a solution having a different acid concentration was injected, the reproducibility was lost.

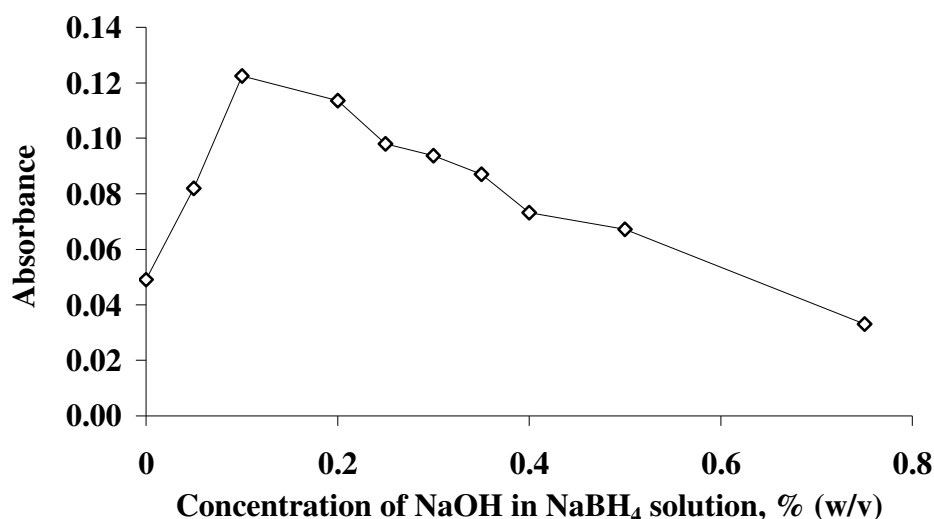


Figure 3.18 Effect of NaOH concentration in reductant solution on the analytical signal of Cd obtained in conventional FI-HGAAS. The signals were obtained by collecting 0.500 mL of 1.0 ng/mL Cd in 0.15 mol/L HCl. Carrier acidity was 0.25 mol/L HCl.

3.6.2.4 Reaction and Stripping Coil Lengths

These two parameters were found to be so dependent on each other that even one could be even eliminated by increasing the length of the other. The experiments were carried out in both conventional FI mode, and W-trap HGAAS in CF mode. The optimization plots for reaction and stripping coils were given in Figure 3.19. The optimum reaction coil length was found to be 60 cm when a 15 cm stripping coil was used. Although shorter stripping coil seems to be predominating, the minimum length of stripping coil was 15 cm due to the physical limitations. However, when no reaction coil was used, a length of 120 cm for stripping coil was found to give the same sensitivity with that was obtained by optimum length of reaction and stripping coils. Therefore, the experiments were carried out by employing either a 60 cm reaction coil and a 15 cm stripping coil or no reaction coil and a 120 cm stripping coil; sample, reductant and carrier gas were merged in a 4-way PTFE connector and the generated to GLS through stripping coil.

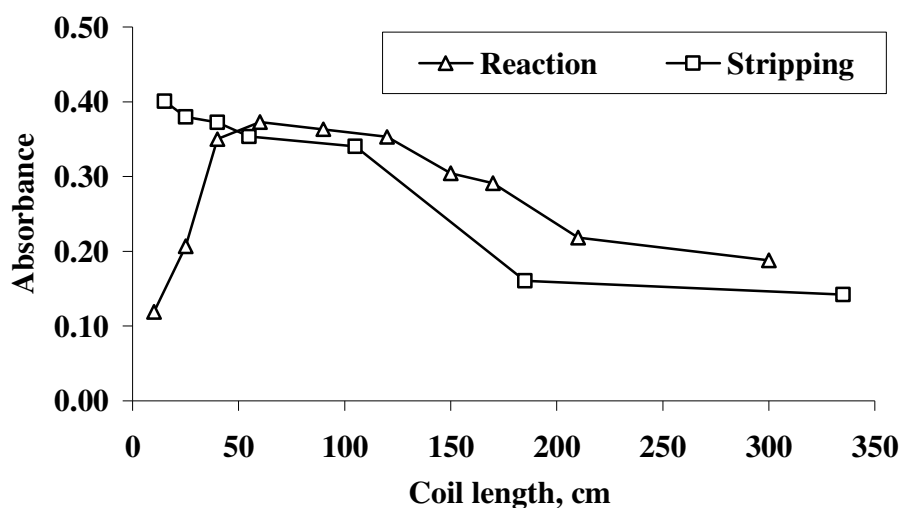


Figure 3.19 Effects of reaction and stripping coil lengths on the analytical signal of Cd obtained in conventional FI-HGAAS. Lengths of reaction and stripping coils were 60 and 15 cm, respectively, as the other parameter was varied. The signals were obtained using 0.100 mL of 5.0 ng/mL Cd in 0.15 mol/L HCl. Carrier was 0.25 mol/L HCl.

3.6.2.5 Reaction Temperature

The effect of reaction temperature on VG of Cd was investigated by using both conventional HGAAS and W-trap system. In order to increase the temperature of reaction coil, it was inserted into a water bath and the temperature was varied by heating water on a hot plate or addition of ice into the bath. Therefore, the effect of temperature was investigated between 0 °C and 98 °C. The plots of reaction coil temperature versus analytical signals of both peak height and peak area obtained from W-trap system are given in Figure 3.20. It was observed that when the temperature of the coil increased, the VG or separation efficiency increased. In the literature there are contradictory statements. Cacho et al. [27] stated the HG efficiency increased with an increase in reaction temperature. However, Sanz-Medel et al. [7] reported that the temperature of reaction has an inverse effect on hydride generation; the lower the temperature, the higher the analytical signal was. The latter group used a cooled system for efficient vapor generation of volatile Cd species. Here, a linear correlation was found between the temperature and the hydride generation efficiency. The analytical signal obtained at 98 °C was about three times higher than that obtained at 25 °C for W-coil HGAAS. Such an increase was also verified by conventional HGAAS in CF mode; the same increase was obtained when the reaction coil was heated. Since the vaporization of water increased at elevated temperatures of reaction solution, the condensation of water on the inner surfaces of GLS, transfer tubings and unheated QTA was increased when the reaction coil temperature was increased. In order to remove the condensed water, the inner surfaces were dried between injections by allowing a flow of Ar at a flow rate of 1 L/min. Although the signal could be increased by increasing the reaction temperature, the experiments were carried out at room temperature, because application is easier since no heating was required. Furthermore, the analysis time was increased due to drying step needed between runs.

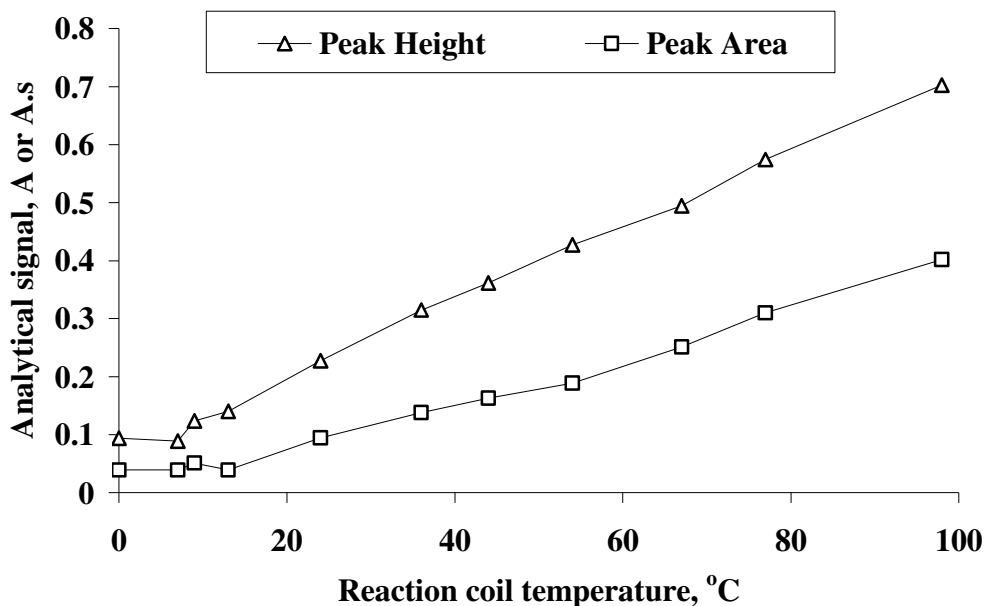


Figure 3.20 Effect of reaction coil temperature on the analytical signal of Cd obtained in CF-W-trap-HGAAS. The signals were obtained by collecting 0.7 mL of 5.0 ng/mL Cd in 0.2 mol/L HCl.

3.6.3 Optimization of Trapping Conditions

3.6.3.1 Placement of W-coil Trap

Since the QTA was not heated by flame and used at room temperature, it was possible to place W-coil as close as possible to the junction point of inlet arm and the horizontal arm. The distance between the trap and the measurement cell was 1 cm which was the minimum attainable distance. The volatile species generated by the HG reaction was trapped on the W-coil and then released as Cd atoms since there was no need to use atomizer as in the cases of Bi and Pb. Therefore, in these studies the W-coil trap was used for both vaporization and atomization of Cd species trapped.

3.6.3.2 Collection and Revolatilization Temperatures

The atomic species of Cd was trapped on the surface of W-coil at relatively lower temperatures when compared to Bi and Pb. The variations in the analytical signal as a function of trapping and releasing temperatures were given in Figure 3.21. The collection temperature range for Cd was relatively wider than that for Bi or Pb. The optimum temperature for collection was found to be between 100 °C and 160 °C. Temperatures higher than 190 °C resulted in a decrease in the signal due to the partial release of trapped species. The trapped species could be revolatilized from the surface at 300 °C completely but the rate of revolatilization was slow. Use of a release temperature less than 750 °C resulted in less reproducible peak heights of analytical signals. A temperature of 1000 °C was used for rapid volatilization that provided more reproducible peak heights.

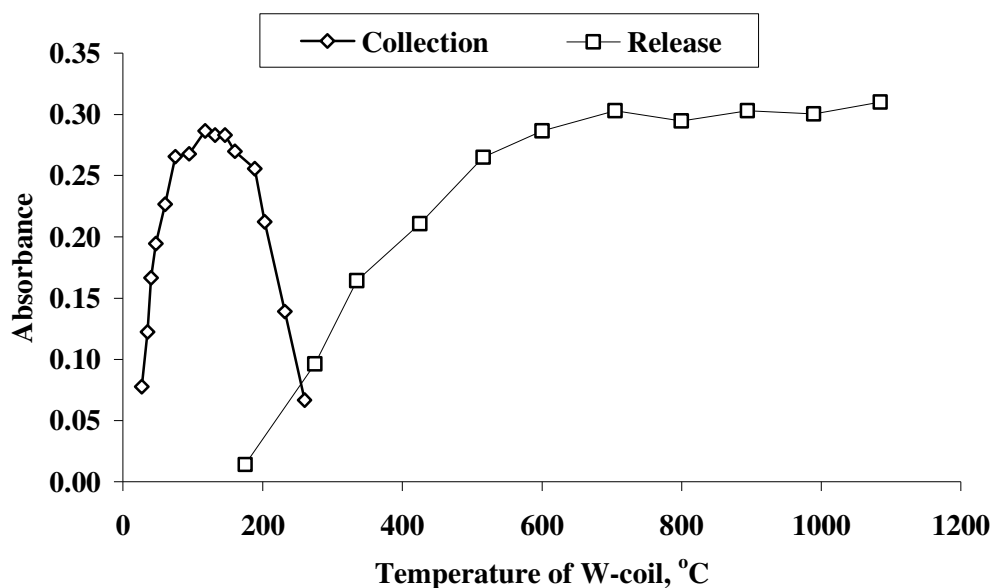


Figure 3.21 The effect of collection and release temperatures on analytical signal for Cd. During the variations of collection and release temperatures, a constant release temperature of 1000 °C and a constant collection temperature of 150 °C, respectively, were employed. The signals were obtained by collecting 0.7 mL of 5.0 ng/mL Cd in 0.2 mol/L HCl.

3.6.3.3 Carrier Gas Flow Rate

The flow rate of H₂ was kept constant at a flow rate at which the oxidation was minimized as in case of Bi and Pb. However slightly higher flow rate of H₂ was required due to higher concentration of NaBH₄ used for Cd. Only the carrier argon flow was varied during the optimization of carrier gas flow rate. The change in the analytical signal as a function of Ar flow rate during collection stage was given in Figure 3.22. The effect was not found to be very critical and the signal remained nearly constant between the flow rates of 150 and 350 mL/min. Above this value, the analytical signal decreased probably they could not find enough time to interact and be captured by W-trap. At lower flow rates, the peak height was also decreased probably due to inefficient hydride separation from the liquid phase and transportation to the trap since the same trend was also observed in conventional hydride generation signal as shown in Figure 3.23. Volatile Cd species must have been separated from the liquid phase and taken into gas phase as soon as possible in order to minimize their re-dissolution in the liquid phase as discussed in previous section where the effect of NaOH concentration was discussed.

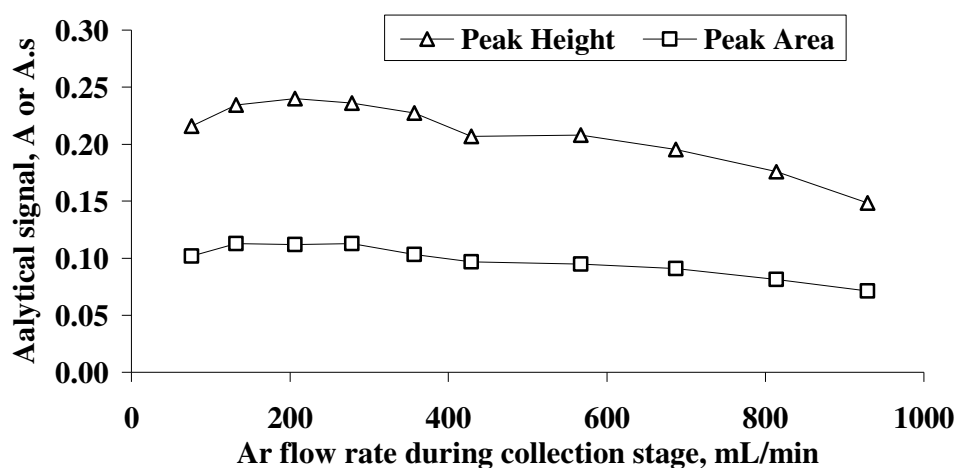


Figure 3.22 The effect of collection Ar flow rate in the carrier gas on the signal of W-trap HGAAS; H₂ flow rate was kept at 150 mL/min. The signals were obtained by collecting 0.7 mL of 5.0 ng/mL Cd in 0.2 mol/L HCl.

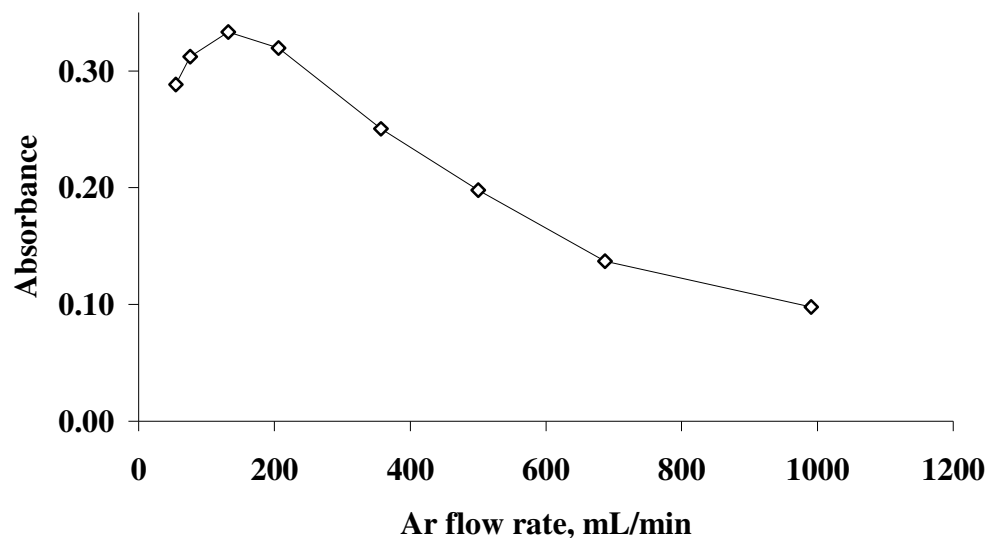


Figure 3.23 Effect of carrier Ar flow rate on the peak height of analytical signal of Cd in conventional FI-HGAAS. The signals were obtained using 0.100 mL of 5.0 ng/mL Cd in 0.15 mol/L HCl. Carrier acidity was 0.25 mol/L HCl.

The effect of Ar flow rate during release stage was not found to be critical for Cd and the relevant graph was given in Figure 3.24. The peak height of analytical signal remained almost constant over a wide range of Ar flow rates between 150 and 800 mL/min. This indicates fast volatilization of Cd atoms from W-trap at 1000 °C. However, the peak area decreased at high Ar flow rates because of short residence time of the atom plug in the QTA. If peak area values are to be used in the experiments, the carrier gas flow rate should be selected less than 200 mL/min. Since peak height values were used, a flow of 270 mL/min was selected as carrier flow rate during both collection and release stages. Therefore similar to Pb, the carrier gas flow rates were the same for both collection and release stages.

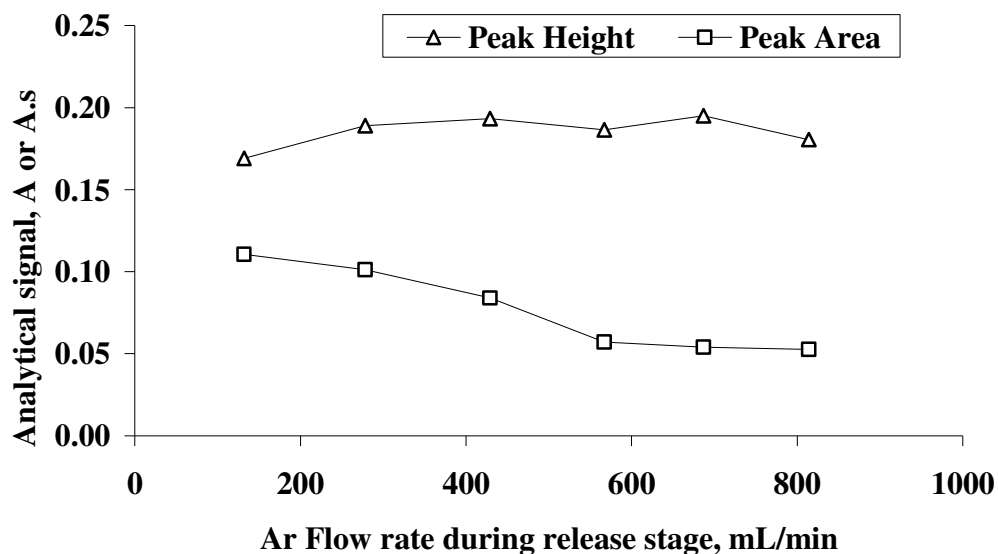


Figure 3.24 The effect of argon flow rate in the carrier gas on the trapping efficiency during collection; H₂ flow rate was kept at 150 mL/min. The signals were obtained by collecting 0.7 mL of 5.0 ng/mL Cd in 0.2 mol/L HCl.

The effect of H₂ on the collection and release processes was also investigated by changing only the H₂ flow rate. In these experiments no reaction coil was used and a 120 cm stripping coil was employed. Hydrogen was introduced at a point between GLS and W-coil; it was not involved in the analyte stripping off the solution. No significant effect of H₂ during collection and release stages were observed.

3.6.3.4 Coating with Pt and Ir

When the W-trap was coated either by Ir or Pt, the collection efficiency did not improve. However, the trapping temperature range extended to lower temperatures: the Cd species trapped efficiently at even room temperature when

the coil was coated with 100 μg of Ir. The highest limit of optimum collecting temperature did not improve and above a collection temperature of 190 $^{\circ}\text{C}$ the analytical signal decreased which meant that Ir did not stabilize Cd species at higher temperatures but increased trapping efficiency at lower temperatures. When W-coil was coated with Pt, the stabilization effect was not significant as for Ir. Iridium as a coating material showed higher stabilization effect at lower temperatures. However, use of these coating materials increased the revolatilization temperatures to above 1300 $^{\circ}\text{C}$ and 1500 $^{\circ}\text{C}$, for Pt and Ir, respectively.

3.6.3.5 Distance between Tip of Transport Capillary and W-trap

Use of PTFE tubing (0.8 mm i.d.) for the transportation of volatile species of Cd to the W-trap allowed to be inserted into inlet arm of quartz T-tube. Therefore, the interaction of Cd species with the inlet arm of quartz T-tube atomizer was minimized. This configuration prevented the possible losses of Cd species on the surface of inlet arm before being collected by W-trap. Since the outer diameter of capillary by which the volatile species were transported to W-trap was smaller than the inner diameter of inlet arm, the capillary was directed into the center of W-coil by using a cladding formed by PTFE tape so that it was fixed at the center of inlet arm. The effect of this distance on the analytical signal was shown in Figure 3.25. It was observed that as the distance between tip of capillary and the W-trap increased, the analytical signal decreased probably due to loss of analyte species on the inner surface of inlet arm. The trapping efficiency was at maximum when the distance was 0.5 cm; shorter distances resulted in degradation of tip made of PTFE since this part was heated to high temperatures at the releasing stage. Therefore during the experiments the distance was kept at its optimum value. When it was varied between release and collection stages, the reproducibility became poorer.

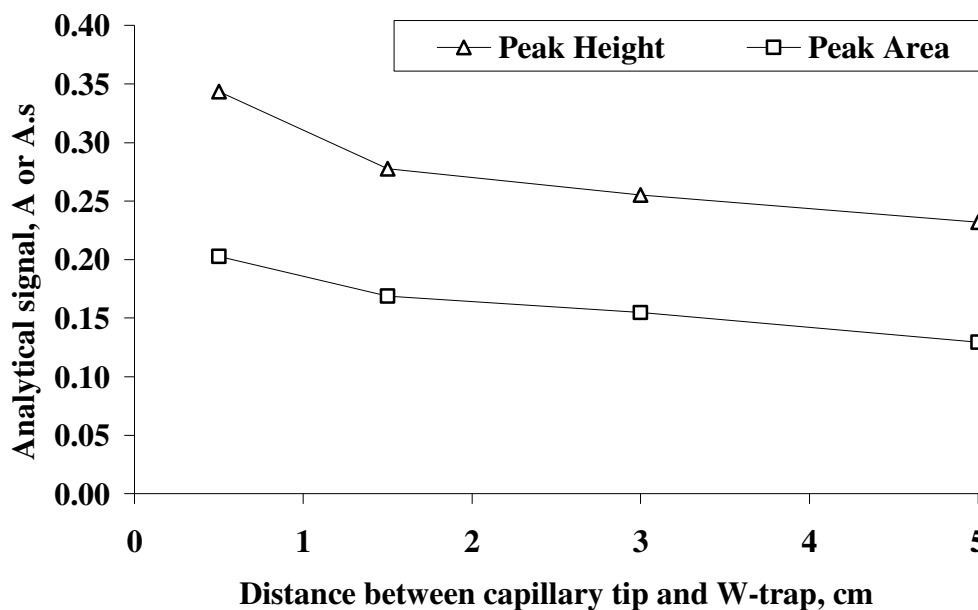


Figure 3.25 Effect of distance between capillary tip and the W-trap on analytical signal. The signals were obtained by collecting 0.7 mL of 5.0 ng/mL Cd in 0.2 mol/L HCl. Collection and release temperatures were 150 °C and 1000 °C, respectively.

3.6.3.6 Stability of Collected Species on the W-Trap

In order to investigate the stability of collected species on the W-coil, the trapped species were released after a period of time. The effect of this time interval between end of the collection step and release step on the analytical signal was given in Figure 3.26. It can be concluded from the figure that the trapped species were stable for at least 12 min. During this period of time, the W-coil was kept at room temperature and the carrier gas passed through the trap. A slight increase was observed when the collected species were released after waiting for a period of 60 seconds. During collection, the inlet arm between W-coil and horizontal arm was heated slightly by the trap and this might decrease the signal by trapping released Cd atoms on quartz surface. When the revolatilization was done

immediately after the collection, signal is reduced. However, this decrease was not significant and the analysis time was increased if a cooling period was used. Therefore no such cooling period was applied during the experiments.

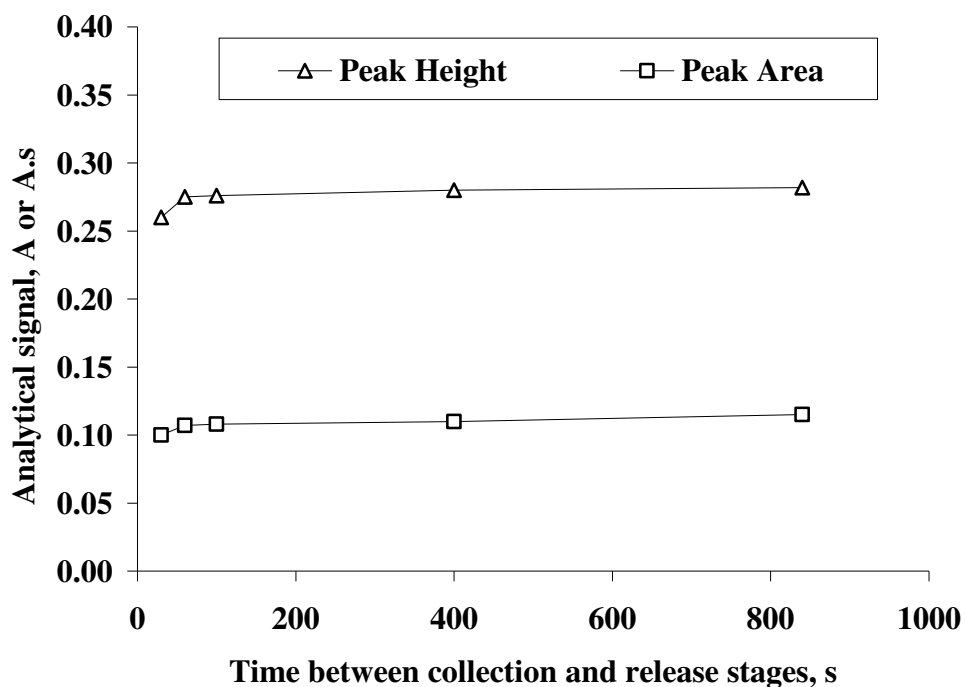


Figure 3.26 Effect of time between collection and release stage on the trap signal of Cd. The signals were obtained by collecting 0.7 mL of 5.0 ng/mL Cd in 0.2 mol/L HCl. Collection and release temperatures were 150 °C and 1000 °C, respectively.

3.6.3.7 Effect of Cooling Time after Releasing Stage

One of the main advantages of W-coil used in the ETAAS systems is its fast cooling rate after each atomization or vaporization cycle. The flow of purge gas was sufficiently high for effective cooling. The length of cooling period after each releasing stage was investigated to observe whether there was a need for cooling between runs or there was a need for activation of W-coil before each collection

cycle. The effect was investigated between 15 s and 7 minutes and the graph was given in Figures 3.27. Only the carrier gas passed through the system at its regular flow rate for both collection and release. The analytical signal did not depend on the cooling time. Moreover, there was no need for the activation of W-coil trap before collection. It can be concluded from the figure that the next collection step can be started just after the release stage. Therefore the analysis time depended on the collection time since the revolatilization took just a few seconds.

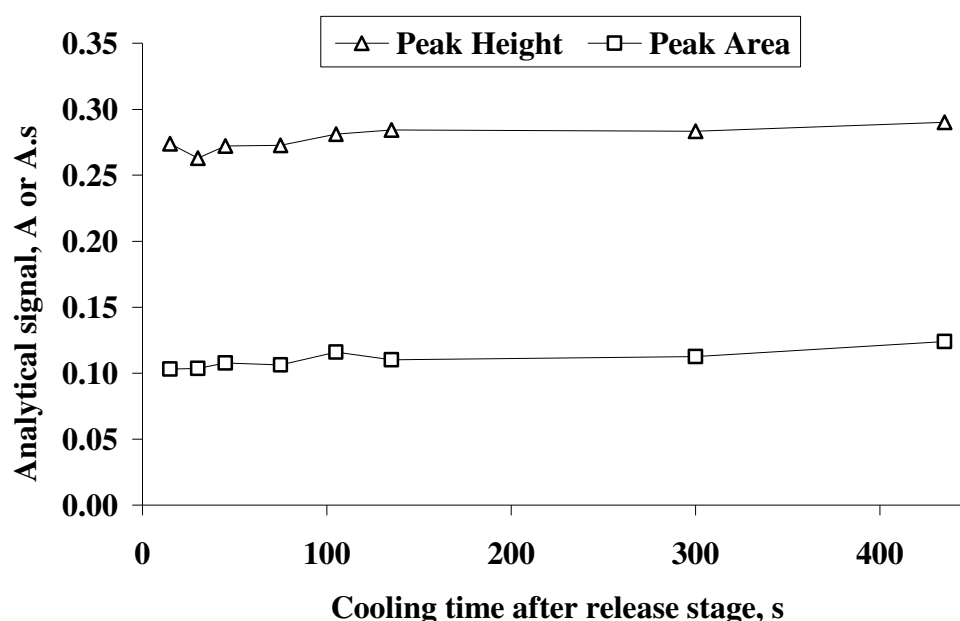


Figure 3.27 Effect of cooling time after each revolatilization stage for Cd. The signals were obtained by collecting 0.7 mL of 5.0 ng/mL Cd in 0.2 mol/L HCl. Collection and release temperatures were 150 °C and 1000 °C, respectively.

3.6.3.8 Length of Transport Tubing between GLS and W-Trap

In conventional HGAAS studies, it was observed that as the distance between GLS and the atom cell increased, the peak height of analytical signal decreased. However, when it was investigated for W-coil HGAAS, such decrease was not

observed. The variations in the analytical signal for peak height and peak area measurements are given in Figure 3.28. The generated Cd species by the reaction with tetrahydroborate could be transported at a distance of at least 70 cm without any significant decrease in the analytical signal by W-coil HGAAS. Thus, the decrease in the peak height of analytical signal obtained by conventional FI-HGAAS (no trap) can be explained by dilution of analyte species but not the loss on the surfaces. But it must be noted that the analyte species were transported through the PTFE tubing (0.8 mm i.d.). If it were transported through a glass tubing, loss on the surfaces was expected; when the distance between capillary tip and W-coil was increased the analytical signal decreased since analyte species came in contact with quartz surface.

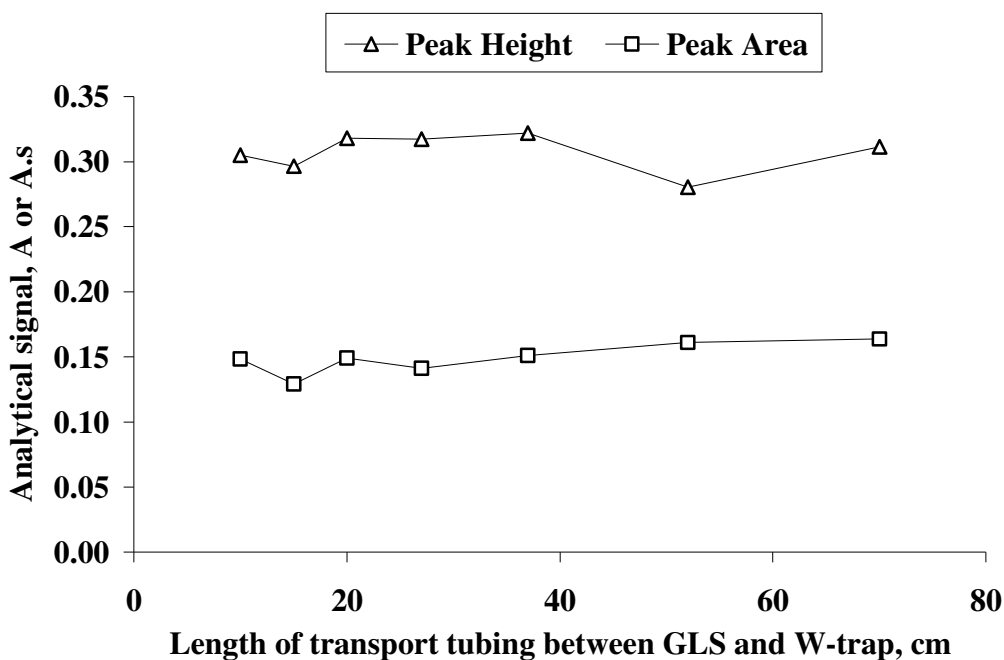


Figure 3.28 The effect of length of PTFE transport tubing between GLS and W-trap. The signals were obtained by collecting 0.7 mL of 5.0 ng/mL Cd in 0.2 mol/L HCl. Collection and release temperatures were 150 °C and 1000 °C, respectively.

3.6.3.9 Distance between W-Trap and Atomizer

The length of transfer tubing between the trap and the atom cell was varied between 10 cm and 110 cm and the analytical signal was recorded. The variation in the analytical signal as a function of distance was given in Figure 3.29. Both peak height and peak area of the analytical signal decreased by 70% when the distance was increased to 50 cm and remained nearly the same up to 110 cm when tygon tubing (3.1 mm i.d.) was used for transportation of released species from the trap. However, if tygon was replaced with a PTFE tubing (4.0 mm i.d.), decrease in the peak area of analytical signal was only 20% at a distance of 110 cm. Although the inner diameters were different for an exact comparison, the tubing with a larger inner diameter was prone to adsorb more than that with a smaller diameter. Therefore, it was clear that Cd atoms were lost on the inner surface of tygon tubing. In order to investigate further, the transfer tubing was replaced with FEP coated tygon tubing with larger inner diameter (6 mm i.d.). In the case of FEP coated tygon tubing the decrease was 30% at 110 cm. Therefore, the Cd species could be transported to long distances but a significant decrease was observed in both peak height and peak area of the analytical signal, especially when a tygon tubing was used. The decrease was less in case of PTFE. For Bi and Pb the decrease in the peak height was more pronounced than that in peak area. However in case of Cd, both in peak area and the peak height decreased together. This may be attributed to the atomic nature of Cd species released from the surface of W-coil.

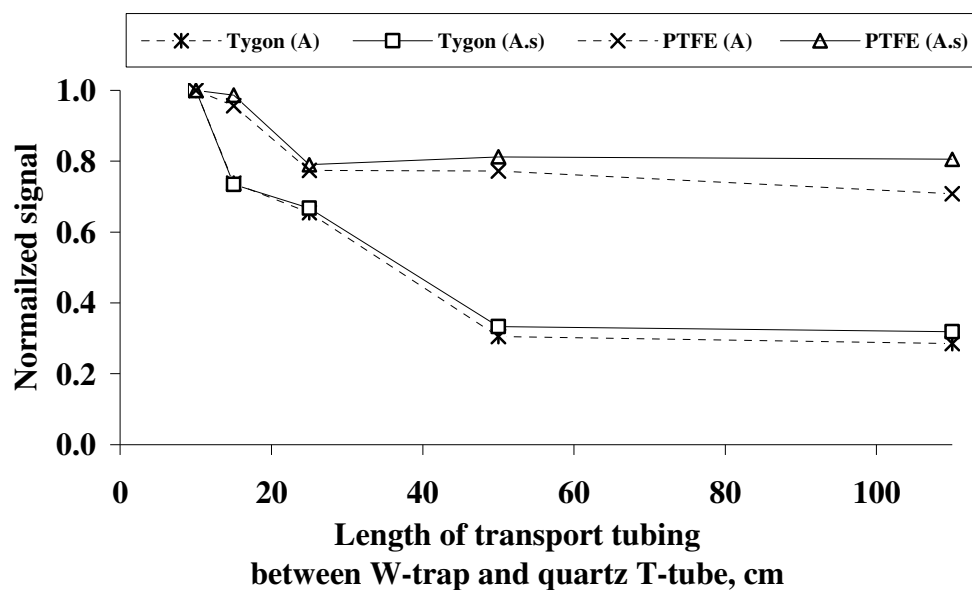


Figure 3.29 The effect of distance between the trap and atomizer on the normalized peak height and peak area signals of Cd.

3.6.4 Relation between Collection Volume and Analytical Signal

The relationship between the collection volume and the analytical signal for both peak height and peak area of analytical signal is given in Figure 3.30. The figure was drawn by injecting 0.5 ng/mL Cd solution in CF mode under optimum conditions with a sample flow rate of 2.1 mL/min. Therefore, it took 2 minutes to collect 4.2 mL sample. The figure shows that both peak area and peak height of the analytical signal was highly correlated with the collection volume up to 4.2 mL with high correlation coefficients. Above this volume a slight negative deviation from the linearity was observed. The analytical signal increased significantly but it was less than expected. A volume of 6 mL can be selected as the sampling volume for further increments in the concentration sensitivity and the detection power of the method. As mentioned before, the selection of collection volume depends on the desired analytical figures of merit. Reagent blank values were not seemed to be significant up to a collection volume of 6.3 mL. Therefore a volume of 4.2 mL can be selected without any reagent blank problems.

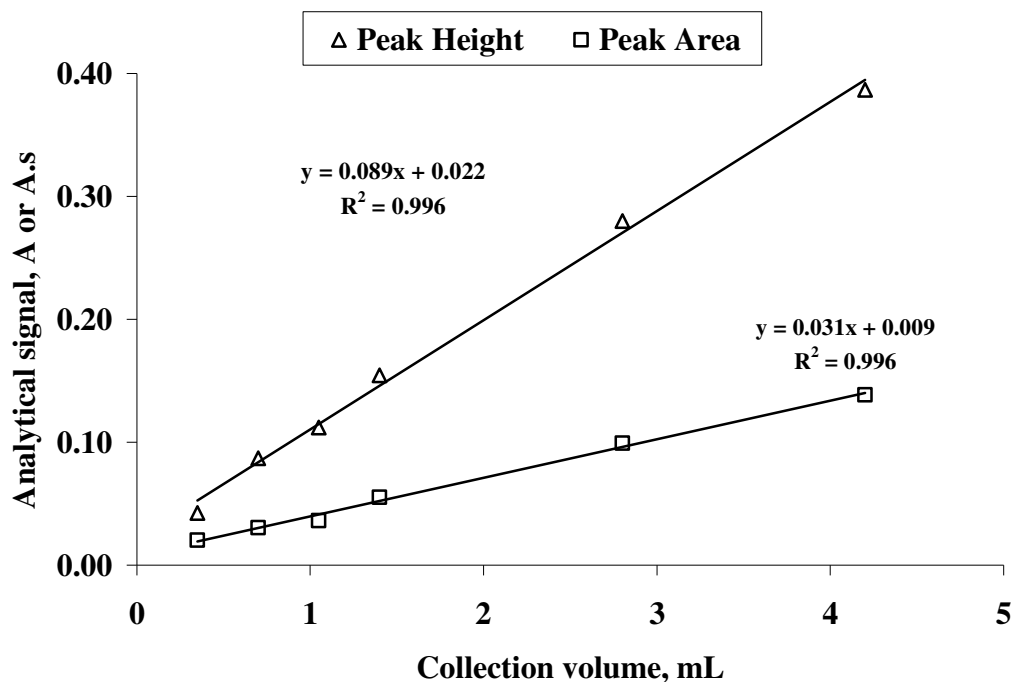


Figure 3.30 Relationship between the collection volume and the analytical signal for both peak area and peak height using 0.50 ng/mL Cd solution under optimized conditions; the flow rate was 2.1 mL/min for both sample and the reductant.

3.6.5 Analytical Signal and Reproducibility

The analytical signal obtained by injection of 4.2 mL of 0.025 ng/mL Cd was given in Figure 3.31. The reproducibility of the measurements was 5.4% RSD for 2 min collection of 0.025 ng/mL Cd solution and better at higher concentrations when the peak height was used. The use of peak area resulted in higher %RSD values (10-15% at this concentration level) as the integrated absorbance values were numerically small due to sharp transient signals as discussed earlier for Bi. Moreover, slight drift in the baseline was also responsible for such poor reproducibility value. The full width at half maximum of analytical signal was around 0.4 s. Although 2.0 s was selected as the integration time, the peak area of

the analytical signal was affected by the lamp noise which resulted in poorer reproducibility.

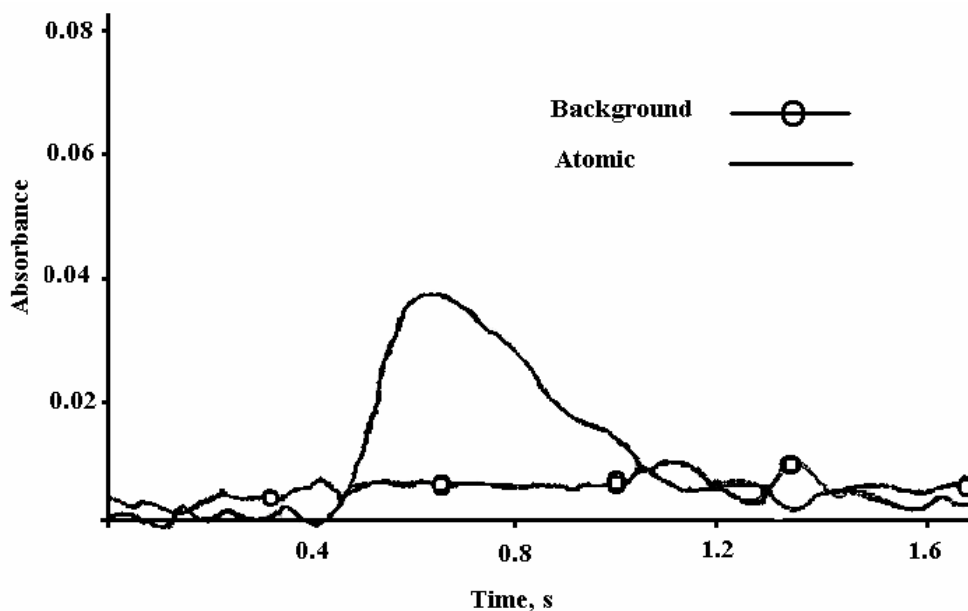


Figure 3.31 The analytical signals for 4.2 mL of 0.025 ng/mL Cd in 0.2 mol/L HCl. Collection at 150 °C and releasing at 1000 °C. 1.5% (w/v) NaBH₄ was used.

Aging of W-coil resulted in an increase in the collection efficiency; the efficiency was found to increase by 20-30% after 600-800 runs when compared to that obtained by new coil. This may be explained by the change of surface characteristics such as porosity. As the surface becomes more porous, the surface area increases and collection efficiency increases.

3.6.6 Calibration Plot

The calibration plot for 2 min collection time which corresponds to a collection volume of 4.2 mL was given in Figure 3.32. Both peak area and peak height of the

analytical signal were found to be linear between the concentrations of 0.025 ng/mL and 0.350 ng/mL. Above this concentration a negative deviation from the linearity was observed. Therefore for 4.2 mL collection volume (2 minutes collection) dynamic range of the calibration graph is between 0.025 and 0.35 ng/mL which is slightly larger than one order of magnitude which is the generally encountered range in HGAAS studies.

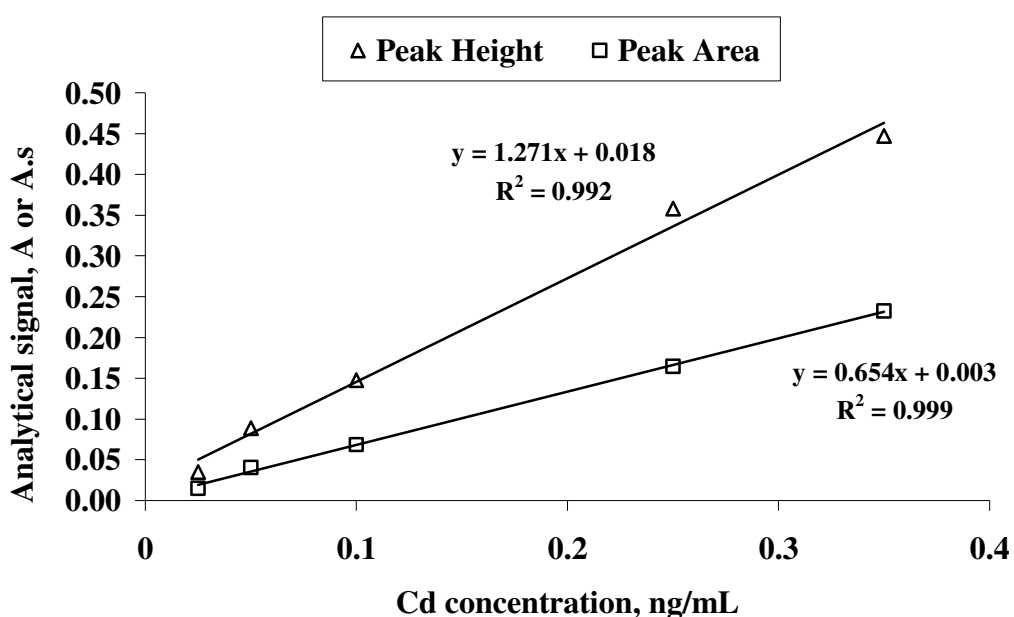


Figure 3.32 The calibration plot of Cd for both peak height and peak area of the analytical signal obtained by W-coil HGAAS. The collection volume was 4.2 mL and aqueous standard solutions were employed; the flow rate was 2.1 mL/min for both sample and reductant.

3.6.7 The Analytical Figures of Merit

The analytical figures of merit of the method for Cd are given in Table 3.4; peak height was used in the calculations. The enhancement factor in limit of detection (3σ) which was calculated by using 0.025 ng/mL was found to be 25 for 4.2 mL collection volume when compared to conventional FI-HGAAS where the injection volume was 0.100 mL and the concentration of Cd was 0.5 ng/mL. The characteristic concentration for 4.2 mL sample volume was calculated as 0.003 ng/mL for peak height which was 31 times lower as compared to conventional FI-HGAAS. When peak area was used the analytical figures was not better than those with the peak height values due to very sharp transient nature of analytical signal.

The limit of detection of the developed method was compared with the literature values in Table 3.5. As seen on the table, the concentration limit of detection value was comparable with the others or better. Although absolute limit of detection of MS system is very low, they are cost prohibitive and not available in most laboratories. Furthermore, the concentration limit of detection was better in our system. The main advantage of W-coil HGAAS is that it can be applied in all laboratories having a simple AAS instrument. When the Cd concentration is in the mid ng/L range, approximately 1-2 minutes are enough for both collection and the measurement of analytical signal. If the concentration is in the low ng/L range, 3-4 minutes are enough for both collection and measurement of analytical signal. A memory effect was observed but it was not cumulative. It was probably arising from the Cd species condensed on the inner walls of GLS as well as the transfer tubings. If blank was injected after a higher concentration of Cd, always a significant signal appeared from blank. If the walls were dried, the memory effect was more. However, the memory signal disappeared after consecutive injections of blank solution. Drying between injections reduced the number of blank injection required to eliminate memory effects.

Table 3.4 Analytical figures of merit and enhancement factors for Cd calculated by using peak height of analytical signal

	FI-HGAAS^a	W-Trap HGAAS^b	Enhancement Factor
Limit of detection, ng/mL	0.100	0.004	25
Characteristic concentration, ng/mL	0.092	0.003	31

a The parameters were calculated by 10 replicate measurements of 0.1 mL of 0.5 ng/mL Cd solution.

b The parameters were calculated by 9 replicate measurements of 4.2 mL of 0.025 ng/mL Cd solution.

Table 3.5 Comparison of the limit of detection and the sample volume of the method with those of others in literature

Method	Concentration LOD, ng/mL	Absolute LOD, pg	Sample Volume, ml	Reference Number
W-Trap HGAAS	0.004	16.8	4.2	This study
W-Coil ETAAS	0.05	0.5	0.01	130
HG <i>in-situ</i> ETAAS	0.002	3.6	1.8	135
HG-AAS	0.01	3	0.3	136
VG-ICP-MS	0.026	2.6	0.100	139
HG <i>in-situ</i> ETAAS	0.06	84	1.4	140
HG <i>in-situ</i> ETAAS	0.005	7	1.4	141

3.6.8 Accuracy of the Method

The accuracy of the method was tested using certified reference materials Oyster Tissue, Tomato Leaves and Sea Water. The certified values and the found values are given in Table 3.6. As indicated on the table, all three SRM results were found to be in good agreement with the certified values. In the analysis of tomato leave SRM, although the digested solutions were further diluted 100 times with 0.20 mol/L HCl, standard addition method was required due to significant matrix interferences. In the determination of Sea Water SRM, the sample was acidified with HCl and direct calibration method was employed. When analyzing Oyster tissue, if the samples were diluted 25 times with 0.2 mol/L HCl, the matrix interferences were significant and the use of direct calibration did not give satisfactory results. However, when digested solutions were further diluted 250 times, matrix interference was eliminated and the direct calibration gave satisfactory results.

Table 3.6 Results of the analysis of standard reference materials and their certified values (n=3 for each measurement)

SRM	Found value	Certified value
Oyster Tissue ^a , µg/g	2.34 ± 0.21	2.48 ± 0.08
Tomato Leaves ^b , µg/g	1.54 ± 0.09	1.52 ± 0.04
Sea Water ^c , nmol/L	0.165 ± 0.007	0.175 ± 0.018

a 0.25 g sample was digested in microwave oven and diluted to 50 mL with deionized water. Then the solutions were further diluted 250 times with 0.2 mol/L HCl and direct calibration method was employed

b 0.25 g sample was digested in microwave oven and diluted to 50 mL with deionized water. Then the solutions were further diluted 25 times with 0.2 mol/L HCl and standard addition method was employed

c Analyzed directly after the solutions were made 0.2 mol/L in HCl. Direct calibration method was employed.

3.7 Lead

3.7.1 Optimization of Hydride Generation Parameters

For the generation of plumbane, the samples were prepared in HCl and reacted with NaBH₄. The flow rate of solutions was 6 mL/min. For phase separation a U-type gas liquid separator was utilized. The length of reaction coil was not found to be very critical and the signal remained nearly constant between 15 and 60 cm. Thus a 30 cm PTFE tubing (0.8 mm i.d.) was used as reaction coil throughout the experiments. No stripping coil was used. The carrier argon was introduced at the entrance of GLS. No signal could be achieved when Pb solutions were prepared in HCl without any oxidizing agent. In order to increase hydride generation efficiency, potassium hexacyanoferrate(III) was used.

3.7.1.1 Concentrations of HCl and NaBH₄

Optimum concentrations of HCl and NaBH₄ were determined by conventional FI-HGAAS (without W-coil trap) using U-type gas liquid separator. The effect of concentration of HCl on the analytical signal was given in Figure 3.33. As it was seen from the figure, HCl concentrations less than 0.03 mol/L and higher than 0.12 mol/L resulted in a decrease in the analytical signal. Between these values, the signal remained nearly the same. Thus 0.06 mol/L was selected as the optimum concentration of HCl in sample solution for hydride generation medium.

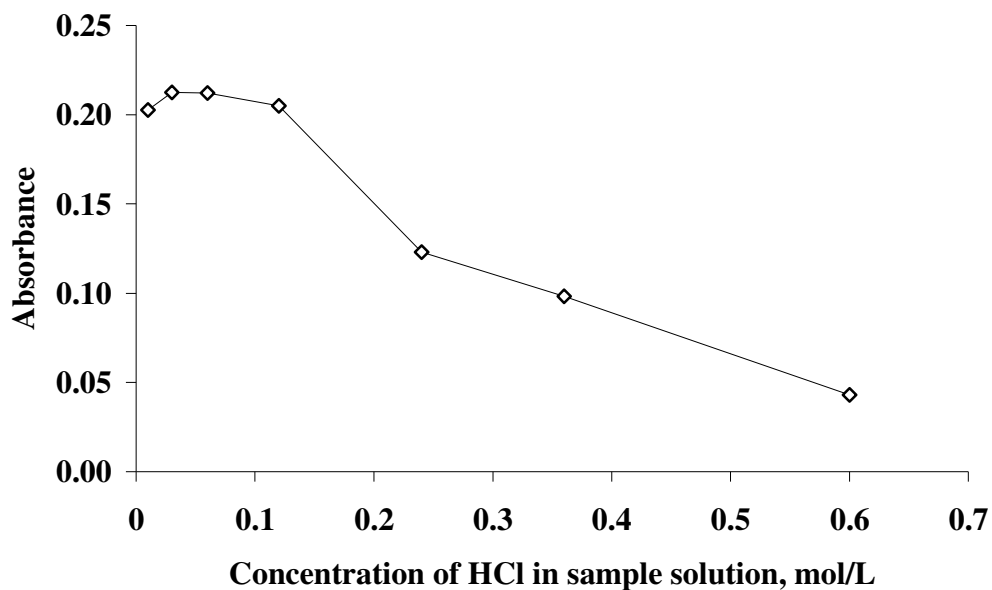


Figure 3.33 Effect of sample acidity on Pb signal in conventional FI-HGAAS. The signals were obtained using 0.500 mL of 10.0 ng/mL Pb in 0.5% (w/v) $K_3Fe(CN)_6$. $NaBH_4$ concentration was 1.0% (w/v).

Optimum $NaBH_4$ concentration was also determined under the same conditions and the optimization graph was given in Figure 3.34. The reductant solutions were prepared daily in 0.1% (w/v) NaOH for the stabilization. A $NaBH_4$ concentration less than 0.5% (w/v) was not found to be adequate for efficient plumbane generation. A slight increase in the analytical signal was observed when the concentration of $NaBH_4$ was increased further, but this increase was not found to be significant and also increased reagent consumption. Therefore, a concentration of 1.0 % (w/v) $NaBH_4$ was found to be optimum for plumbane generation.

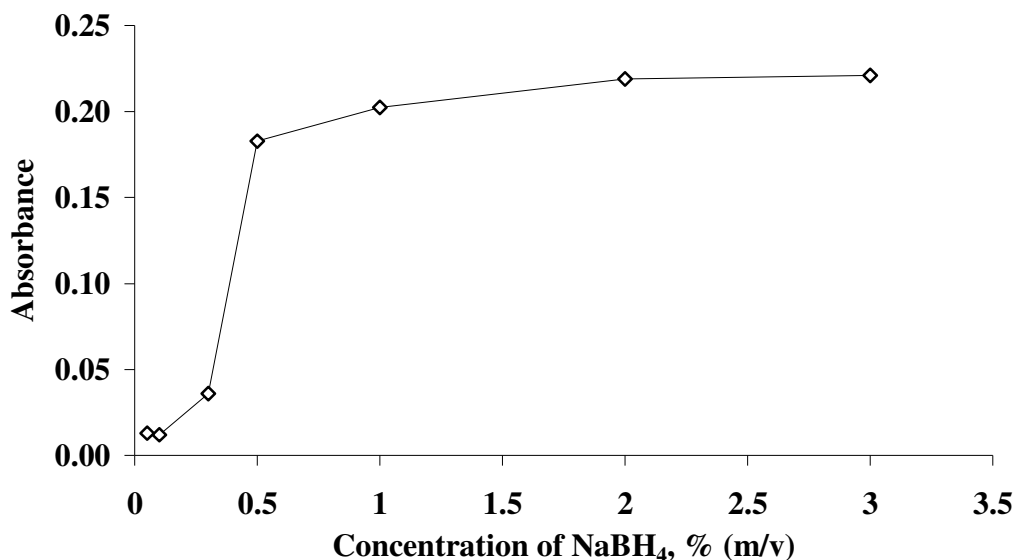


Figure 3.34 Effect of NaBH₄ concentration on Pb signal in conventional FI-HGAAS. The signals were obtained using 0.500 mL of 10.0 ng/mL Pb in 0.06 mol/L HCl and 0.5% (w/v) K₃Fe(CN)₆.

3.7.1.2 Concentration of Oxidizing Reagent in the Reaction Medium

The hydride generation efficiency for Pb in acidified sample solution was very low unless an oxidant was added; even no signal could be observed. For the effective generation of volatile species of lead by NaBH₄ reduction, it was necessary to use oxidizing reagents such as potassium hexacyanoferrate (III), hydrogen peroxide etc. reported in the literature that was summarized in the introduction. In this study, no signal was achieved from sample solutions prepared in only HCl at optimum concentrations. In order to increase the generation efficiency, some oxidants used in the literature were tested. These were H₂O₂, nitroso-R salt (1-nitroso-2-naphthol-3,6-disulphonic acid disodium salt) and potassium hexacyanoferrate(III) (K₃Fe(CN)₆). Use of H₂O₂ did not improve the analytical signal and almost no signal was obtained under the optimized HCl and NaBH₄

concentrations. The highest analytical signal was obtained when $\text{K}_3\text{Fe}(\text{CN})_6$ was used as the hydride generation medium. Tyson et al. [159] also found superior sensitivity with $\text{K}_3\text{Fe}(\text{CN})_6$ among some other oxidizing reagents tested.

The increase in the efficiency of plumbane generation, although not proven, is attributed to the oxidizing effect of the reagent since the common properties of reagents that increased efficiency are their oxidizing properties. Such increase in the generation efficiency was explained by the formation of $\text{Pb}(\text{IV})$ ions in the solution [5]. However the oxidizing power of $\text{K}_3\text{Fe}(\text{CN})_6$ is lower than that of H_2O_2 ; the latter did not improve the analytical signal. In addition, an organic compound, PAN-S, does not have any oxidizing character and its effect can not be accounted for the formation of $\text{Pb}(\text{IV})$. However, it was used for the generation of plumbane in the literature [155]. Therefore the increase in the efficiency was possibly the result of chelated $\text{Pb}(\text{II})$ which is kinetically more easily reduced by NaBH_4 than free $\text{Pb}(\text{II})$ [155].

The dependence of analytical signal on $\text{K}_3\text{Fe}(\text{CN})_6$ concentration is given in Figure 3.35. Addition of $\text{K}_3\text{Fe}(\text{CN})_6$ into the solution of analyte significantly increased the analytical signal up to a concentration of 0.5% (w/v). Although the increase was continued up to 2%, 0.5% (w/v) was selected as the working concentration because the solid $\text{K}_3\text{Fe}(\text{CN})_6$ contained significant amount of Pb as a contaminant which was found to be the limiting factor in the trap experiments. An attempt was made to synthesize it in the laboratory starting from solid KCN and FeCl_3 . The analysis of the reactants by ETAAS showed that they were also contaminated with significant amounts of Pb, so the synthesis was not further pursued.

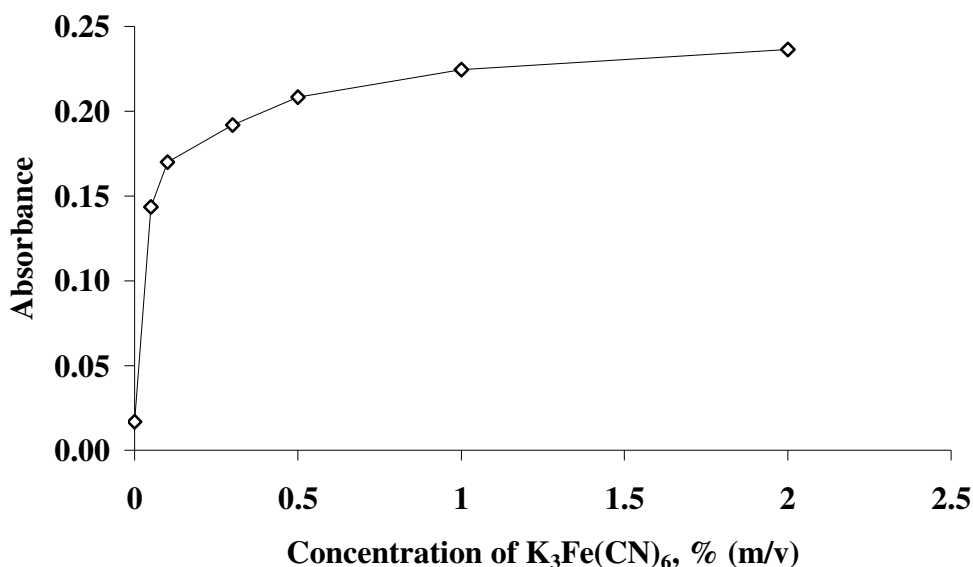


Figure 3.35 Effect of concentration of $K_3Fe(CN)_6$ on analytical signal in conventional FI-HGAAS. The signals were obtained using 0.500 mL of 10.0 ng/mL Pb in 0.06 mol/L HCl.

In addition to $K_3Fe(CN)_6$, nitroso-R salt was also found to increase hydride generation efficiency but its effect was much less; the sensitivity was about 6 times less. The change in the analytical signal as a function of nitroso-R salt concentration was given in Figure 3.36. The analytical signal was increased gradually and linearly up to a concentration of 1.5% (w/v). Above this concentration, the linearity was lost and a plateau was reached. Although the increase in the sensitivity was lower than that of $K_3Fe(CN)_6$, it was also considered that if it has lower reagent blank values, then it could be used in trap studies instead of $K_3Fe(CN)_6$. However, it was found that it also contained significant amount of Pb as contaminant. Another problem with this reagent was that the solubility in water was limited. The dissolution process was slow and even a 2% (w/v) solution contained undissolved solid material.

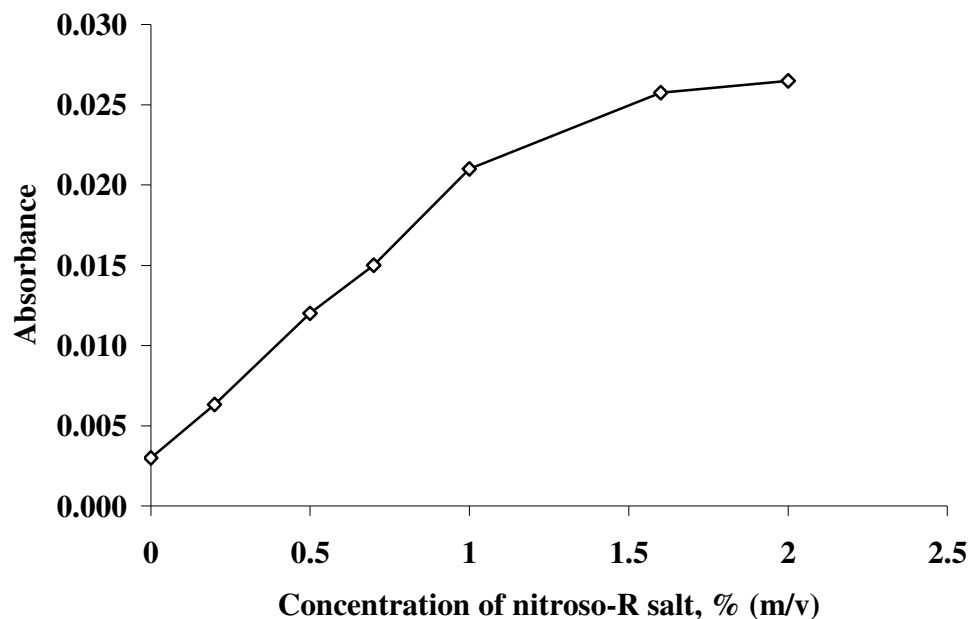


Figure 3.36 Effect of nitroso-R salt concentration on analytical signal in conventional FI-HGAAS. The signals were obtained using 0.500 mL of 10.0 ng/mL Pb in 0.06 mol/L HCl.

3.7.2 Optimization of Trapping Conditions

3.7.2.1 Collection and Revolatilization Temperatures

Collection and release temperatures were optimized by considering the trap signal at the end of collection. While one was being optimized, the other one was kept constant at its optimum value. The optimization plot for trapping and releasing temperatures are given in Figure 3.37. The optimum trapping temperature was found to be 350 °C as measured at the center of coil; at higher temperatures the collected species were lost and a decrease in the analytical signal was observed. A temperature of 500-600 °C was enough for revolatilization of all of trapped Pb

species from the surface but the revolatilization was rather slow and the signals were broad. The peak height of analytical signal increased linearly up to a release temperature of 1200 °C and reached to a plateau. A temperature of 1300 °C was necessary for rapid and reproducible volatilization of Pb species so that the use of peak height in signals was justified. Above this temperature, no further enhancement was observed in the peak height of analytical signal. Similar to Bi, when higher temperatures were employed in the collection step, the surface of quartz around the coil started to collect Pb species which are then observed as a secondary peak next to the analytical peak at high release temperatures. At the optimum trapping and release temperatures, there was only one analytical peak observed and no signal was observed from quartz.

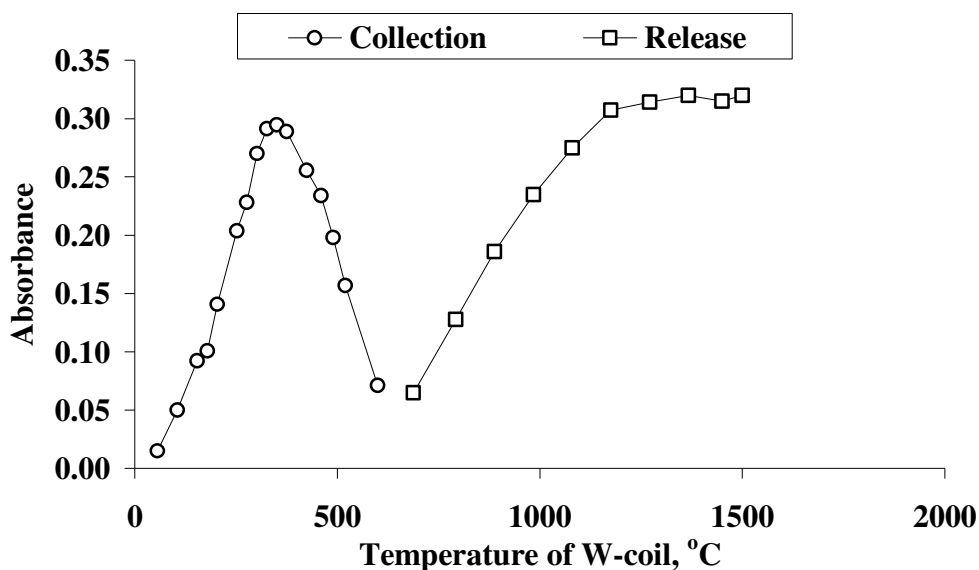


Figure 3.37 The effect of collection and release temperatures on analytical signal for 5.0 ng Pb. During the variations of collection and release temperatures, a constant release temperature of 1300 °C and a constant collection temperature of 350 °C, respectively, were employed.

3.7.2.2 Carrier Gas Flow Rate

Since the trapping temperature of plumbane was slightly higher than that of Bi, a higher hydrogen flow rate was required for the minimization of oxidation of W-coil. The flow rate of H₂ was kept constant at 100 mL/min; the lower H₂ flow rates caused the oxidation of W-coil and resulted in relatively higher background absorption. The optimum collection and release Ar flow rates were investigated independent from each other while keeping the H₂ flow rate constant. The optimization graphs for Ar flow rates during collection and revolatilization were given in Figure 3.38 and 3.39, respectively. In contrast to Bi where collection and release Ar flow rates were different from each other, the optimum collection and release Ar flow rates were found to be almost the same for Pb. During collection Ar flow rate was not very critical and the signal remained almost the same between 100 and 400 mL/min, above which a decrease was observed in the analytical signal. The effect of Ar flow rate during revolatilization was found to be more important than that in collection step. Higher analytical signals were obtained when the release Ar flow rate was kept at 210 mL/min. When it was increased further the analytical signal decreased due to dilution of analyte by the carrier gas. Therefore, the Ar flow rate for both collection and release steps was found to be optimum at 210 mL/min; therefore it was not needed to vary the flow rate between collection and release stages. The effect of H₂ flow rate on the collection and release was also investigated for Pb and no significant effect was observed; a value of 100 mL/min has been applied for H₂ flow rate in both stages.

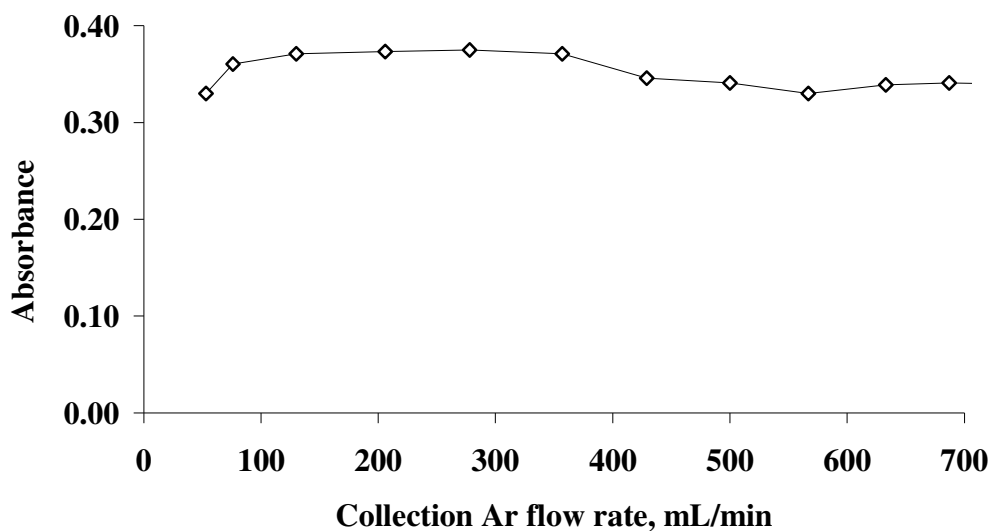


Figure 3.38 Effect of collection Ar flow rate on the analytical signal obtained by W-coil HGAAS; H₂ flow rate was 100 mL/min, release Ar flow rate was 210 mL/min; 0.500 mL of 10 ng/mL Pb was used.

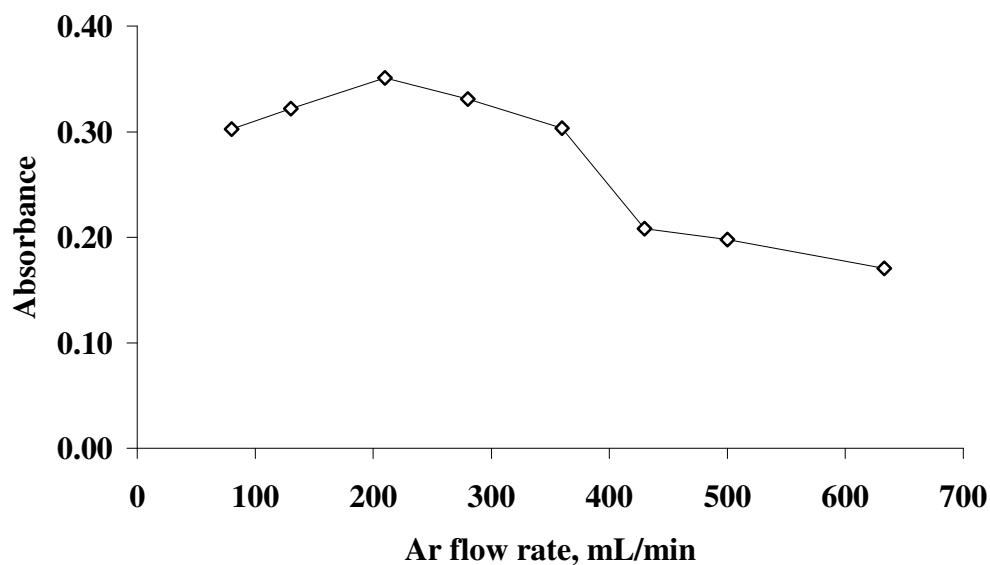


Figure 3.39 Effect of release Ar flow rate on the analytical signal obtained by W-coil HGAAS; H₂ flow rate was 100 mL/min, collection Ar flow rate was 210 mL/min; 0.500 mL of 10 ng/mL Pb was used.

3.7.2.3 Coating with Pd, Pt and Ir

In the collection stage there was significant breakthrough signal due to untrapped plumbane. This was an indication of low trapping efficiency. In order to increase the trapping efficiency, the surface of W-coil was coated with Ir, Pd and Pt which were generally used for the stabilization of analyte species in ETAAS. These elements have been widely used for *in-situ* trapping in graphite furnaces. It was shown that, Pt was an efficient coating material for the *in-situ* preconcentration of Se in W cuvette [82]. The coil was treated with 100 µg of each of these elements. The coating was carried out by addition of 25 µl aliquots of 1000 mg/L stock solution. The process was repeated 4 times by drying injected solution between injections. At the end, the coil was heated to release temperature under H₂ environment for the reduction of coated metal to its elemental form. In this study, the coating materials were not investigated in detail and the amount of coating material was not optimized.

Coating with Pd resulted in very irreproducible signals. It was observed that Pd was not stable on the coil. The releasing required higher temperatures; as high as 1800 °C or more. The collection efficiency was not increased any more. Therefore it did not provide any advantage.

When the coil was coated with Pt, a slight increase, approximately 20-40%, was observed in the trapping efficiency. Furthermore, the range of optimum collection temperature was improved. The temperature range of uncoated W-coil for efficient collection was between 300 °C and 350 °C. By coating with Pt this range was broadened and the W-coil was capable of trapping the volatile species of Pb in between 200 °C and 500 °C. The analytical signals obtained from Pt coated W-coil as a function of coil temperature is given in Figure 3.40.

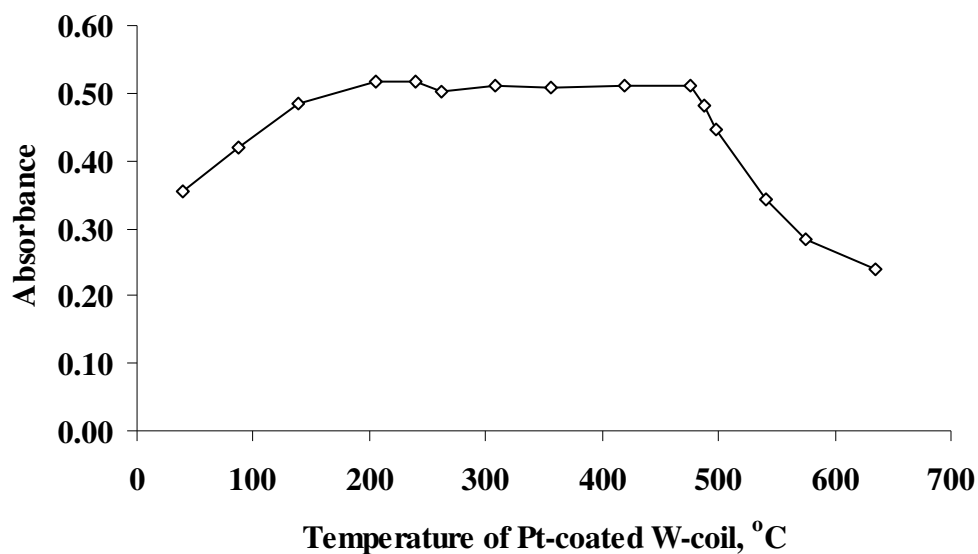


Figure 3.40 The dependence of analytical signal on the collection temperature of Pt coated W-coil for 5.0 ng Pb. During the variations of collection temperature, a constant release temperature of 1300 °C was employed.

Coating the W-coil with Ir significantly increased the optimum trapping temperature to about 450 °C. Approximately a 2-fold increase was observed in the sensitivity but the optimum temperature range for collection was decreased. In other words, slight variations in the collection temperature resulted in high changes in responses.

Although Ir-coating resulted in a 2-fold increase in the sensitivity, it was not used since it required higher collection temperatures and the slight changes in the collection temperature resulted in significant changes in the analytical signal since the maximum signal was limited to a narrow temperature range. The increase in the collection efficiency by using Pt coating was only 20-40% and this can be achieved by collection higher sample volumes. Therefore, in order to simplify the procedure, these coating was not preferred. However, it was shown that the trapping efficiency could be increased by coating the W-coil.

3.7.2.4 Distance between W-Trap and Atomizer

The length of transfer tubing between the trap and atomizer was varied between 10 cm and 45 cm and the analytical signal was observed. The change in the analytical signal as a function of the distance was given in Figure 3.41. When the length of tygon transport tubing used for the transportation of volatilized species was increased from 10 cm to 45 cm, the full width at half maximum of the analytical signal was increased and peak height signal was decreased by 43%. If the peak area was considered, the decrease in the analytical signal was not found to be significant indicating significant peak broadening. The decrease in the peak height of analytical signal was mostly due to dilution of volatile analyte species during the transportation since the peak height was much more affected than peak area. Since the volatilized species were transported to a distance of about half a meter, they were probably molecular or converted to molecular species just after their volatilization. The fact that no signal could be obtained by the volatilized species when sent to unheated QTA supports this idea.

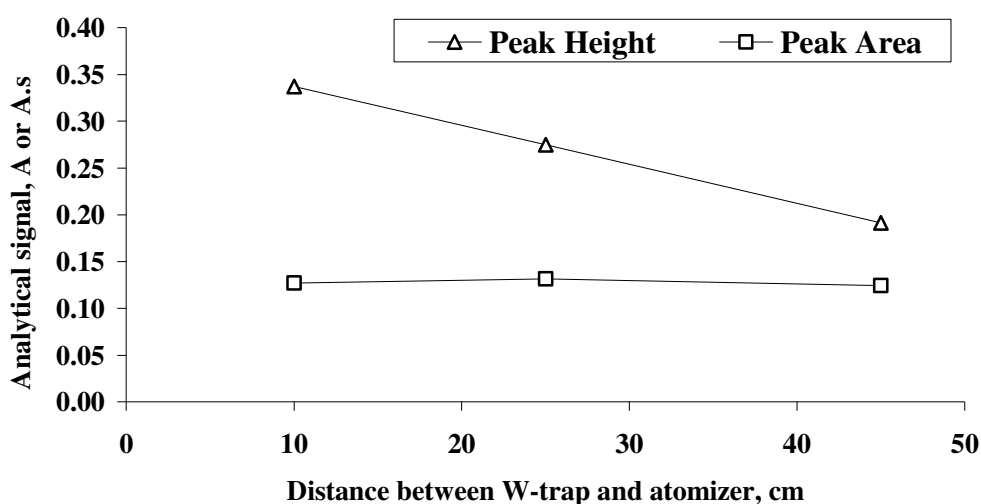


Figure 3.41 The effect of distance between the trap and atomizer on both peak height and peak area signals of Pb. 0.500 mL of 10 ng/mL Pb was used.

3.7.2.5 Tandem W-Trap Arrangement

During the trapping studies, it was observed that a significant amount of Pb species were not trapped on the trap and there always appeared a breakthrough signal when the concentration of Pb was appropriate for direct measurements. A tandem W-trap arrangement was designed to collect these untrapped Pb species. Two identical traps were consecutively coupled so that the species that were not trapped on the first one would be trapped on the second one. In order to accomplish these experiments, both trap temperatures were kept at collection temperature. After the trapping was complete, the revolatilized species from the first and the second traps were sent to the atomizer in separate experiments. It was observed that the peak area of the analytical signal obtained from the first trap (closer to GLS) was approximately 6 times higher than that was obtained from the second one. If the untrapped species remained as hydride and reached to the second trap, the analytical signal of second trap should be approximately 16% less than that of the analytical signal from the first trap since the total efficiency of W-trap was 14%. Therefore the untrapped Pb species were either decomposed and turned into another form or lost before reaching to second trap.

3.7.3 Relation between Collection Volume and Analytical Signal

The relation between analytical signal and the collection volume was investigated in CF mode. As already mentioned the blank reagents, mostly $K_3Fe(CN)_6$, were contaminated by Pb. The blank reagent gave an analytical signal equal to that would be obtained by using approximately 0.2 ng/mL Pb solution. The relation between collection volume and peak height of analytical signal given in Figure 3.42 was obtained by using blank reagents. The solution of 0.5% (w/v) $K_3Fe(CN)_6$, which was blank, was continuously pumped and the generated plumbane was trapped on the coil. The analytical signal obtained by using blank was significant even the collection volume was as low as 1.0 mL. As it is seen on the figure, the

analytical signal increases almost linearly up to at least 40 mL which corresponds to 6.5 min collection time. If the collection volume is to be increased, the reagent blanks must be decreased by applying appropriate purification methods so that the collection volume can be increased up to 40 mL. The linear relation was an indication of stability of Pb species on the coil ($R^2 = 0.978$). No further investigation was carried out on the stability of Pb species on the coil.

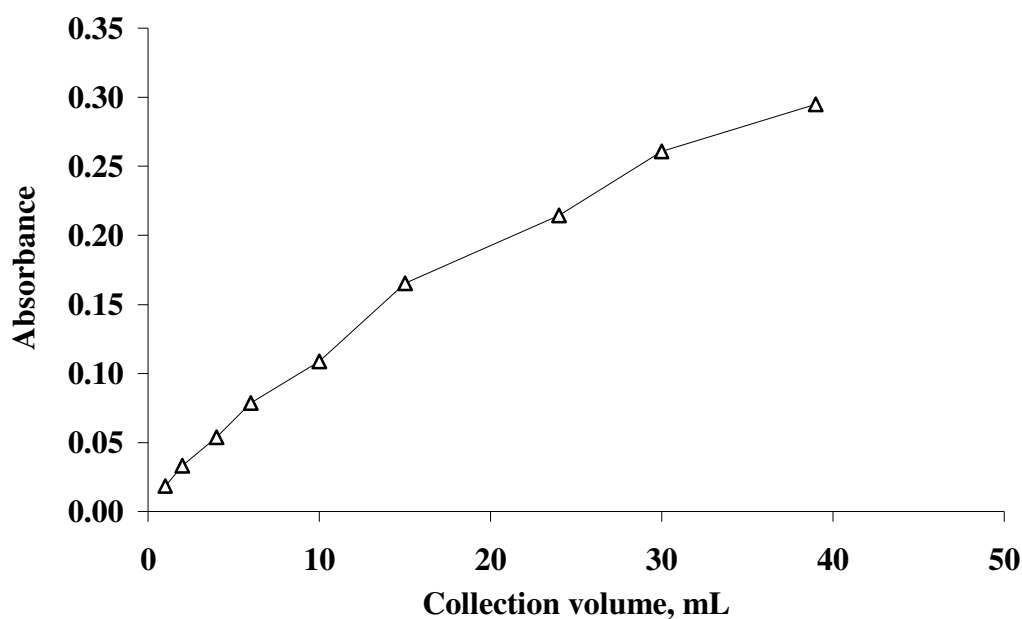


Figure 3.42 Analytical signal versus collection volume obtained by using reagent blank solutions: 0.5% (w/v) $K_3Fe(CN)_6$ in 0.06 mol/L HCl and 1.0% $NaBH_4$ (w/v) (reagent blanks gave a signal equal to that obtained from 0.2 ng/mL Pb, and no Pb was added); collection temperature, 350 °C; release temperature, 1300 °C.

3.7.4 Analytical Signal and Reproducibility

The analytical signal obtained from 0.5 mL of 10 ng/mL Pb (5.0 ng Pb) was shown in Figure 3.43. The full width at half maximum of the analytical signal was approximately 0.3 s. In addition, the peak was tailed. The signal shapes obtained

under different conditions of concentration or collection volume, were similar to the one shown here. Less than 5% RSD ($n=7$) was obtained by replicate measurements of reagent blanks (0.2 ng/mL) for a collection volume of 15 mL (2.5 min collection). As discussed for Bi and Cd, the reproducibility of the peak area measurements was poorer than that of peak height values because of very sharp signals which resulted numerically small peak area values. Moreover, since the integration period was longer than the basewidth of the analytical signal, small drifts in the baseline and also tailing of the analytical signal resulted in higher %RSD values. Therefore, higher relative standard deviation was observed when the peak area values were taken into account; typically 10-15% RSD values were obtained.

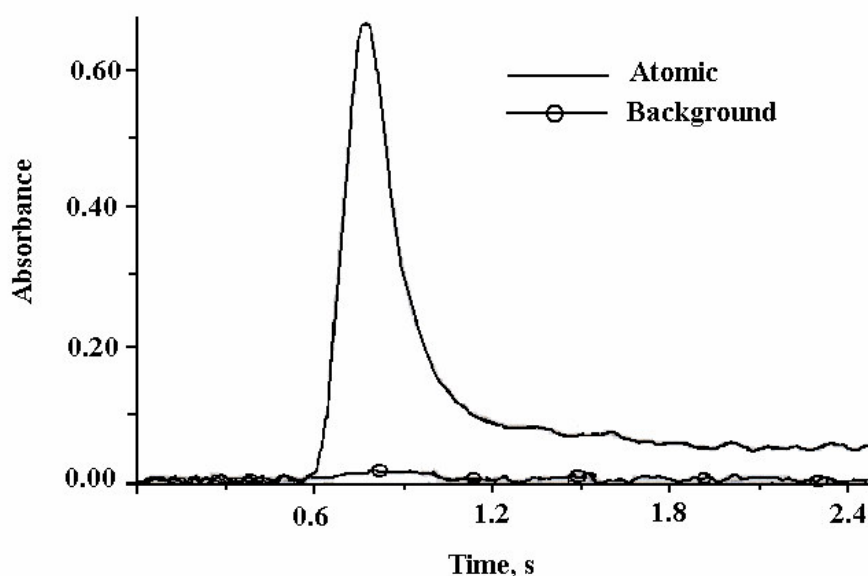


Figure 3.43 The analytical signals for 2.0 mL of 5.0 ng/mL Pb; Collection at 350 °C and releasing at 1300 °C.

3.7.5 Calibration Plot

The calibration plot drawn by using peak height and peak area for 2.0 mL of aqueous standard solutions was given in Figure 3.44; no blank correction was

made. It was found that the plot was linear between the concentrations of 0 and 3.0 ng/mL for peak height for 2 mL collection volume (20 s collection). The peak area was also found to be linearly correlated with the concentration, but the precision was poor due to very sharp transient signals as discussed earlier. Since the reagent blank values due to high Pb content of $K_3Fe(CN)_6$ was significant, the signal obtained from only blank was significant even at a collection volume of 1.0 ml.

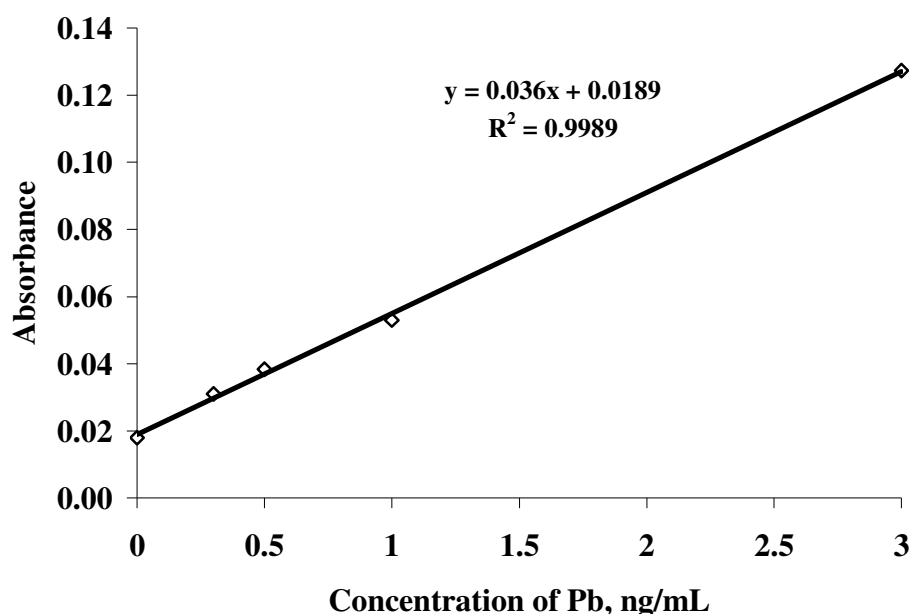


Figure 3.44 The calibration plot drawn by using peak height for 2.0 mL of aqueous standard solutions of Pb in 0.5% (w/v) $K_3Fe(CN)_6$ under optimum conditions (No blank correction was made).

3.7.6 The Analytical Figures of Merit

The total efficiency for trapping, releasing and transportation to the atomizer for trapping was calculated by comparing the peak area values of the signals obtained by conventional FI-HGAAS (no W-trap) and that obtained by W-trap HGAAS

under the same carrier gas flow rates. These experiments showed that the total efficiency was 14% and the rest was either untrapped or lost between trap and atomizer.

High reagent blank values were the limiting factor for the enhancement of figures of merit for Pb. The blank solution already contained 0.2 ng/mL Pb. The same problem was also observed elsewhere where the same reagent was used for efficient hydride generation [155, 159]. Therefore the characteristic mass and the limit of detection was calculated from the blank solution for both conventional FI HGAAS and W-trap HGAAS. The analytical figures of merit of the method for Pb were given in Table 3.7; peak height was used for the calculation of parameters. The limit of detection values of both conventional FI-HGAAS and W-trap HGAAS were calculated using 0.5% (w/v) $K_3Fe(CN)_6$. The enhancement factor in the limit of detection (3σ) found to be 12 for 2.0 mL collection volume when compared to conventional FI-HGAAS where the injection volume was 0.500 mL. The characteristic concentration of W-trap HGAAS for 2.0 mL collection volume was calculated as 0.011 ng/mL for peak height which was 20 times lower as compared to conventional FI-HGAAS whose characteristic concentration was 0.18 ng/mL of Pb. The observed enhancement factor in the sensitivity could not be reached in the limit of detection due to high blank values, since the solution used for calculation of LOD contained significant amount of Pb.

When peak area was used the improvement in analytical figures was as much as for peak height values due to sharp transient nature of analytical signal. The enhancement factor in the limit of detection was only 3. The characteristic mass for conventional FI HGAAS was 0.15 ng whereas that of W-trap HGAAS was 1.0 ng since the collection efficiency was only 14% and also the signal was very sharp. Therefore use of peak area did not provide any advantage.

Table 3.7 Analytical figures of merit and enhancement factors for Pb calculated by using peak height of analytical signal.

	FI-HGAAS ^a	W-Trap HGAAS ^b	Enhancement Factor
Limit of detection, ng/mL	0.180	0.015	12
Characteristic concentration, ng/mL	0.23	0.011	20
Characteristic mass^c, ng	0.15	1.0	-

a The parameters were calculated by 10 replicate measurements of 0.500 mL of blank solution containing 0.2 ng/mL Pb in FI mode.

b The parameters were calculated by 10 replicate measurements of 2.0 mL of blank solution containing 0.2 ng/mL Pb in CF mode.

c Characteristic mass values were calculated by using peak area values obtained at optimum working conditions for each method.

The limit of detection of the developed method was compared with the literature values in Table 3.8. As seen on the table, the concentration limit of detection value was comparable with other hydride generation systems or better. The LOD of ICP-MS is lower than ours but as mentioned its cost is relatively higher than the simple and low cost method presented here. If reagent blank values are reduced, the analytical figures of merit can be improved further by using higher sample volumes since the linearity between collection volume and analytical signal is conserved up to 40 mL.

The effects of interfering elements were not studied. Copper have been assigned as one of the most interfering transition metal. Brindle et al. studied the interferences of transition metals and showed that Cu is the most interfering element; presence of 1 µg/mL Cu decreased the analytical signal obtained from 20 ng/mL Pb by 48% [158]. In the same study, it was reported that when the concentration of Fe(III) and Mn(II) was 1 µg/mL, the decrease in the analytical signal was 8% by each metal. Therefore at higher concentrations of these elements, interference should be

expected. Dilution of sample and collection of larger volumes may be required; the reagent blanks must be reduced.

Table 3.8 Comparison of the limit of detection and the sample volume of the method with those of others in literature

Method	Concentration LOD, ng/mL	Absolute LOD, pg	Sample Volume, ml	Reference Number
W-Trap HGAAS	0.015	30	2.0	This study
W-Coil ETAAS	0.63	6.3	0.010	129
HG <i>in-situ</i> ETAAS	0.500	250	0.5	157
ETAAS	0.93	9.3	0.010	147
DCP-AES	0.7	350	0.500	158
HG-ICP-MS	0.007	3.5	0.5	161
HG <i>in-situ</i> ETAAS	0.03	30	1.0	159
HG <i>in-situ</i> ETAAS	0.06	30	0.500	163

3.7.7 Accuracy of the Method

The accuracy of the method was tested using certified reference materials, Metals on Soil/Sediment #4 (Ultra Scientific) and NIST SRM 278 Obsidian Rock. The certified and found values are given in Table 3.9. The results of analysis of both SRM were found to be in good agreement with the certified values. In the analysis of soil/sediment, the digested solutions were further diluted 100 times with blank

solution. The digests of obsidian SRMs were further diluted 25 times with blank solution and then injected. The determination of Pb in the SRM solutions was performed in FI mode with a sample volume of 0.500 mL. Each injection took approximately 20 seconds. Since reagent blank, 0.5% (w/v) $K_3Fe(CN)_6$, contained significant Pb as contaminant, a solution containing only 0.06 mol/L HCl was used as carrier solution in order to decrease the blank values. Significant signal was obtained from 0.500 mL of reagent blank solution which was also injected together with sample and standards. No matrix interference was encountered during the analysis. Direct calibration method was applied since no matrix interference was observed during the determination.

Table 3.9 Results of the analysis of standard reference materials and their certified values (n=3 for each measurement)

SRM	Found value	Certified value
Soil/Sediment^a, $\mu\text{g/g}$	96.1 ± 5.0	95.3 ± 5.3
Obsidian Rock^b, $\mu\text{g/g}$	16.0 ± 1.1	16.4 ± 0.2

a 0.100 g sample was digested in microwave oven and diluted to 100 mL with 0.06 mol/L HCl. The solutions were further diluted 100 times with 0.5% (w/v) $K_3Fe(CN)_6$ in 0.06 mol/L HCl just before the measurements.

b 0.250 g sample was digested in microwave oven and diluted to 100 mL with 0.06 mol/L HCl. The solutions were further diluted 25 times with 0.5% (w/v) $K_3Fe(CN)_6$ in 0.06 mol/L HCl just before the measurements.

CHAPTER IV

CONCLUSIONS

Novel analytical techniques for the determination of Bi, Cd and Pb have been developed by using on-line preconcentration on heated W-coil and revolatilization. The methods provide relatively easy, low cost and fast on line preconcentration and determination of Bi, Cd and Pb at ng/L range. Furthermore they can be applied in laboratories having a simple AAS instrument and a hydride generation system with a very low additional cost. The system can be easily manufactured in any laboratory.

A regular W-coil atomizer was not used since its geometry is not ideal for trapping. A W-coil extracted from a commercial halogen lamp was employed. The inlet arm of the T-tube was chosen for the best trapping geometry; the trapping efficiency depends on the alignment of W-coil in the inlet arm.

The analytical signals are very sharp due to fast heating rate of W coil which allowed the use of peak height values; half widths are less than a second. The peak area values are rather small which resulted in a decrease in the reproducibility and enhancement factors. However if peak area values are to be used, the heating rate and the carrier gas flow rate can be reduced in order to improve reproducibility.

The total efficiency of trapping and revolatilization for Bi was 23% and the achieved limit of detection for Bi was 0.0027 ng/mL for 18 mL sample volume.

Revolatilized Bi species can be transported for at least 50 cm without any significant decrease in the peak area; however peak heights were decreased due to broadening. The enhancement factor in the sensitivity was 130 with 18 mL sample volume.

The generation of atomic species of Cd by tetrahydroborate reduction is rather problematic when compared to Bi and Pb due to the atomic nature of volatile species. The decrease in the analytical signal of Cd in the presence of O₂ in conventional HG can also be attributed to atomic nature. However this must be investigated further. A close control of experimental parameters is required for efficient and reproducible vapor generation. The efficiency of generation of Cd atoms is linearly correlated by the reaction coil temperature. A significant decrease was observed in both peak height and peak area when the distance between trap and atomizer was 25 cm. The decrease depends on the tubing material used for transportation. The sensitivity was improved 31 times when compared to conventional HG. The limit of detection achieved with 4.2 mL sample volume was 0.015 ng/mL.

Among the tested reagents used to increase plumbane generation efficiency, K₃Fe(CN)₆ is the best but it has high blank values. High reagent blanks is the major problem for the improvement in the LOD for Pb. Characteristic concentration was improved 20 times for 2.0 mL collection volume when compared to conventional HGAAS. The limit of detection was 0.015 ng/mL for 2.0 mL sample volume. The analytical figures of merit for Pb can be improved further using sample volumes of up to 4 mL. However, reagent blanks must be purified for the achievement of enhancement factors close to that was obtained for Bi. The total trapping and revolatilization efficiency is 14%. Revolatilized Pb species can be transported for at least 45 cm without any significant reduction in the peak area however peak heights were decreased due to broadening.

The achieved concentration limits of detection are well comparable with that of *in-situ* trapping in the literature. Although absolute limits of detection of ICP-MS systems are much lower than presented here, the concentration limits are comparable. However ICP-MS systems are cost prohibitive.

The revolatilized species of Bi and Pb are either molecular or short living atomic in nature; since no signal was observed when quartz T-tube was not heated. However Cd is revolatilized from the surface as its atomic species. Rather convenient transport properties of revolatilized species suggest that they can be transported to another detection system such as ICP or ICP-MS that will improve the limit of detection.

In order to extend the applicability of this method for other analytes there are three requirements: 1. The analyte must be volatilized; Hg and all the hydride forming elements fulfill this requirement. 2. The analyte must be collected on a suitable trap; including W-coil there may be several other metal traps that could be used for this purpose. 3. Trapped analyte must be thermally revolatilized and then atomized in an absorption cell. It seems that the method can be applied to some other hydride forming elements using electrically heated metal wires.

The following article (Reference 104) was published from this work.

O. Cankur, N. Ertas, O.Y. Ataman, Determination of bismuth after on-line preconcentration by trapping on resistively heated W-coil and hydride generation atomic absorption spectrometry, *Journal of Analytical Atomic Spectrometry* 2002, Vol 17, 603-609.

REFERENCES

1. B. Welz, M. Sperling, *Atomic Absorption Spectrometry*, 3rd Edition, Wiley-VCH Verlag GmbH, Germany, 1999.
2. D.L. Tsalev, Vapor generation or electrothermal atomic absorption spectrometry?-Both!, *Spectrochimica Acta Part B* 2000, Vol 55, 917-933.
3. A. Montaser, D. Golightly, *Inductively Coupled Plasmas in Analytical Atomic Spectrometry*, 2nd Edition, VCH Publishers Inc., New York, 1992.
4. S.S. Kannamkumarath, K. Wrobel, K. Wrobel, C. B'Hymer, J.A. Caruso, Capillary electrophoresis-inductively coupled plasma-mass spectrometry: an attractive complementary technique for elemental speciation analysis-Review, *Journal of Chromatography A* 2002, Vol 975, 245-266.
5. J. Dědina, D.L. Tsalev, *Hydride Generation Atomic Absorption Spectrometry*, John Wiley and Sons Ltd., Chichester, 1995.
6. D.L. Tsalev, Hyphenated vapour generation atomic absorption spectrometric techniques, *Journal of Analytical Atomic Spectrometry* 1999, Vol 14, 147-162.
7. A. Sanz-Medel, M.C. Valdés-Hevia y Temprano, N. Bordel García, M.R. Fernández de la Campa, Generation of cadmium atoms at room temperature using vesicles and its application to cadmium determination by cold vapor atomic spectrometry, *Analytical Chemistry* 1995, Vol 67, 2216-2223.
8. R.K. Skogerboe, D.L. Dick, D.S. Pavlica, F.E. Lichte, Injection of samples into flames and plasmas by production of volatile chloride, *Analytical Chemistry* 1975, Vol 47, 568-570.
9. P.N. Vijan, Feasibility of determining ultratrace amounts of nickel by carbonyl generation and atomic absorption spectrometry, *Atomic Spectroscopy* 1980, Vol 1, 143-144.

10. T.W. Brueggemeyer, J.A. Caruso, Determination of lead in aqueous samples as the tetramethyl derivative by atomic absorption spectrometry, *Analytical Chemistry* 1982, Vol 54, 872-875.
11. S. Rapsomanikis, O.F.X. Donard, J.H. Weber, Speciation of lead and methyllead ions in water by chromatography/atomic absorption spectrometry after ethylation with sodium tetraethylborate, *Analytical Chemistry* 1986, Vol 58, 35-38.
12. R.E. Sturgeon; S.N. Willie, S.S. Berman, Atomic absorption determination of lead at picogram per gram levels by ethylation with *in situ* concentration in a graphite furnace, *Analytical Chemistry* 1989, Vol 61, 1867-1869.
13. W. Holak, Gas-sampling technique for arsenic determination by atomic absorption spectrophotometry, *Analytical Chemistry* 1969, Vol 41, 1712-1713.
14. R.C. Chu, G.P. Barron, P.A.W. Baumgarner, Arsenic determination at sub-microgram levels by arsine evolution and flameless atomic absorption spectrophotometric technique, *Analytical Chemistry* 1972, Vol 44, 1476-1479.
15. H.C. Freeman, J.F. Uthe, An improved hydride generation apparatus for determining arsenic and selenium by atomic absorption spectroscopy, *Atomic Absorption Newsletter* 1974, Vol 13, 75-76.
16. F.E. Lichte, R.K. Skogerboe, Emission spectrometric determination of arsenic, *Analytical Chemistry* 1972, Vol 44, 1480-1482.
17. W.B. Robbins, J.A. Caruso, Development of hydride generation methods for atomic spectroscopic analysis, *Analytical Chemistry* 1979, Vol 51, 889A-899A.
18. F.J. Fernandez, D.C. Manning, The determination of As at sub-microgram levels by AA spectrophotometry, *Atomic Absorption Newsletter* 1971, Vol 10, 86-88.
19. J. Agterdenbos, D. Box, A study on the generation of hydrogen selenide and decomposition of tetrahydroborate in hydride generation atomic absorption spectrometry, *Analytica Chimica Acta* 1986, Vol 188, 127-135.
20. R.S. Braman, L.L. Justen, C.C. Foreback, Direct volatilization-spectral emission type detection system for nanogram amounts of arsenic and antimony, *Analytical Chemistry* 1972, Vol 44, 2195-2199.

21. A. D'Ulivo, V. Loreti, M. Onor, E. Pitzalis, R. Zamboni, Chemical vapor generation atomic spectrometry using amineboranes and cyanotrihydroborate(III) reagents, *Analytical Chemistry* 2003, Vol 75, 2591-2600.
22. X.-D. Tian, Z.-X. Zhuang, B. Chen, X.-R. Wang, Movable reduction bed hydride generator coupled with inductively coupled plasma optical emission spectrometry for determination of hydride forming elements, *Analyst* 1998, Vol 123, 627-632.
23. N. Maleki, A. Safavi, Z. Ramezani, Determination of lead by hydride generation atomic absorption spectrometry (HGAAS) using a solid medium for generating hydride, *Journal of Analytical Atomic Spectrometry* 1999, Vol 14, 1227-1230.
24. W.-W. Ding, R.E. Sturgeon, Evaluation of electrochemical hydride generation for the determination of arsenic and selenium in sea water by graphite furnace atomic absorption with *in situ* concentration, *Spectrochimica Acta Part B* 1996, Vol 51, 1325-1334.
25. A. D'Ulivo, C. Baiocchi, E. Pitzalis, M. Onor, R. Zamboni, Chemical vapor generation for atomic spectrometry. A contribution to the comprehension of reaction mechanisms in the generation of volatile hydrides using borane complexes, *Spectrochimica Acta Part B* 2004, Vol 59, 471-486.
26. F. Laborda, E. Bolea, M.T. Baranguan, J.R. Castillo, Hydride generation in analytical chemistry and nascent hydrogen: when is it going to be over?, *Spectrochimica Acta Part B* 2002, Vol 57, 797-802.
27. J. Cacho, I. Beltrán, C. Nerin, Generation of volatile cadmium species in an organic medium, *Journal of Analytical Atomic Spectrometry* 1989, Vol 4, 661-663.
28. X.-W. Guo, X.-M. Guo, Determination of cadmium at ultratrace levels by cold vapor atomic absorption spectrometry, *Journal of Analytical Atomic Spectrometry* 1995, Vol 10, 987-991.
29. R.E. Sturgeon, J. Liu, V.J. Boyko, V.T. Luong, Determination of copper in environmental matrices following vapor generation, *Analytical Chemistry* 1996, Vol 68, 1883-1887.
30. H. Sun, R. Suo, Y. Lu, Determination of zinc in food using atomic fluorescence spectrometry by hydride generation from organized media, *Analytica Chimica Acta* 2002, Vol 457, 305-310.

31. X.-M. Guo, B. Huang, Z. Sun, R. Ke, Q. Wang, Z.-B Gong, Preliminary study on a vapor generation technique for nickel without using carbon monoxide by inductively coupled plasma atomic emission spectrometry, *Spectrochimica Acta Part B* 2000, Vol 55, 943-950.
32. P. Pohl, W. Zyrnicki, Study of chemical vapor generation of Au, Pd, and Pt by inductively coupled plasma atomic emission spectrometry, *Journal of Analytical Atomic Spectrometry* 2001, Vol 16, 1442-1445.
33. A.S. Luna, R.E. Sturgeon, R.C. de Campos, Chemical vapor generation: atomic absorption by Ag, Au, Cu and Zn following reduction of aquo ions with sodium tetrahydroborate(III), *Analytical Chemistry* 2000, Vol 72, 3523-3531.
34. Y.-L. Feng, J.W. Lam, R.E. Sturgeon, Expanding the scope of chemical vapor generation for noble and transition metals, *Analyst* 2001, Vol 126, 1833-1837.
35. T. Matoušek, J. Dědina, M. Vobecký, Continuous flow chemical vapour generation of silver for atomic absorption spectrometry using tetrahydroborate (III) reduction-system performance and assessment of the efficiency using instrumental neutron activation analysis, *Journal of Analytical Atomic Spectrometry* 2002, Vol 17, 52-56.
36. Y.-L. Feng, R.E. Sturgeon, J.W. Lam, Chemical vapor generation characteristics of transition and noble metals reacting with tetrahydroborate(III), *Journal of Analytical Atomic Spectrometry* 2003, Vol 18, 1435-1442.
37. N. Panichev, R.E. Sturgeon, Atomic absorption by free atoms in solution following chemical reduction from the ionic state, *Analytical Chemistry* 1998, Vol 70, 1670-1676.
38. R. Burtovyy, E. Utzig, M. Tkacz, Studies of the thermal decomposition of copper hydride, *Thermochimica Acta* 2000, Vol 363, 157-163.
39. G.D. Barbaras, C. Dillard, A.E. Finholt, T. Wartik, K.E. Wilzbach, H.I. Schlesinger, The preparation of the hydrides of zinc, cadmium, beryllium, magnesium and lithium by the use of lithium aluminum hydride, *Journal of American Chemical Society* 1951, Vol 73, 4585-4590.
40. K. Fujita, T. Takada, Effect of temperature on generation and decomposition of the group Vb Element hydrides and estimation of the kinetic stability of gaseous bismuth hydride by atomic absorption spectrometry, *Talanta* 1986, Vol 33, 203-207.

41. F.J. Fernandez, Atomic absorption determination of gaseous hydrides utilizing sodium borohydride reduction, *Atomic Absorption Newsletters* 1973, Vol 12, 93-97.
42. J. Dědina, Quartz tube atomizers for hydride generation atomic absorption spectrometry: mechanism of selenium atomization and fate of free atoms, *Spectrochimica Acta Part B* 1992, Vol 47, 689-700.
43. B. Welz, T. Guo, Formation and interpretation of double peaks in flow injection hydride generation atomic absorption spectrometry, *Spectrochimica Acta Part B* 1992, Vol 47, 645-658.
44. B. Welz, M. Melcher, Investigations on atomisation mechanisms of volatile hydride-forming elements in a heated quartz cell: Part 1. Gas-phase and surface effects; Decomposition and atomisation of arsine, *Analyst* 1983, Vol 108, 213-224.
45. M. Johansson, D.C. Baxter, K.E.A. Ohlsson, W. Frech, Mechanism of formation and spatial distribution of lead atoms in quartz tube atomizers, *Spectrochimica Acta Part B* 1997, Vol 52, 643-656.
46. S. Tesfalidet, G. Wikander, K. Irgum, Determination of hydrogen radicals in analytical flames using electron spin resonance spectroscopy applied to direct investigations of flame-based atomization units for hydride generation atomic absorption spectrometry, *Analytical Chemistry* 1999, Vol 71, 1225-1231.
47. K. Jin, M. Taga, Determination of lead by continuous-flow hydride generation and atomic absorption spectrometry: comparison of malic acid-dichromate, nitric acid-hydrogen peroxide and nitric acid-peroxodisuphate reaction matrices in combination with sodium tetrahydroborate, *Analytica Chimica Acta* 1982, Vol 143, 229-236.
48. X.J. Feng, B. Fu, Determination of arsenic, antimony, selenium, tellurium and bismuth in nickel metal by hydride generation atomic fluorescence spectrometry, *Analytica Chimica Acta* 1998, Vol 371, 109-113.
49. A. D'Ulivo, L. Gianfranceschi, L. Lampugnani, R. Zamboni, Masking agents in the determination of selenium by hydride generation technique, *Spectrochimica Acta Part B* 2002, Vol 57, 2081-2094.
50. A.B. Volynsky, Mechanisms of action of platinum group modifiers in electrothermal atomic absorption spectrometry, *Spectrochimica Acta Part B* 2000, Vol 55, 103-150.

51. X. Hou, B.T. Jones, Tungsten devices in analytical atomic spectrometry, *Spectrochimica Acta Part B* 2002, Vol 57, 659-688.
52. K.A. Wagner, K.E. Levine, B.T. Jones, A simple, low cost, multielement atomic absorption spectrometer with a tungsten coil atomizer, *Spectrochimica Acta Part B* 1998, Vol 53, 1507-1516.
53. V. Krivan, P. Barth, C. Schnürer-Patschan, An electrothermal atomic absorption spectrometer using semiconductor diode lasers and a tungsten coil atomizer: Design and first applications, *Analytical Chemistry* 1998, Vol 70, 3525-3532.
54. X. Hou, K.E. Levine, A. Salido, B.T. Jones, M. Ezer, S. Elwood, J.B. Simeonsson, Tungsten coil devices in atomic spectrometry: Absorption, fluorescence, and emission, *Analytical Sciences* 2001, Vol 17, 175-180.
55. P. Barth, S. Hauptkorn, V. Krivan, Improved slurry sampling electrothermal vaporization system using a tungsten coil for inductively coupled plasma atomic emission spectrometry, *Journal of Analytical Atomic Spectrometry* 1997, Vol 12, 1351-1358.
56. T. Maruta, T. Takeuchi, Determination of trace amounts of chromium by atomic absorption spectrometry with a tantalum filament atomizer, *Analytica Chimica Acta* 1973, Vol 66, 5-11.
57. S. Ahsan, S. Kaneco, K. Ohta, T. Mizuno, Y. Taniguchi, Direct determination of cadmium in calcium drug samples using electrothermal atomic absorption spectrometry with a metal tube atomizer and thiourea as a matrix modifier, *Talanta* 1999, Vol 48, 63-69.
58. K. Ohta, S.-I. Itoh, T. Mizuno, Electrothermal atomization atomic absorption spectrometry of cadmium with a platinum tube atomizer, *Talanta* 1991, Vol 38, 871-874.
59. *CRC Handbook of Chemistry and Physics*, 52nd Edition, The Chemical Rubber Co., USA, 1971-1972.
60. M.F. Giné, F.J. Krug, V.A. Sass, B.F. Reis, J.A. Nobrega, H. Berndt, Determination of cadmium in biological materials by tungsten coil atomic absorption spectrometry, *Journal of Analytical Atomic Spectrometry* 1993, Vol 8, 243-245.
61. X. Hou, B.T. Jones, Field instrumentation in atomic spectroscopy, *Microchemical Journal* 2000, Vol 66, 115-145.

62. A.S. Ribeiro, M.A.Z. Arruda, S. Cadore, Determination of bismuth in metallurgical materials using a quartz tube atomizer with tungsten coil and flow injection-hydride-generation atomic absorption spectrometry, *Spectrochimica Acta Part B: Atomic Spectroscopy* 2002, Vol 57, 2113-2120.
63. A.S. Ribeiro, M.A.Z. Arruda, S. Cadore, A quartz tube atomizer with tungsten coil: a new system for vapor atomization in atomic absorption spectrometry, *Journal of Analytical Atomic Spectrometry* 2002, Vol 17, 1516 - 1522.
64. W. Lund, B.V. Larsen, The application of electrodeposition techniques to flameless atomic absorption spectrometry Part I. Determination of cadmium with a tungsten Filament, *Analytica Chimica Acta* 1974, Vol 70, 299-310.
65. W. Lund, B.V. Larsen, The application of electrodeposition techniques to flameless atomic absorption spectrometry Part II. Determination of cadmium in sea water, *Analytica Chimica Acta* 1974, Vol 72, 57-62.
66. W. Lund, B.V. Larsen, The application of electrodeposition techniques to flameless atomic absorption spectrometry Part III. Determination of cadmium in urine, *Analytica Chimica Acta* 1976, Vol 81, 319-324.
67. E.J. Czobik, J.P. Matoušek, The application of electrodeposition on a tungsten wire to furnace atomic absorption spectrometry, *Spectrochimica Acta Part B* 1980, Vol 35, 741-751.
68. E.W. Wolff, M.P. Landy, D.A. Peel, Preconcentration of cadmium, copper, lead, and zinc in water at the 10^{-12} g/g level by adsorption onto tungsten wire followed by flameless atomic absorption spectrometry, *Analytical Chemistry* 1981, Vol 53, 1566-1570
69. Jr F. Barbosa, F.J. Krug, É.C. Lima, On-line coupling of electrothermal preconcentration in tungsten coil electrothermal atomic absorption spectrometry for determination of lead in natural waters, *Spectrochimica Acta Part B* 1999, Vol 54, 1155-1166.
70. S.I. Itoh, S. Kaneco, K. Ohta, T. Mizuno, Determination of bismuth in environmental samples with Mg-W cell-electrothermal atomic absorption spectrometry, *Analytica Chimica Acta* 1999, Vol 379, 169-173.
71. H. Matusiewicz, R.E. Sturgeon, Atomic spectrometric detection of hydride forming elements following *in situ* trapping within a graphite furnace, *Spectrochimica Acta Part B* 1996, Vol 51, Iss 4, 377-397.

72. D.S. Lee, Determination of bismuth in environmental samples by flameless atomic absorption spectrometry with hydride generation, *Analytical Chemistry* 1982, Vol 54, 1682-1686.
73. R.E. Sturgeon, S.N. Willie, S.S. Berman, Hydride generation atomic-absorption determination of antimony in seawater with in-situ concentration in a graphite furnace, *Analytical Chemistry* 1985, Vol 57, 2311-2314.
74. D.L. Tsalev, A. D'Ulivo, L. Lampugnani, M. Di Marco, R. Zamboni, Thermally stabilized iridium on an integrated, carbide-coated platform as a permanent modifier for hydride-forming elements in electrothermal atomic absorption spectrometry Part 2. Hydride generation and collection, and behaviour of some organoelement species, *Journal of Analytical Atomic Spectrometry* 1996, Vol 11, 979-988.
75. R.E. Sturgeon, S.N. Willie, G.I. Sproule, P.T. Robinson, S.S. Berman, Sequestration of volatile element hydrides by platinum group elements for graphite furnace atomic absorption, *Spectrochimica Acta Part B* 1989, Vol 44, 667-682.
76. L. Zhang, Z.M. Ni, X.-Q. Shan, *In situ* concentration of metallic hydrides in a graphite furnace coated with palladium, *Spectrochimica Acta Part B* 1989, Vol 44, 339-346.
77. L. Zhang, Z.M. Ni, X.-Q. Shan, *In situ* concentration of metallic hydrides in a graphite furnace coated with palladium- Determination of Bismuth, Germanium and Tellurium, *Spectrochimica Acta Part B* 1989, Vol 44, 751-758.
78. Y.-P. Liao, H.O. Haug, Investigation of stable coatings for *in situ* trapping of Se and Te in flow-injection hydride generation and graphite furnace atomic absorption spectrometry for automated determination, *Microchemical Journal* 1997, Vol 56, 247-258.
79. H.O. Haug, Y.-P. Liao, Investigation of the automated determination of As, Sb and Bi by flow-injection hydride generation using in-situ trapping on stable coatings in graphite furnace atomic absorption spectrometry, *Fresenius Journal of Analytical Chemistry* 1996, Vol 356, 435-444.
80. S. Garboś, M. Wałcerz, E. Bulska, A. Hulanicki, Simultaneous determination of Se and As by hydride generation atomic absorption spectrometry with analyte concentration in a graphite furnace coated with zirconium, *Spectrochimica Acta Part B* 1995, Vol 50, 1669-1677.

81. J. Murphy, P. Jones, G. Schlemmer, I.L. Shuttler, S.J. Hill, Investigations into the simultaneous determination of bismuth and selenium by 'in atomizer trapping' electrothermal atomic absorption spectrometry, *Analytical Communications* 1997, Vol 34, 359-362.
82. B. Dočekal, P. Marek, Investigation of *in situ* trapping of selenium and arsenic hydrides within tungsten tube atomizer, *Journal of Analytical Atomic Spectrometry* 2001, Vol 16, 831-837.
83. Jr F. Barbosa, S.S. de Souza, F.J. Krug, *In situ* trapping of selenium hydride in rhodium-coated tungsten coil electrothermal atomic absorption spectrometry, *Journal of Analytical Atomic Spectrometry* 2002, Vol 17, 382-388.
84. V. Majidia, N. Xu, R.G. Smith, Electrothermal vaporization, part 1: Gas phase chemistry- Review, *Spectrochimica Acta Part B* 2000, Vol 55, 3-35.
85. G. Ertaş, J.A. Holcombe, Determination of absolute transport efficiencies of Be, Cd, In, Pb and Bi for electrothermal vaporization sample introduction into an inductively coupled plasma using an in-line electrostatic precipitator, *Spectrochimica Acta Part B* 2003, Vol 58, 1597-1612.
86. M.A. Belarra, M. Resano, F. Vanhaecke, L. Moens, Direct solid sampling with electrothermal vaporization/atomization: what for and how?, *Trends in Analytical Chemistry* 2002, Vol 21, 828-839.
87. T. Kantor, Electrothermal vaporization and laser ablation sample introduction for flame and plasma spectrometric analysis of solid and solution samples-Review, *Spectrochimica Acta Part B* 2001, Vol 56, 1523-1563.
88. D.C. Grégoire, R.E. Sturgeon, Analyte transport efficiency with electrothermal vaporization inductively coupled plasma mass spectrometry, *Spectrochimica Acta Part B* 1999, Vol 54, 773-786.
89. U. Schäffer, V. Krivan, A graphite furnace electrothermal vaporization system for inductively coupled plasma atomic emission spectrometry, *Analytical Chemistry* 1998, Vol 70, 482-490.
90. T. Kantor, Interpreting some analytical characteristics of thermal dispersion methods used for sample introduction in atomic spectrometry, *Spectrochimica Acta Part B* 1988, Vol 43, 1299-1320.

91. J. Bernhardt, T. Buchkamp, G. Hermann, G. Lasnitschka, Transport efficiencies and analytical determinations with electrothermal vaporization employing electrostatic precipitation and electrothermal atomic spectroscopy, *Spectrochimica Acta Part B* 1999, Vol 54, 1821-1829.
92. H.T. Uggerud, W. Lund, Use of palladium and iridium as modifiers in the determination of arsenic and antimony by electrothermal vaporization inductively coupled plasma mass spectrometry, following *in situ* trapping of the hydrides, *Journal of Analytical Atomic Spectrometry* 1997, Vol 12, 1169-1174.
93. H. Matusiewicz, M. Koprás, Simultaneous determination of hydride forming elements (As, Bi, Ge, Sb, Se) and Hg in biological and environmental reference materials by electrothermal vaporization–microwave induced plasma-optical emission spectrometry with their *in situ* trapping in a graphite furnace, *Journal of Analytical Atomic Spectrometry* 2003, Vol 18, 1415-1425.
94. C.C. Chang, S.J. Jiang, Determination of Hg and Bi by electrothermal vaporization inductively coupled plasma mass spectrometry using vapor generation with *in situ* preconcentration in a platinum-coated graphite furnace, *Analytica Chimica Acta* 1997, Vol 353, 173-180.
95. J.P. Matoušek, R. Iavetz, K.J. Powell, H. Louie, Mechanistic studies on the trapping and desorption of volatile hydrides and mercury for their determination by electrothermal vaporization-inductively-coupled plasma mass spectrometry, *Spectrochimica Acta Part B* 2002, Vol 57, 147-155.
96. K. Dittrich, H. Berndt, J.A.C. Broekaert, G. Schaldach, G. Tölg, Comparative study of injection into a pneumatic nebuliser and tungsten coil electrothermal vaporisation for the determination of rare earth elements by inductively coupled plasma optical emission spectrometry, *Journal of Analytical Atomic Spectrometry* 1988, Vol 3, 1105-1110.
97. K. Levine, K.A. Wagner, B.T. Jones, Low-cost, modular electrothermal vaporization system for inductively coupled plasma atomic emission spectrometry, *Applied Spectroscopy* 1998, Vol 52, 1165-1171.
98. N. Shibata, N. Fudagawa, M. Kubota, Electrothermal vaporization using a tungsten furnace for the determination of rare-earth elements by inductively coupled plasma mass spectrometry, *Analytical Chemistry* 1991, Vol 63, 636-640.

99. S. Hauptkorn, V. Krivan, B. Gercken, J. Pavel, Determination of trace impurities in high-purity quartz by electrothermal vaporization inductively coupled plasma mass spectrometry using the slurry sampling technique, *Journal of Analytical Atomic Spectrometry* 1997, Vol 12, 421-428.
100. Y. Okamoto, Direct determination of lead in biological samples by electrothermal vaporization inductively coupled plasma mass spectrometry (ETV-ICP-MS) after furnace-fusion in the sample cuvette-tungsten boat furnace, *Fresenius Journal of Analytical Chemistry* 2000, Vol 367, 300-305.
101. Y. Okamoto, R. Kikkawa, Y. Kobayashi, T. Fujiwara, External furnace-fusion digestion for the direct determination of lead in rock samples by inductively coupled plasma mass spectrometry (ICP-MS) using the tungsten boat furnace-sample cuvette technique, *Journal of Analytical Atomic Spectrometry* 2001, Vol 16, 96-98.
102. C. Bruhn, H. Berndt, M.L. Tristao, Low-temperature hydride furnace modified for the atomic absorption spectrometric determination of metals with low appearance temperatures, *Analytica Chimica Acta* 1987, Vol 193, 361-365.
103. I. Osama, M.S. Thesis, *Determination of Cadmium by Cold Vapour Generation Atom Trapping Atomic Absorption Spectrometry*, Middle East Technical University, Ankara, June 2000.
104. O. Cankur, N. Ertaş, O.Y. Ataman, Determination of bismuth after on-line preconcentration by trapping on resistively heated W-coil and hydride generation atomic absorption spectrometry, *Journal of Analytical Atomic Spectrometry* 2002, Vol 17, 603-609.
105. B. Dočekal, Ş. Güçer, A. Selecká, Trapping of hydride forming elements within miniature electrothermal devices: Part I. Investigation of collection of arsenic and selenium hydrides on a molybdenum foil strip, *Spectrochimica Acta Part B* 2004, Vol 59, 487-495.
106. X.-M. Guo, X.-W. Guo, Determination of ultra-trace amounts of selenium by continuous flow hydride generation AFS and AAS with collection on gold wire, *Journal of Analytical Atomic Spectrometry* 2001, Vol 16, 1414-1418.
107. P.J. Sadler, H. Li, H. Sun, Coordination chemistry of metals in medicine: target sites for bismuth, *Coordination Chemistry Reviews* 1999, Vol 185-186, 689-709.

108. J.L. Burguera, M. Burguera, C. Rivas, C. Rondon, P. Carrero, M. Gallignani, Determination of bismuth in biological samples using on-line flow-injection microwave-assisted mineralization and precipitation/dissolution for electrothermal atomic absorption spectrometry, *Talanta* 1999, Vol 48, 885-893.
109. D.M. Taylor, D.R. Williams, *Trace element medicine and chelation therapy*, The Royal Society of Chemistry, Cambridge, 1995.
110. Bi Applications and Trends, <http://www.bismuth.be/Appl.html> and <http://www.bismuth.be/news.html>.
111. S. Cadore, N. Baccan, Continuous hydride generation system for the determination of trace amounts of bismuth in metallurgical materials by atomic absorption spectrometry using an on-line stripping-type generator/gas-liquid separator, *Journal of Analytical Atomic Spectrometry* 1997, Vol 12, 637-642.
112. S. Cadore, A.P. dos Anjos, N. Baccan, Determination of bismuth in urine and prescription medicines using atomic absorption with an on-line hydride generation system, *Analyst* 1998, Vol 123, 1717-1719.
113. R. Pamphlett, M. Stoltenberg, J. Rungby, G. Danscher, Uptake of bismuth in motor neurons of mice after single oral doses of bismuth compounds, *Neurotoxicology and Teratology* 2000, Vol 22, 559-563.
114. P. Schramel, I. Wendler, J. Angerer, The determination of metals (antimony, bismuth, lead, cadmium, mercury, palladium, platinum, tellurium, thallium, tin and tungsten) in urine samples by inductively coupled plasma-mass spectrometry, *Int Arch. Occup. Environmental Health* 1997, Vol 69, 219-223.
115. H. Li, B.M. Keohane, H. Sun, P.J. Sadler, Determination of bismuth in serum and urine by direct injection nebulization inductively coupled plasma mass spectrometry, *Journal of Analytical Atomic Spectrometry* 1997, Vol 12, 1111-1114.
116. S. Moyano, J.A. Gásquez, R. Olsina, E. Marchevsky, L.D. Martinez, Pre-concentration system for bismuth determination in urine using FI-ICP- AES with ultrasonic nebulization, *Journal of Analytical Atomic Spectrometry* 1999, Vol 14, 259-262.
117. J.B.B. da Silva, M.B.O. Giacomelli, A.J. Curtius, Determination of bismuth in aluminium and in steel by electrothermal atomic absorption spectrometry after on-line separation using a minicolumn of activated carbon, *Analyst* 1999, Vol 124, 1249-1253.

118. E.N. Pollock, S.J. West, The generation and determination of covalent hydrides by atomic absorption, *Atomic Absorption Newsletters* 1973, Vol 12, 6-8.
119. H.D. Fleming, R.G. Ide, Determination of volatile hydride-forming metals in steel by atomic absorption spectrometry, *Analytica Chimica Acta* 1976, Vol 83, 67-82.
120. M. Bedard, J.D. Kerbyson, Determination of trace bismuth in copper by hydride evolution atomic absorption spectrophotometry, *Analytical Chemistry* 1975, Vol 47, 1441-1444.
121. B. Vanloo, R. Dams, J. Hoste, Determination of bismuth and lead in steel and cast iron by hydride generation and zeeman atomic absorption spectrometry, *Analytica Chimica Acta* 1983, Vol 151, 391-400.
122. O. Aöstrom, Flow injection analysis for the determination of bismuth by atomic absorption spectrometry with hydride generation, *Analytical Chemistry* 1982, Vol 54, 190-193.
123. S. Moyano, R.G. Wuilloud, R.A. Olsina, J.A. Gásquez, L.D. Martinez, On-line preconcentration system for bismuth determination in urine by flow injection hydride generation inductively coupled plasma atomic emission spectrometry, *Talanta* 2001, Vol 54, 211-219.
124. H. Matusiewicz, M. Kopras, A. Suszka, Hydride generation graphite furnace atomic absorption determination of bismuth in clinical samples with *in situ* preconcentration, *Microchemical Journal* 1995, Vol 52, 282-289.
125. J. Murphy, G. Schlemmer, I.L. Shuttler, P. Jones, S.J. Hill SJ, Simultaneous multi-multielement determination of hydride forming elements by “in-atomiser trapping” electrothermal atomic absorption spectrometry on an iridium-coated graphite tube, *Journal of Analytical Atomic Spectrometry* 1999, Vol 14, 1593-1600.
126. S.E. Manahan, *Toxicological Chemistry and Biochemistry*, 3rd Edition, CRC Press LLC, USA, 2003.
127. M. Radojevic, V.N. Bashkin, *Practical Environmental Analysis*, The Royal Society of Chemistry, Cambridge, 1999.
128. E. Lückner, Analysis of the distribution of lead, cadmium and mercury in the avian kidney by means of direct solid sampling electrothermal atomic absorption spectrometry, *Fresenius Journal of Analytical Chemistry* 1997, Vol 358, 848-853.

129. C.G. Bruhn, N.A. San Francisco, J.Y. Neira, J.A. Nóbrega, Determination of cadmium and lead in mussels by tungsten coil electrothermal atomic absorption spectrometry, *Talanta*, 1999, Vol 50, 967-975.
130. C.G. Bruhn, J.Y. Neira, G.D. Valenzuela, J.A. Nobrega, Determination of cadmium in hair and blood by tungsten coil electrothermal atomic absorption spectrometry with chemical modifiers, *Talanta* 1999, Vol 48, 537-549.
131. Y. Hirano, J. Nakajima, K. Oguma, Y. Terui, Determination of traces of cadmium in natural water samples by flow injection on-line preconcentration-graphite furnace atomic absorption spectrometry, *Analytical Sciences* 2001, Vol 17, 1073-1077.
132. A. D'Ulivo, Y. Chen, Determination of cadmium in aqueous samples by vapor generation with sodium tetraethylborate(III) reagent, *Journal of Analytical Atomic Spectrometry* 1989, Vol 4, 319-322.
133. M.C. Valdés-Hevia y Temprano, M.R. Fernández de la Campa, A. Sanz-Medel, Generation of volatile cadmium species with sodium tetrahydroborate from organized media: application to cadmium determination by inductively coupled plasma atomic emission spectrometry, *Journal of Analytical Atomic Spectrometry* 1993, Vol 8, 847-852.
134. L. Ebdon, P. Goodall, S.J. Hill, P.B. Stockwell, K.C. Thompson, Ultra-trace determination of cadmium by vapor generation atomic fluorescence spectrometry, *Journal of Analytical Atomic Spectrometry* 1993, Vol 8, 723-729.
135. L. Lampugnani, C. Salvetti, D.L. Tsalev, Hydride generation atomic absorption spectrometry with different flow systems and in-atomizer trapping for determination of cadmium in water and urine-overview of existing data on cadmium vapour generation and evaluation of critical parameters, *Talanta* 2003, Vol 61, 683-698.
136. C. Vargas-Razo, J.F. Tyson, Determination of cadmium by flow injection-chemical vapor generation-atomic absorption spectrometry, *Fresenius Journal of Analytical Chemistry* 2000, Vol 366, 182-190.
137. Y.-L. Feng, R.E. Sturgeon, J.W. Lam, Generation of atomic and molecular cadmium species from aqueous media, *Analytical Chemistry* 2003, Vol 75, 635-640.
138. X. Guo, X. Guo, Studies on the reaction between cadmium and potassium tetrahydroborate in aqueous solution and its application in atomic fluorescence spectrometry, *Analytica Chimica Acta* 1995, Vol 310, 377-385.

139. T.-J. Hwang, S.-J. Jiang, Determination of cadmium by flow injection isotope dilution inductively coupled plasma mass spectrometry with vapour generation sample introduction, *Journal of Analytical Atomic Spectrometry* 1997, Vol 12, 579-584.
140. H.G. Infante, M.L.F. Sánchez, A. Sanz-Medel, Ultratrace determination of cadmium by atomic absorption spectrometry using hydride generation with in-situ preconcentration in a palladium-coated graphite atomizer, *Journal of Analytical Atomic Spectrometry* 1996, Vol 11, 571-575.
141. H.G. Infante, M.L.F. Sanchez, A. Sanz Medel, Vesicular hydride generation - *In situ* preconcentration - electrothermal atomic absorption spectrometry determination of sub-parts-per-billion levels of cadmium, *Journal of Analytical Atomic Spectrometry* 1997, Vol 12, 1333-1336.
142. P. Bermejo-Barrera, J. Moreda-Pinheiro, A. Moreda-Pinheiro, A. Bermejo-Barrera, Use of flow injection cold vapour generation and preconcentration on coated graphite tubes for the determination of cadmium in sea-water by electrothermal atomic absorption spectrometry, *Journal of Analytical Atomic Spectrometry* 1996, Vol 11, 1081-1086.
143. M. Patriarca, A. Menditto, B. Rossi, T.D.B. Lyon, G.S. Fell, Environmental exposure to metals of newborns, infants and young children, *Microchemical Journal* 2000, Vol 67, 351-361.
144. H.T. Odum, *Heavy Metals in the Environment Using Wetlands for Their Removal*, CRC Press LLC, USA, 2000.
145. R.T. Daher, Trace metals (lead and cadmium exposure screening), *Analytical Chemistry* 1995, Vol 67, 405R-409R.
146. Y. Zhou, R.A. Zañão, Jr F. Barbosa, P.J. Parsons, F.J. Krug, Investigations of a W-Rh permanent modifier for the determination of Pb in blood by electrothermal atomic absorption spectrometry, *Spectrochimica Acta Part B* 2002, Vol 57, 1291-1300.
147. P.R.M. Correia, E. Oliveira, P.V. Oliveira, Simultaneous determination of Cd and Pb in foodstuffs by electrothermal atomic absorption spectrometry, *Analytica Chimica Acta* 2000, Vol 405, 205-211.
148. P.J. Parsons, H. Qiao, K.M. Aldous, E. Mills, W. Slavin, A low-cost tungsten filament atomizer for measuring lead in blood by atomic absorption spectrometry, *Spectrochimica Acta Part B* 1995, Vol 50, 1475-1480.

149. Y. Zhou, P.J. Parsons, K.M. Aldous, P. Brockman, W. Slavin, Rhodium as permanent modifier for atomization of lead from biological fluids using tungsten filament electrothermal atomic absorption spectrometry, *Spectrochimica Acta Part B* 2002, Vol 57, 727-740.
150. K.C. Thompson, D.R. Thomerson, Atomic-absorption studies on determination of antimony, arsenic, bismuth, germanium, lead, selenium, tellurium and tin by utilising the generation of covalent hydrides, *Analyst* 1974, Vol 99, 595-601.
151. P.N. Vijan, G.R. Wood, Semi-automated determination of lead by hydride generation and atomic-absorption spectrophotometry, *Analyst* 1976, Vol 101, 966-973.
152. Y. Madrid, C. Camara, Lead hydride generation atomic absorption spectrometry: an alternative to electrothermal atomic absorption spectrometry- A review, *Analyst* 1994, Vol 119, 1647-1658.
153. J. Li, Y. Liu, T. Lin, Determination of lead by hydride generation atomic absorption spectrometry Part 1. A new medium for generating hydride, *Analytica Chimica Acta* 1990, Vol 231, 151-155.
154. S.-Z. Zhang, H.-B. Han, Z.-M. Ni, Determination of lead by hydride generation atomic absorption spectrometry in the presence of nitroso-R salt, *Analytica Chimica Acta* 1989, Vol 221, 85-90.
155. H. Chen, F. Tang, C. Gu, I.D. Brindle, The influence of chelating reagents on plumbane generation: determination of lead in the presence of PAN-S, *Talanta* 1993, Vol 40, 1147-1155.
156. G. Samanta, D. Chakraborti, Flow injection atomic absorption spectrometry for the standardization of arsenic, lead and mercury in environmental and biological standard reference materials, *Fresenius Journal of Analytical Chemistry* 1997, Vol 357, 827-832.
157. H.O. Haug, Study on stable coatings for determination of lead by flow-injection hydride generation and *in situ* concentration in graphite furnace atomic absorption spectrometry, *Spectrochimica Acta Part B* 1996, Vol 51, 1425-1433.
158. I.D. Brindle, R. McLaughlin, N. Tangtreamjitmun, Determination of lead in calcium carbonate by flow-injection hydride generation with dc plasma atomic emission detection, *Spectrochimica Acta Part B* 1998, Vol 53, 1121-1129.

159. J.F. Tyson, R.I. Ellis, G. Carnrick, F. Fernandez, Flow injection hydride generation electrothermal atomic absorption spectrometry with in-atomizer trapping for the determination of lead in calcium supplements, *Talanta* 2000, Vol 52, 403-410.
160. M. Ikeda, Nishibe, S. Hamada, R. Tujino, Determination of lead at the ng ml^{-1} level by reduction to plumbane and measurement by inductively-coupled plasma emission spectrometry, *Analytica Chimica Acta* 1981, Vol 125, 109-115.
161. J. Li, F. Lu, T. Umemura, K. Tsunoda, Determination of lead by hydride generation inductively coupled plasma mass spectrometry, *Analytica Chimica Acta* 2000, Vol 419, 65-72.
162. S. Chen, Z. Zhang, H. Yu, W. Liu, M. Sun, Determination of trace lead by hydride generation-inductively coupled plasma-mass spectrometry, *Analytica Chimica Acta* 2002, Vol 463, 177-188.
163. P. Bermejo-Barrera, J. Moreda-Pinheiro, A. Moreda-Pinheiro, A. Bermejo-Barrera, Direct trace determination of lead in estuarine water using *in situ* preconcentration of lead hydride on Ir, Zr and W-coated graphite tubes, *Analytica Chimica Acta* 1998, Vol 368, 281-289.
164. D.K. Korkmaz, N. Ertaş, O.Y. Ataman, A novel silica trap for lead determination by hydride generation atomic absorption spectrometry, *Spectrochimica Acta Part B* 2002, Vol 57, 571-580.
165. T. Matoušek, M. Johansson, J. Dědina, W. Frech, Spatially resolved Absorption measurements of antimony atom formation and dissipation in quartz tube atomizers following hydride generation, *Spectrochimica Acta Part B* 1999, Vol 54, 631-643.
166. Z.F. Queiroz, P.V. Oliveira, J.A. Nobrega, C.S. Silva, I.A. Rufini, S.S. de Sousa, F.J. Krug, Surface and gas phase temperatures of a tungsten coil atomizer, *Spectrochimica Acta Part B* 2002, Vol 57, 1789-1799.
167. D.T. Burns, N. Chimpalee, M. Harriott, Applications of a slotted tube atom trap and flame atomic absorption spectrometry: determination of bismuth in copper-based alloys with and without hydride generation, *Analytica Chimica Acta* 1995, Vol 311, 93-97.
168. O. Cankur, O.Y. Ataman, Effect of exhaustion hood flow rate in flow injection cold vapor and hydride generation atomic absorption spectrometry, *Analytical Letters* 2004, Vol 37, 1025-1034.

VITA

Oktay Cankur was born in Bandırma, Balıksir on June 23, 1974. He was graduated from Göl Öğretmen Lisesi, Kastamonu in 1990. He received his B.S. degree from the Chemistry Education Department of the Middle East Technical University. He received his M.S. degree from Chemistry Department of the same university in 1998. Then, he started his PhD studies in the same year. He worked as teaching assistant in chemistry Department of Middle East Technical University between 1995 and 2004.